

# Arabian Journal of Chemistry

---

**Editor -in- Chief**

**Prof. Abdulrahman A . Alwarthan**

Chemistry Department  
King Saud University,  
Riyadh, Saudi Arabia  
E-mail: [awarthan@ksu.edu.sa](mailto:awarthan@ksu.edu.sa)

**Vice-editors -in- Chief**

**Prof. Sultan T. Abu-Orabi**

Tafila Technical University/President  
Tafila, P.O. Box 179, Jordan,  
Jordanian Chemical Society  
Arab Union of Chemists/Secretary General  
E-mail: [abuorabi@excite.com](mailto:abuorabi@excite.com)

**Prof. Yousry M. Issa**

Chemistry Department  
Cairo University, Cairo  
Egypt  
E-mail: [yousrymi@yahoo.com](mailto:yousrymi@yahoo.com)

# EDITORIAL BOARD

**Prof. Belkheir Hammouti**

Director, Laboratory of Applied Chemistry and Environment  
Faculty of Science  
University of Mohammed Premier  
Morocco  
E-mail: hammoutib@yahoo.com

**Prof. Mamia El Rhazi**

Chemistry Department  
Faculty of Science and Technology  
Hassan II University-Mohammedia  
Morocco  
E-mail: elrhazim@hotmail.com

**Prof. Hassan M. Al-Hazimi**

Chemistry Department  
Science College, King Saud University  
Saudi Arabia  
E-mail: hhazimi@ksu.edu.sa

**Prof. Hamad Z. Al-Khathlan**

Chemistry Department  
Science College, King Saud University  
Saudi Arabia  
E-mail: Khathlan@ksu.edu.sa

**Prof. Ibrahim A. Jibril**

Chemistry Department  
Yarmouk University  
Irbid, Jordan  
E-mail: iajibril@yahoo.com

**Prof. El Sayed H. El Ashry**

Chemistry Department  
Faculty of Science  
University of Alexandria  
Alexandria, Egypt  
E-mail: eelashry60@hotmail.com

**Dr. Lassaad Baklouti**

Laboratoire de Chimie des Interactions Moleculaires  
Faculte de Sciences de Bizerte  
7021 Zarzouna, Tunisie  
E-mail: bakloutilassaad@yahoo.fr

**Prof. Saad M. H. Ayoub**

Chemistry Department  
Elneleen University  
Khartoum, Sudan

E-mail:

**Prof. Abdalsalam A. Daffaalla**

Chemistry Department  
Science College, Sudan University of Science and Technology  
P.O.Box: 407  
Khartoum, Sudan  
E-mail: aadafa@hotmail.com

**Prof. Ahmed-Yacine Badjah-Hadj-Ahmed**

University of Science and Technology  
Houari Boumediene  
Faculty of Chemistry  
BP 32 El Alia.  
16111 Bab Ezzouar  
Algiers, Algeria  
E-mail: Ybadjah@hotmail.com

**Abdelkader Bengueddach**

laboratoire de Chimie des Materiaux  
Department of Chemistry  
Faculty of Science  
University of Oran  
P.O.Box 1524 el Mnouar  
31000-Oran, Algeria  
E-mail: aek-bengueddach@univ.oran.dz

**Mohammad Hourani**

Department of Chemistry, Al Balqa Applied  
University, Al-Salt, Jordan.  
E-mail: mhouran@bau.edu.jo

**Prof. Mahmoud F. Farhat**

Professor of Organic Chemistry  
Chemistry Department  
Faculty of Science  
Al-Fateh University  
P.O.Box: 13494  
Tripole, Libya  
E-mail: mf\_farhat@yahoo.com

**Prof. Nouria A. Al-Awadi**

Professor of Organic Chemistry  
Department of Chemistry  
Faculty of Science  
P.O.Box: 5969 Safat-13060  
Kuwait University  
E-mail: eam\_hc5@kuc01.kuniv.edu.kw

**Dr. Abdulaziz A. AlNajjar**

Applied Science, College of Technological Studies,  
Public Authority of Applied Education and Training  
P.O. Box 34484 Adeilia, 73255, Kuwait  
e-mail: anajjar\_55@yahoo.com

**Dr. Ameera Saeed Al-Haddad**

University of Bahrain, Kingdom of Bahrain ,  
Department of Chemistry, P.O. Box 32028, Isa Town,  
Kingdom of Bahrain  
E=mail: ameera@sci.uoh.bh

# INTERNATIONAL ADVISORY BOARD

**Prof. Issa Yavari**

Chemistry Department  
Tarbiat Modarres University  
Tehran, Iran  
E-mail: yavarisa@modares.ac.ir

**Dr. Paul S. Francis**

School of Life and Environmental Sciences  
Deakin University, Geelong  
Victoria 3217, Australia  
E-mail: psf@deakin.edu.au

**Prof. Jose Martinez Calatayud**

Chemistry Department  
University of Valencia  
Valencia, Spain  
E-mail: jose.martinez@uv.es

**Prof. Robert G. Michel**

Department of Chemistry  
University of Connecticut  
55 North Eagleville Road  
Storrs, CT 06269-3060  
E-mail: robert.g.michel@uconn.edu

**Prof. Motaza M. Khater**

Chemistry Department  
Cairo University  
Cairo, Egypt  
E-mail: motazakhater117@yahoo.com

**Prof. Jacques Vicens**

Directeur de recherche at CNRS  
UMR 7178-CNRS  
Institut Pluridisciplinaire Hubert Curien  
Universite Louis Pasteur de Strasbourg  
Laboratoire de Conception Moléculaire  
ECPM  
25, rue Becquerel  
F-67087  
France  
E-mail: vicens@chimie.u-strasbg.fr

**Prof. Jean-Michel KAUFFMANN**

Free University of Brussels  
Lab, Instrumental Analysis and Bioelectrochemistry  
Pharmaceutical Institute, ULB 205/6  
Campus Plaine  
B-1050 Brussels, Belgium  
E-mail: jmkauf@ulb.ac.be

**Prof. Essam Khamis Al-Hanash**

Vice-Dean for Graduate Studies & Research.

Faculty of Science, Mohram Bey, Alexandria University.  
Alexandria, Egypt  
E-mail: ekaijac@yahoo.com

**Prof. Bryan R. Henry**

University of Guelph  
Department of Chemistry  
Guelph, Ontario N1G 2W1  
Canada  
E-mail: Chmhenry@uoguelph.ca

**Prof. Samy El-Shall**

Department of Chemistry,  
Virginia Commonwealth University  
Richmond, Virginia 23284-2006  
USA  
E-mail: mselshal@vcu.edu.

**Prof. JIN, JUNG-IL(M)**

35-41Ku-Ui 2-Dong  
Kwang-Jin Ku, Seoul 133-202, Korea  
Chemistry Department and Center for Electro-and Photo-  
Responsive Molecules, College of Sciences,  
Korea University  
5-1 Anam-Dong, Seoul 136-701, Korea  
E-mail: jijin@korea.ac.kr, jijin@kcsnet.or.kr

**Prof. Alan Townshend**

The University of Hull  
Department of Chemistry  
Hull, HU6 7RX  
United Kingdom  
E-mail: a.townshend@hull.ac.uk

**Dr. Danielle M. Cleveland**

18347 woodland Ridge Drive # 14  
Spring Lake, MI 49456  
E-mail: danielle.cleveland@uconn.edu

**Prof. Yuhan Sun**

Institute of Coal Chemistry  
Chinese Academy of Sciences  
P.O.Box: 165, Taiyuan, Shanxi, 030001, PR. China  
E-mail: yhsun@sxicc.ac.cn

**Prof. Ishaque Khan**

Director, Materials and Chemical Synthesis Program  
Department of Biological Chemical and Physical Sciences  
College of Science and Letters  
Room 125, E1  
10W, 32nd Street  
Chicago, IL 60616-3793  
E-mail: khan@117.edu

# INTERNATIONAL ADVISORY BOARD

**Prof. Mikhail M. Krayushkin**

Head of Laboratory of Heterocyclic Compounds  
N.D.Zelinsky Institute of Organic Chemistry,  
Russian Academy of Sciences  
119991, Moscow, Leninsky Prospekt 47, Russia  
E-mail: mkray@ioc.ac.ru

**Prof. Volker Schurig,**

Institute of Organic chemistry,  
University of Tübingen, Auf der Morgenstelle 18, 72076  
Tübingen, Germany  
E-mail: Volker.schurig@uni-tuebingen.de

**Prof. Angel Rios Castro**

Department of Analytical Chemistry and food Tech.,  
Faculty of Chemistry  
University of Castilla- La Mancha  
AV. Camilo Jose Cela. 10, E-13004 Ciudad Real, Spain.  
Phone: +34 926 295232 /Fax: +34 926 295318  
E-mail: angel.rios@uclm.es

**Prof. Faiza M. Al-Kharafi**

Department of Chemistry  
Faculty of Science  
Kuwait University  
Kuwait  
E-mail: chesc@kuc01.kuniv.edu.kw

# Author Guidelines

## Scope and Description

Arabian Journal of Chemistry (AJC) is an international quarterly peer-reviewed research journal issued by the Arab Union of Chemists, and published by the Saudi Chemical Society, Riyadh, Saudi Arabia. The Journal publishes new and original Research Articles, Short Communications, Technical Notes, Feature Articles and Review Articles encompassing all fields of chemistry, experimental and theoretical, written either in English or Arabic.

## Introduction to Authors

Instructions to authors concerning manuscript organization and format apply to hardcopy submission by mail, and also to electronic online submission via the Journal homepage website (under construction).

## Manuscript Submission

1- Hardcopy: The Original and three copies of the manuscript, together with a covering letter from the corresponding author, should submitted to the:

Editor-in-chief:  
Prof. Abdulrahman. A. Alwarthan  
Editor-in-Chief  
Arabian Journal of Chemistry  
Chemistry Department, Faculty of Science  
King Saud University  
P.O.Box: 2455, Riyadh-11451  
Saudi Arabia  
Tel: 00966 1 4676005  
Fax: 00966 1 4675888  
E-mail:awarthan@ksu.edu.sa

2- Online: follow the instructions at the journal homepage website.

Original Research Articles, Communications and Technical Notes are subject to critical review by at least two referees. Authors are encouraged to suggest names of competent reviewers. Feature Articles in active chemistry research fields, in which the author's own contribution and its relationship to other work in the field constitutes the main body of the article, appear as a result of an invitation from the Editorial Board, and will be so designated. The author of a Feature Article will be asked to provide a clear, concise and critical status report of the field as an introduction to the article. Review Articles on active and rapidly changing chemistry research fields will also be published. Authors of Review Articles are encouraged to submit two-page proposals to the Editor-in-Chief for approval. Manuscripts submitted in Arabic should also include an Abstract and Keywords in English.

## Organization of the Manuscript

Manuscripts not exceeding 30 pages should be typed double-

spaced on one side of high quality white A4 sheets (21.6×27.9 cm) with 3.71 cm margins, using Microsoft Word 2000 or a later version thereof. The sections should be arranged in the following order: Title Page, Abstract, Keywords, Introduction, Materials and Methods, Results, Discussion, Conclusion, Acknowledgments, Abbreviations (if any), References, Tables, a list of Figure Captions, and Figures. Only the first letters of words in the Title, Headings and Subheadings are capitalized. Headings should be in bold while Subheadings in italic fonts.

**Title Page:** Includes the title of the article, authors' names with full first names and middle initials, and affiliations. The affiliation should comprise the department, institution (university or company), city and state and should be typed as a footnote to the author's name. The name and complete mailing address, telephone and fax numbers, and e-mail address of the author responsible for correspondence (who is designated with an asterisk) should also be included for office purposes. The title should be carefully, concisely and clearly constructed to highlight the emphasis and content of the manuscript, which is very important for information retrieval.

**Abstract:** A one paragraph abstract not exceeding 200 words is required, which should be arranged to highlight the purpose, methods used, results and major findings, with the results comprising no less than 50% of the abstract.

**Keywords:** A list of 4-6 keywords, which express the precise content of the manuscript for indexing purposes, should follow the abstract.

**Introduction:** Should present the purpose of the studies to be reported and their relationship to earlier work in the field, but it should not be an extensive review of the literature (e.g., should not exceed 1 ½ typed pages).

**Materials and Methods:** Should be sufficiently informative to allow competent reproduction of the experimental procedures presented, yet concise enough not to be repetitive of earlier published procedures. Note that all unusual hazards in the chemicals, equipment or procedures used in the study must be clearly identified.

**Results:** Should present results in Tables and Figures plus some complimentary data in the Text without extensive discussion of results.

**Discussion:** Should be concise and focusing on the interpretation of the results without repetition of same results.

**Conclusion:** Should be a brief account of the major findings of the study not exceeding one typed page at the most.

**Nomenclature:** Registered trade names should be capitalized whenever they are used, while trade or trivial names should not be capitalized. The chemical name or composition should be given in parentheses at the first occurrence of that name. Nomenclature should be systematic conforming to those used by the Chemical Abstracts Service and recommended by IUPAC and IUBMB.

**Abbreviations:** Abbreviations are to be used sparingly, otherwise

provide a notation section indicating all nonstandard abbreviations on a separate page prior to the references section. The metric system should be used for all measurements, which must be indicated in lower case letters (e.g., g, kg, m, ml, s), while Standard International (SI) units are to be used conforming to IUPAC. Define all symbols used in equations and formulas. Include a list of all symbols in the notation section when extensively used.

**Acknowledgments:** Acknowledgments, including those for grant and financial support, should be typed in one paragraph directly preceding the References section.

**References:** References should be typed double-spaced and numbered sequentially in the order in which they are cited in the text. References should be cited in the text by the appropriate Arabic numerals, which are superscripted while enclosed in square brackets. Titles of journals are abbreviated according to the Chemical Abstracts Service Source Index (American Chemical Society). Authors are responsible for the accuracy of the references. The style and punctuation should conform to the following examples:

#### 1. Journal Article:

For journals that are not paginated continuously throughout the year (e.g., page numbering does not continue from issue to the next), the volume number should be followed by the issue number in regular parentheses. In contrast, only the volume number is required for journals that are paginated continuously throughout the year. Examples:

- a) Metallo, S. J.; Kane, R. S.; Holmlin, R. E.; Whitesides, G. M., *J. Am. Chem. Soc.* 2003, 125, 4534-4540.
- b) Stevens, M. J., *Langmuir* 1999, 15, 2773-2778.
- c) Walmsley, I.; Rabitz, H., *Phys. Today* 2003, 56(8), 43-49.
- d) Freemantle, M., *Chem. Eng. News* 1988, 76(28), 15-16.

#### 2. Books with authors, No Editors:

- a) Calvert, J. G.; Pitts, J. N., *Photochemistry*; Wiley: New York, 1966, pp 156-186.
- b) Zewail, A. H., *Femtochemistry-Ultrafast Dynamics of the Chemical Bond*; World Scientific: Singapore, 1994; Vol. I, pp 52-58.

#### 3. Books with Authors and Editors:

- a) *The carbohydrates: Chemistry and Biochemistry*; Pigman, W. W., Ed.; Academic Press: New York, 1970; pp 45-50.
- b) Hilman, L. W., In *Dye Laser Principles with Applications*; Durate, F. J.; Hilman, L. W.; Eds.; Academic press: New York, 1990; Chapter 1.
- c) Lochbrunner, S.; Stock, K.; De waele, V.; Riedle, E., *Ultrafast Excited-State Proton Transfer: Reactive Dynamics by Multidimensional Wavepacket Motion*. In *Femtochemistry and Femtobiology: Ultrafast dynamics in Molecular Science*; Douhal, A.; Santamaria, J., Eds.; World Scientific: Singapore, 2002; pp 202-212.
- d) *Femtochemistry and Femtobiology: Ultrafast Reaction Dynamics at Atomic Scale Resolution*; Sundstrom, V., Ed.; World Scientific: Singapore, 1997; Chapter 2.

**4. Technical Report:** Schneider, A. B. Technical Report No. 1234-56, 1985; ABC Company, New York.

**5. Patent:** Kealy, T. J. US Patent 3 062 820, 1962; *Chem. Abstr.* 1963, 58, 9101.

#### 6. Thesis:

Flink, S. *Sensing Monolayers on Gold and Glass*. Ph.D. Thesis,

University of Twente, Enschede, the Netherlands, 2000.

#### 7. Conference or Symposium Proceedings:

Huber, O.; Szejtli, J. *Proceedings of the IV International Symposium on Cyclodextrins*; Munchen; Kluwer Academic Publishers: Dordrecht, 1988.

#### 8. Software Acquired from a Company:

Alchemy: A Molecular Modeling System for the IBMPC; Tripos Associates, Inc.: St. Louis, MO, 1988.

#### 9. Software Accessed through the Internet:

CLOGP Program. Daylight Chemical Information systems, Inc. <http://www.daylight.com/daycgi/clogp>.

#### 10. Internet Source:

Should include Author names (if any), Title, Internet website, URL, and (date of access).

#### 11. Prepublication Online Articles (Already accepted for publication):

Should include Author names (if any), Title of Digital Database, Database Website, URL, and (date of access).

**Tables:** Tables should be numbered with Arabic numerals and referred to by number in the Text (e.g., Table 1). Each Table should be typed on a separate page with the legend above the Table, while explanatory footnotes, which are indicated by superscript lowercase letters, should be typed below the Table.

**Illustrations:** Figures, drawings, diagrams, charts and photographs are to be numbered in a consecutive series of Arabic numerals in the order in which they are cited in the text. Computer-generated illustrations and good-quality digital photographic prints are accepted. They should be black and white originals (not photocopies) provided on separate pages and identified with their corresponding numbers. Actual size graphics should be provided, which need no further manipulation, with lettering (Arial or Helvetica) not smaller than 4.5 points, lines no thinner than 0.5 points, and each of uniform density. All color should be removed from graphics except for those graphics to be considered for publication in color. If graphics are to be submitted digitally, they should conform to the following minimum resolution requirements: 1200 dpi for black and white line art, 600 dpi for grayscale art, and 300 dpi for color art. All graphic files must be saved as TIFF images, and all illustrations must be submitted in the actual size at which they should appear in the journal. Note that good quality hardcopy original illustrations are required for both online and mail submissions of manuscripts.

**Text Footnotes:** The use of text footnotes is to be avoided. When their use is absolutely necessary, they should be typed at the bottom of the page to which they refer, and should be cited in the text by a superscript asterisk or multiples thereof. Place a line above the footnote, so that it is set off from the text.

**Supplementary Material:** Authors are encouraged to provide all supplementary materials that may facilitate the review process, including any detailed mathematical derivations that may not appear in whole in the manuscript, crystallographic information files (CIFs) and cited preprints. As to CIF files, the author must deposit the corresponding CIFs with the Cambridge Crystallographic Data Centre (CCDC). The E-mail address of CCDC is: [deposit@ccdc.cam.ac.uk](mailto:deposit@ccdc.cam.ac.uk).

The deposited material is indicated in the manuscript by a footnote as follows:

Supplementary data: Crystallographic data for the structural



analysis reported in this paper have been deposited with the Cambridge Crystallographic Data Centre, CCDC, Number (...). Copies of the information may be obtained free of charge from Director, CCDC, 12 Union Road, Cambridge, CB2 1EZ, UK (Fax: +44-1223-336033; e-mail; deposit@ccdc.cam.ac.uk, home page: <http://www.ccdc.cam.ac.uk>).

**Theoretical Calculations:** Reporting the results of electronic structure calculations should follow the guidelines in J. E. Boggs (Pure and Appl. Chem. 1998, 70(4), 1015-1018). Reporting force field parameters and other energy surface data should follow the guidelines in D. J. Raber and W. C. Guida (Pure and Appl. Chem. 1998, 70(10), 2047-2049). Both sets of guidelines are available online at the IUPAC Website ( <http://www.iupac.org/reports/1998/index.html> ).

**X-Ray Data:** X-ray data presented in the text and/or tables should provide information on the empirical formula, unit cell dimensions (a, b, c in pm or Å;  $\alpha$ ,  $\beta$ ,  $\gamma$  in degrees) with corresponding standard error estimates, number of formula units in the unit cell, density (measured or calculated), crystal system, space group symbol, diffractometer type, radiation, and monochromator used, temperature, data collection mode, the  $\theta$ -range and reciprocal lattice segments, number of reflections measured, number of symmetry-independent reflections, cut-off criterion, linear absorption coefficient, absorption correction method, method of solution and refinement, positional and atomic displacement parameters, final R and Rw. A table of selected bond distances and bond angles may also be included.

**Revised Manuscript and Computer Disks:** Following the acceptance of a manuscript for publication and the incorporation of all required revisions, authors should submit an original and one more copy of the final manuscript typed double-spaced plus a 3½" disk containing the complete manuscript in Microsoft Word for

Windows 2000 or a later version thereof. Original Figures should be submitted with the final, revised manuscript even if art is submitted electronically. All graphic files must be saved as TIFF images, and all illustrations must be submitted in the actual size at which they should appear in the journal. A list of the software programs used for text, art and file names on the disk should also be provided. Label the Disk with the author's last name, title of the manuscript, and date. Package the disk in a disk mailer or protective cardboard.

**Reprints:** Twenty (20) reprints are provided to the author responsible for correspondence free of charge. For orders of more reprints, a reprint order form and prices will be sent with article proofs, which should be returned directly to the Editor for processing.

#### **Copyright**

Submission is an admission by the authors that the manuscript has neither been previously published nor is being considered for publication elsewhere. A statement transferring copyright from the authors to Saudi Chemical Society is required before the manuscript can be accepted for publication. The necessary form for such transfer is supplied by the Editor-in-Chief with the article proofs. Reproduction of any part of the contents of a published work is forbidden without a written permission by the Editor-in-Chief.

#### **Disclaimer**

Articles, communication or editorials published by AJC represent the sole opinions of the authors. The publisher shoulders no responsibility or liability whatsoever for the use or misuse of the information published by AJC.

#### **Indexing**

AJC is currently applying for indexing and abstracting to all related International Services, including the Chemical Abstract Service and the Science Citation Index Service



## Arabian Journal of Chemistry

### Table of Contents

Volume 1, Number 2	Page
The Importance of Chirality in Nature and Methods of the Separation of Enantiomers by Chiral Chromatography . V. Schurig	111-122
Determination of Essential Elements in Milk and Urine of Camel And in Nigella sativa Seeds Amirah S. Al-Attas	123-130
Determination of Indoleamine 2, 3- dioxygenase activity in tissues of Arabian Camel ( <i>Camelus dromedarius</i> ) N. J. Siddiqi and A. S. Alhomida	131-135
Application of Oxidative Coupling Reactions for the Estimation of Sildenafil Citrate in Bulk Sample and Dosage Forms Safwan Ashour, Khalil Alkourdi	137-144
Use of Solid Superbase (Na/FAP) as Efficient Catalyst in Facile Construction of a Carbon-Carbon and Carbon-Hetero Atom Bonds Mohamed Zahouily, Bahija Mounir, Ahmed Rayadh, M. Abdellah Bahlaoui, Saïd Sebti	145-160
Palladium(II)/diamine/phosphine and phosphine-free complexes as catalysts for Heck reactions I. Warad, A. Al-Warthan, S. Al-Reseyes, N. Al-Zaqri, M. Fattoh and M. Al-Kahtani	161-169
Catalytic Oxidation of CO pollutant over NiO induced by some transition metal oxides Mohammed A. Al-Omair	171-181
Synthesis and Reactions of Some Novel Quinoxalines Derivatives Haya A. Abubshait	183-199
Synthesis and Characterization of the Gallosilicate Mesoporous Molecular sieve Ga-SBA-15 L. CHERIF, R. BOURI, K. SAIDI, A. BENGUEDDACH, J. FRAISSARD	201-208
Spectrophotometric Determination of Enrofloxacin, Lomefloxacin and Ofloxacin in Pure and in Dosage Forms Through Ion-Pair Complex Formation Alaa S. Amin , Hassan A. Dessouki, and Ibrahim A. Agwa	209-215
Synthesis and Characterization of Two Novel Salent Type Symmetrical Schiff Base Ligands Iran Shiekhshoaie	217-218

## The Importance of Chirality in Nature and Methods of the Separation of Enantiomers by Chiral Chromatography

### Review article

V. Schurig<sup>1</sup>

<sup>1</sup>*Institute of Organic Chemistry, University of Tübingen, Auf der Morgenstelle 18,  
72076 Tübingen, Germany*

[volker.schurig@uni-tuebingen.de](mailto:volker.schurig@uni-tuebingen.de)

The historic development of the concept chirality and its importance in natural sciences is described. The principle of the separation of enantiomers by chiral chromatography is outlined.

**KEYWORDS:** Chirality, homochiral, heterochiral, enantiomers, chiral stationary phase, enantioselective chromatography

In the treatise „*Prolegomena zu einer jeden künftigen Metaphysik, die als Wissenschaft wird auftreten können*“, [1] the Prussian philosopher Immanuel Kant (1724-1804) adopted the phenomenon of handedness in his arguments about ‘incongruent counterparts’ in the context of a debate between philosophers on the nature of space (Fig. 1, translated): „what can be more similar and in every part

more alike to my hand or to my ear, than their images in the mirror? And yet I cannot put such a hand as is seen in the mirror in the place of its original; for if this is a right hand, that in the mirror is a left one ... (they cannot be made congruent); the glove of one hand cannot be employed for the other”.

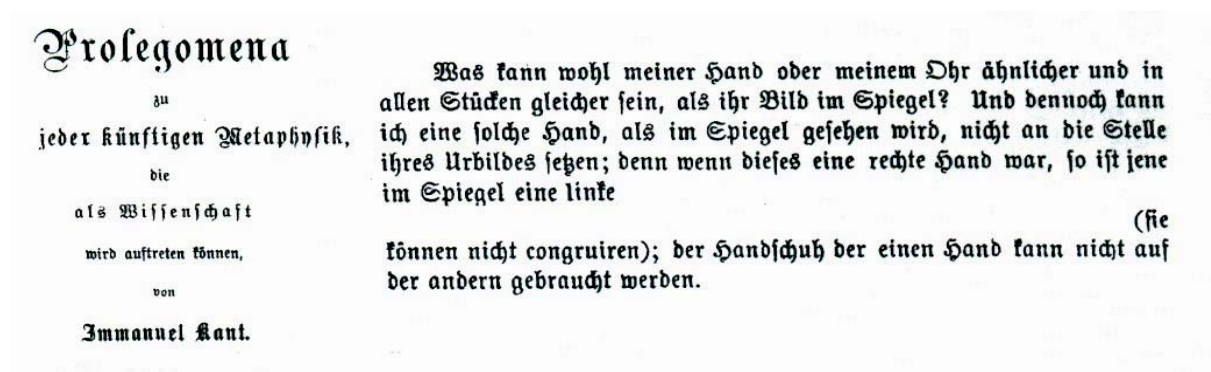


Figure 1: Title and prose of the *Prolegomena* of Immanuel Kant (1783).

Kant went on to mention "widersinnig gewundene Schnecken (absurdly twisted snails)" as another vivid

example of "incongruent things" (Fig. 2).[1]



Figure 2: Escargots forming incongruent mirror images. Left specimen: very rare; right specimen: common.

As proposed by Sir William Thomson (Lord Kelvin), the property of nonsuperimposability (incongruence) of an object on its mirror image is called *chirality* referring to handedness (from Greek: *kheir* = hand). Lord Kelvin states: "I call any geometrical figure, or group, of points, *chiral*, and say that it has chirality, if its image in a plane mirror cannot be brought to coincide with itself. Two equal and similar right hands are homochirally similar. Equal and

similar right and left hands are heterochirally similar ... "[2] Mislow inferred that the meaning of "similar" in this context is synonymous with "congruent". [3] The definition of chirality by Lord Kelvin implies that two right hands (or two left hands) represent a *homochiral* pair, whereas a right and a left hand resemble a *heterochiral* pair (Fig. 3).



A homochiral pair

A heterochiral pair

Figure 3: Homochiral and heterochiral assemblies of hands. The homochiral combination is required to shake hands and the heterochiral combination is involved to clasp one's hands.

The terms homo- and heterochiral apply also to helical objects as exemplified for double helices.[4] The depicted artefacts (Fig. 4) from the eternal town of Rome are intriguing as the heterochiral array represents a perfect *meso*-assembly (part and counterpart are related by

reflection) whereas no symmetry plane exists in the homochiral arrangement. It may be noted that the main motif, carved into marble, possesses the same helical twist as the DNA double helix elucidated by Watson and Crick in 1953. [5]



Figure 4: Homochiral (left) and heterochiral (right) double-twisted columns. Provenance: St-Paul-outside-the-fields, Rome, Italy (1222-30).

Vladimir Prelog extended the definition of chirality as defined for macroscopic objects to the realm of microscopic objects such as molecules prevailing in stereochemistry. In his Nobel Prize Lecture, he provided the following definition: [6] “An object is chiral if it cannot be brought into congruence with its mirror image by translation and rotation. Such objects are devoid of symmetry elements which include reflection: mirror planes, inversion centers, or improper rotational axes.” This definition applies to objects and symmetry operations in the three-dimensional space. It should be noted that an object  $A-B / B-A$  is chiral in a one-dimensional world (*lineland*). Yet the counterparts can be brought into congruence in the two-dimensional space by rotation. A scalene triangle is chiral in the two dimensional world (*flatland*) and the counterparts (which can be differentiated by a clockwise or anticlockwise configuration of ABC) can be superimposed in the three-dimensional space by rotation. Kant already anticipated geometries in space of

higher dimensionality and hence his incongruent hands in the three-dimensional world (*spaceland*) are rendered congruent in the four-dimensional space. [7] According to August F. Möbius (1827) incongruent images obtained by reflection in  $n$ -dimensional space are congruent by rotation in an  $(n+1)$ th dimension. [7]

The early nineteenth century witnessed the origins of stereochemistry which arose from optics and mineralogy. Following the discovery of plane-polarized light by Malus (1809), the phenomenon of optical rotation was discovered by Arago (1811) in quartz crystals and by Biot (1815) in liquids (turpentine), in solutions of solids (camphor, sucrose, tartaric acid) and in gases. [8] Sir John Herschel’s observation (1822) [9,10] that a causal relationship exists between the sense of hemihedrism (then called *plagiëdrism* according to the mineralogist Haüy) of quartz crystals and the (positive or negative) sign of the optical rotation of plane-polarized light paved the way to Louis Pasteur’s momentous discovery (1848) that

hemihedry and optical rotation are also correlated in ammonium sodium tartrate crystals.[11,12] Hemihedrism implies that certain facets of the crystal produce

nonsuperimposable species which are related as incongruent object and mirror image (Fig. 5).

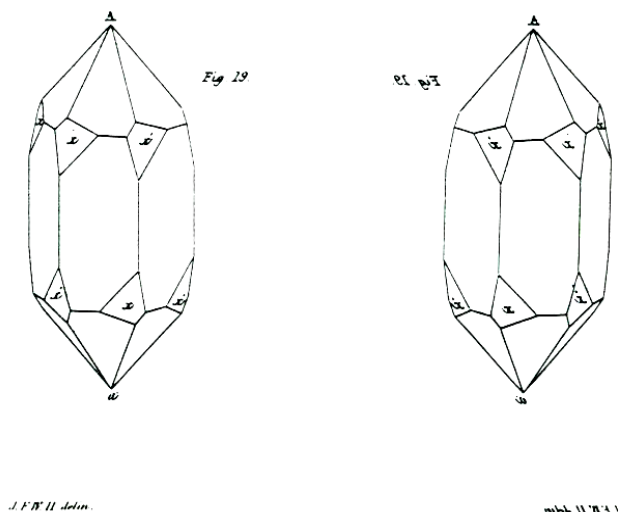


Figure 5: Hemihedrism of quartz crystals (left: original drawing by John Herschel (*J.F.W. delin*) as Fig. 19 in Ref. 9, right: constructed mirror image). [10]

In 1860 Pasteur drew a far-reaching analogy between enantiomorphous crystals (Greek: *enantios* = opposite and *morphe* = form, this term was introduced by Naumann in 1856[13]) and enantiomeric molecules in solution (Greek: *enantios* = opposite and *meros* = sharing part). According to Pasteur, both solid state crystals and molecules in solution rotate plane-polarized light due to dissymmetry.

Pasteur's insight that the optical activity of tartaric acid in solution is a manifestation of "dissymétrie moléculaire", [14] marks the beginning of stereochemistry. Moreover, Pasteur was convinced that molecular dissymmetry represents one of the most fundamental signatures of life ("dissymmetry, this is life") and he continued to assert his belief in the cosmic (physical) origin of molecular dissymmetry.[15] Pasteur separated the enantiomers of a 1:1 mixture of tartaric acid (known as the racemate or racemic mixture) by three independent methods: (i) crystallization of a conglomerate formed by ammonium sodium tartrate and separating the

enantiomorphous crystals with tweezers, (ii) kinetic resolution via enzymatic transformation (e.g., by *Penicillium glaucum*) and (iii) transformation to diastereomeric salts using an optically active auxiliary compound (see Chapter 7 in Ref. [8]).

Thus, save for chromatographic resolution (chromatography had not yet been invented), Pasteur discovered all principles of enantioseparation which are still extensively used today. Pasteur, however, failed to interpret his enormous insights in line with the emerging valence and molecular structure theory of Kekulé and contemporaries. [7] In fact, Pasteur was not aware of the chemical constitution of tartaric acid and he did not relate dissymmetry to a single molecule.

The unequivocal criterion for optical activity is chirality and a chiral molecule always exists as a pair of incongruent enantiomers. Based on those stereochemical perceptions, the *tetrahedral configuration* of the stereogenic carbon atom linked to four different ligands (e.g., in lactic acid)

was independently deduced by Van't Hoff in Utrecht (1874) [16] and by Le Bel in Paris (1874). [17] These two scientists thereby paved the way to modern stereochemistry.

The phenomenon of chirality is of eminent importance for the creation of life. Almost all building blocks of biopolymers, such as amino acids and sugars, are chiral and as a consequence they exhibit the phenomenon of mirror image incongruence. A unique signature of life is the enantioenrichment of chiral building blocks toward complete homochirality. Indeed, in all self-replicating systems (viruses, bacteria, plants, animals, humans) only one enantiomeric form is found in nature, *i.e.*, *L*-configured  $\alpha$ -amino acids and *D*-configured sugars (*L* = *levo* = left, *D* = *dextro* = right). The tetrahedral configuration of the simplest chiral  $\alpha$ -amino acid alanine,

forming a pair of incongruent enantiomers according to Van't Hoff and Le Bel, is depicted in Figure 6. This educational slide (presented in German) misses its didactic objective in that it could be understood that *L*-alanine resides in the left hand, while *D*-alanine is present in the right hand. Of course, both human hands are only comprised of *L*-amino acids. Therefore, the right and left hands in the understanding of Kant (*vide supra*) represent *apparent* enantiomers only at a macroscopic scale. At the molecular level, the dissymmetric building blocks of the hands are homochiral. In this respect it is intriguing to note that strictly homochiral building blocks can nevertheless be employed by nature to create right and left handed forms of shells, *e.g.*, the enantiomeric snails depicted in Figure 2.

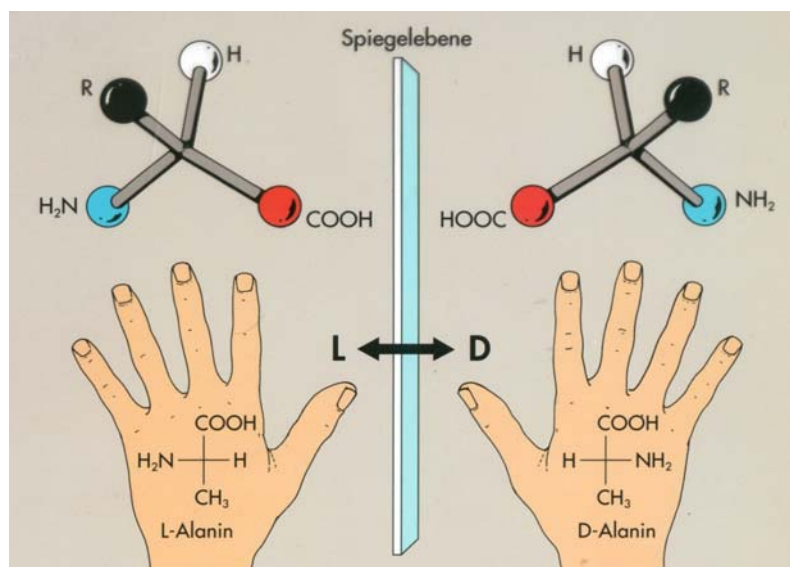


Figure 6: The simplest chiral  $\alpha$ -amino acid alanine. Top: tetrahedral configuration ( $R = CH_3$ ), Bottom: *Fischer projection* with the amino group on the left side (= *L*) and the amino group on the right side (= *D*) (Source: Fonds der chemischen Industrie, Germany).

Even on the verge of the third millennium, two basic questions are still not answered: (i) how was homochirality

created on prebiotic Earth and (ii) why were *L*-amino acids and *D*-sugars selected, *i.e.*, no mirror image life exists on

Earth composed of energetically equivalent (ignoring quantum mechanical effects, *vide infra*) *D*-amino acids and *L*-sugars. The genesis of homochirality on primordial Earth is still a "mystery.[18]" Enantiomeric bias may have occurred on Earth itself or may have its origin from space. Therefore a space craft is now on the way to a comet in the solar system to probe, *inter alia*, extraterrestrial homochirality. [19] The requirement of homochirality in

overcoming undesired structural complexity becomes immediately obvious when the formation of small peptides from chiral amino acids is considered (Fig. 7). The number of stereoisomers of an *n*-mer peptide obtained from *n* racemic amino acids is  $2^n$ . However, just one stereoisomeric *n*-mer peptide is formed when only homochiral *L*-amino acids are employed for peptide synthesis.

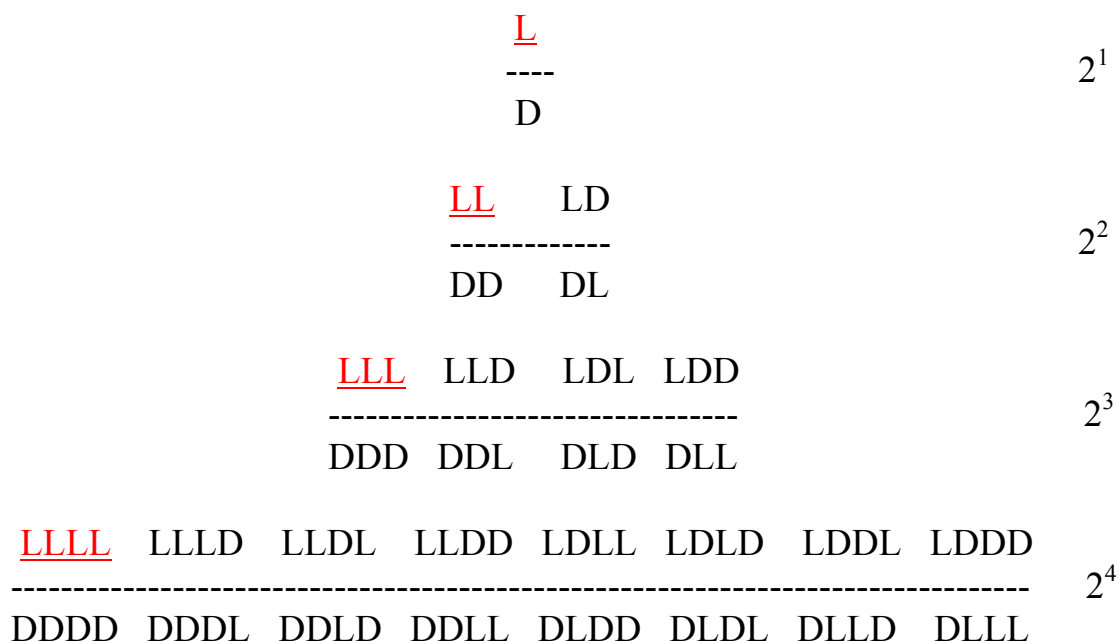


Figure 7: Stereochemical complexity of peptide formation from racemic *D,L*-amino acids. Only a single *all-L*-peptide (in red) is formed from homochiral *L*-α-amino acids.

Enantiomers are often referred to as having identical physical and chemical properties (with the exception of their chiroptics, i.e., optical rotation and circular dichroism). This statement is correct only when enantiomers are present in a strictly achiral (symmetric) environment which does not exist on Earth. In a chiral environment, enantiomers may be discriminated in the

same way as Kant argued that the right hand *D* and the left hand *L* are differentiated by a right hand glove *D'*. This is due to the diastereomeric relationship between *DD'* and *LD'*. The enantiomers of flavour and fragrance molecules may indeed invoke different olfactory sensations (Fig. 8). [20]



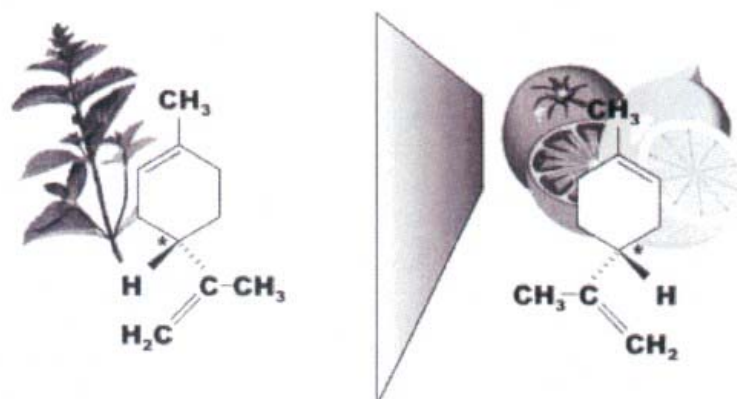


Figure 8: Configurational formulae of *R*- and *S*-limonene [20].

For example dextrorotatory *R*-limonene elicits a citrus (lemon-orange) scent while levorotatory *S*-limonene has a turpentine-like (mint) odour. In citrus fruits only the *R*-form is found [21] (*R* = *rectus* = right, *S* = *sinister* = left, according the Cahn-Ingold-Prelog (CIP) nomenclature [22]). Indeed, the impression gained when smelling a fragrant substance depends on its handedness because our receptors are chiral and one-handed. This principle holds true for all kinds of biogenic substrate-receptor, selectand-

selector, donor-acceptor, host-guest or antigen-antibody interactions and applies also to chiral pharmaceuticals [23].

Very often only one enantiomer (the *eutomer*) displays the desired pharmacological effect while the other enantiomer (the *distomer*) may be inefficient or even toxic. The three-point rule which can be considered as a simplified model of the *lock-and-key concept* of enzyme specificity advanced by Emil Fischer (1894), offers a self-explanatory rationale for the enantiomeric discrimination between a chiral substrate and a chiral receptor (Fig. 9).

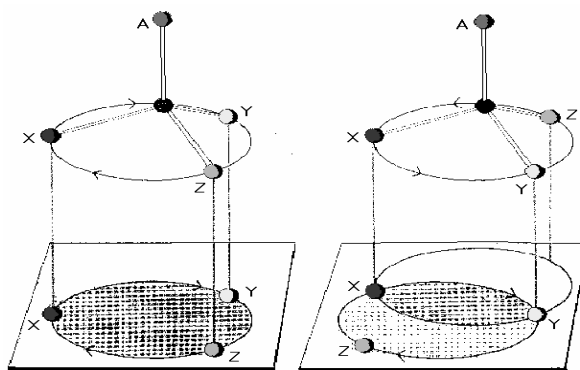


Figure 9: Three-point attachment (left) and two-point attachment (right) of oppositely-configured enantiomers with a planar receptor with only one accessible site (Source: Natta, Giulio & Farina, Mario: Struktur und Verhalten von Molekülen im Raum, Verlag Chemie, Weinheim, Germany)

Legislation authorities are wary on the role of chirality in drug use as a consequence of the tragic events involving the sedative drug  $\alpha$ -(*N*-phthalimido)glutarimide) (thalidomide = Contergan produced by Grünenthal, Germany). The drug was prescribed to pregnant women who experienced morning sickness and anxieties.

Unfortunately, it caused severe birth defects in new-born children. Thalidomide exists as an equal mixture

of *S*-(-)- and *R*-(+)-enantiomers (Fig. 10). It was marketed as the 1:1 racemic mixture. Experiments with rodents indicated that the sedating and anti-nausea effects reside in the *R*-(+)-eutomer, whereas the *S*-(-)-distomer harbours the undesired teratogenic effects on the foetus.

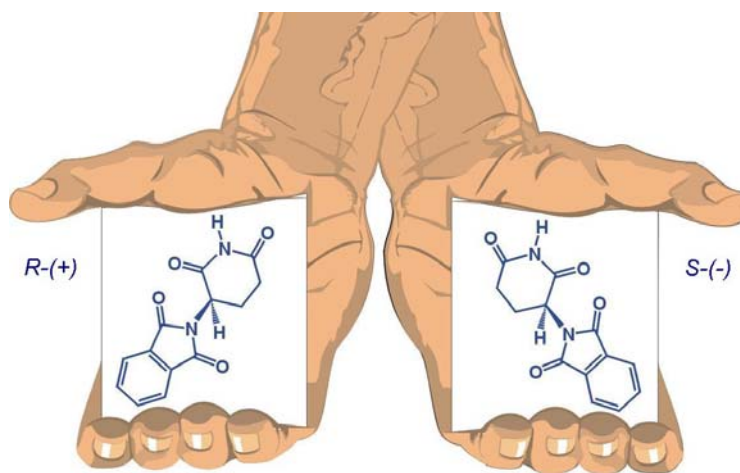


Figure 10: The enantiomers of thalidomide (Contergan).

Nowadays legislation authorities require from pharmaceutical companies that they supply only the active eutomer, and not the racemic mixture containing 50% inactive or even toxic ballast. However, the chemical synthesis of a chiral drug in an achiral environment furnishes only the racemic mixture. The access to single enantiomers (‘racemic switch’) is cumbersome and expensive and amounts to estimated 250 billion US \$ production costs annually. Incidentally, the case of thalidomide may give rise to a serious misconception. The stereogenic carbon atom of thalidomide in the glutarimide ring is configurationally *labile* due to hydrogen tautomerism. Therefore thalidomide enantiomerizes in the liver, i.e., the right-handed molecule is inverted to the left-handed molecule (and *vice versa*). The half life of a single

enantiomer is only 5 - 6 hrs at 35°C and pH 8. [24] Therefore the assertion that the thalidomide disaster might have been avoided if only the *R*-eutomer had been administered to humans is invalid since the eutomer is interconverted far too quickly to the undesired distomer by *in vivo* enantiomerization. Nevertheless in most cases enantiomeric drugs are configurationally stable and the ‘racemic switch’ is fully justified and requested by legislative authorities such as the FDA. [25]

To prove that a drug is indeed enantiomerically pure, modern analytical methods for the determination of enantiomeric compositions are utilized such as chiroptical methods, enantioselective NMR-spectroscopy and enantioselective chromatography. [26] Enantiomeric analyses are also important in many other fields (Fig. 11).

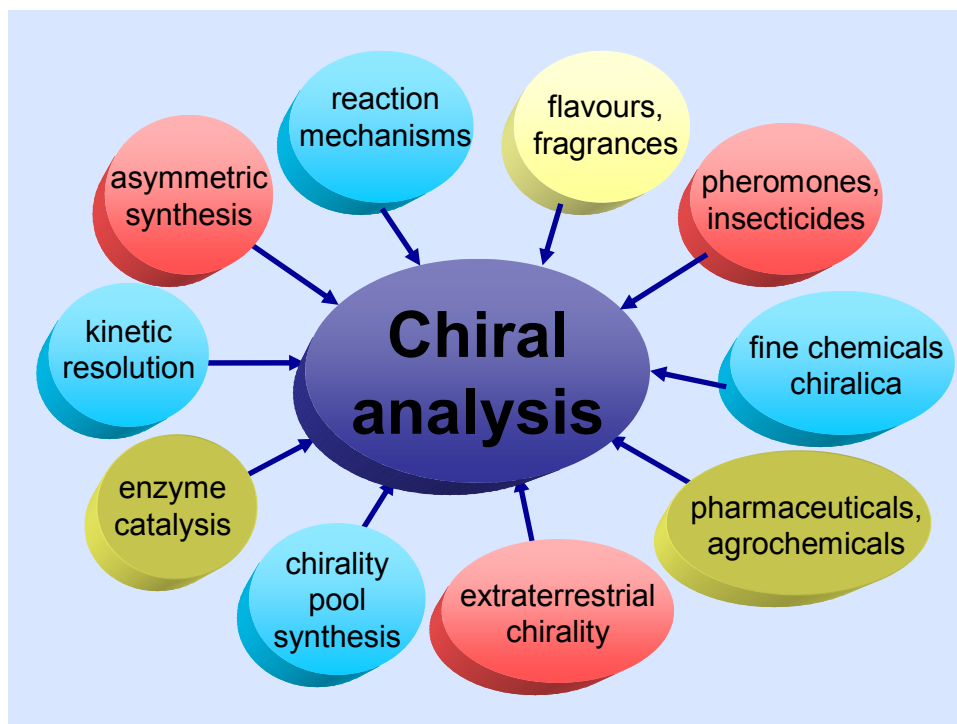


Figure 11: Enantiomeric analyses as required in many different fields of research and applications.

In analogy to Kant, who distinguished a right hand from a left hand by a right-handed glove, the enantiomers *D* and *L* can be distinguished in the chiral environment of an enantiomerically pure chiral auxiliary agent or chiral solvent *D'*. An enantiomeric discrimination arises when the single enantiomer of the chiral auxiliary interacts reversibly (or irreversibly) with the two enantiomers of the chiral substrate to produce the distinct diastereomeric associates (*DD'* and *LD'*). Diastereomers possess different physical and spectroscopic properties and can thus be distinguished in an achiral environment. One important technique for the separation of enantiomers is *chromatography*. Chromatography (from Greek: *chroma* = colour and

*graphein* = writing) was discovered by Michael Zswett (1903). [27] In fact, Zswett in Russian means colour.

Chromatography is based on the distribution of an analyte between two phases in a tube called column: one phase is stationary while the other phase is mobile. For the separation of enantiomers, either diastereomers are preformed and separated on an *achiral* stationary phase (indirect method) or diastereomeric associates are formed within the column in the presence of a *chiral* stationary phase (CSP) (direct method). For the separation of enantiomers by the latter method, again the principle of Kant can be adapted (Fig. 12).

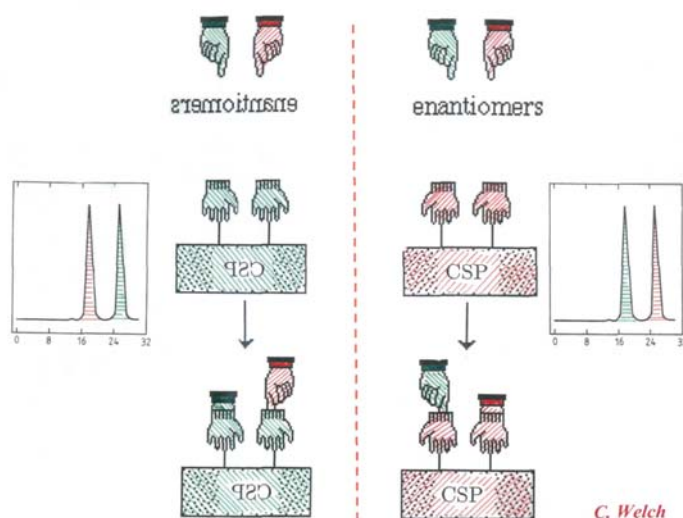


Figure 12: Scheme of the chromatographic separation of enantiomers on a chiral stationary phase (CSP) according to Christopher Welch, Merck Inc., USA.

The right-handed chiral stationary phase distinguishes the right- and left-handed molecules in the same way that a right hand fits in a right-handed glove and it is retarded as compared to the left hand which leaves the column first (right side of Fig. 12). When the chirality of the system is switched (left side of Fig. 12) and a left-handed chiral stationary phase is employed, peak inversion occurs and the left-handed molecule is now eluted second. The translation of the description (Fig. 12) into real practice has been very difficult but it is now solved satisfactorily. The first practical example of the resolution of a racemate by chiral chromatography, a method which was not yet available to Pasteur (*vide supra*), constitutes the partial enantioseparation of Tröger's base (Fig. 13) by liquid chromatography on the CSP *D*-lactose hydrate by Prelog

and Wieland (1944). [28] The first direct separation of  $\alpha$ -amino acid derivatives on CSPs comprising of  $\alpha$ -amino acid selectors by gas chromatography was described by Gil-Av et al. (1966). [29] This was the starting point of an enormous development utilizing also dipeptides, chiral metal complexes and modified cyclodextrin as CSPs in enantioselective gas chromatography. These developments will be reviewed in a subsequent account.



Figure 13: The enantiomers of Tröger's base. This compound contains two stereogenic nitrogen atoms which are stable toward molecular inversion through a rigid bicyclic structure of the molecule[28].

#### Cited References:

- [1] Kant, I., Prolegomena zu einer jeden künftigen Metaphysik die als Wissenschaft wird auftreten können, 1783 (English translation: <http://philosophy.eserver.org/kant-prolegomena.txt> (cf. first part, section 13).
- [2] Kelvin, W.T., Baltimore Lectures on Molecular Dynamics and the Wave Theory of Light, C. J. Clay: London, 1904, 602-642.
- [3] Mislow, K., *Croatia Chemica Acta*, 1996, *69*, 485-511.
- [4] Schurig, V., *Enantiomer*, 1996, *1*, 147-149.
- [5] Watson, J.D., Crick, F.H.C., *Nature*, 1953, *171*, 737.
- [6] Prelog, V., *Science*, 1976, *193*, 17-23.
- [7] Cintas, P., *Angew. Chem. Int. Ed.*, 2007, *46*, 4016-4024.
- [8] Eliel, E.L.; Wilen, S.H., *Stereochemistry of Organic Compounds*; Wiley: New York, 1994, 2-6.
- [9] Herschel, J.F.W., *Cambridge Philos. Soc. Trans. I*, 1822, 43-52.
- [10] Schurig, V., *Enantiomer*, 1997, *2*, 135-142.
- [11] Pasteur, L., *Compt. Rend. Acad. Sci.*, 1848, *26*, 535 & *Ann. Chim. Phys.*, 1948, *24*, 442-459.
- [12] Kauffman, G.B., Bernal, I., Schütt, H.-W., *Enantiomer*, 1999, *4*, 33-45.
- [13] Gal, J., *Chirality*, 2007, *19*, 89-98.
- [14] Pasteur, L., *De La Dissymétrie Moléculaire*, in: *Leçons de Chimie Professées en 1860*, Lib. Hachette: Paris, 1861, 1-48.
- [15] Pasteur, L., *La Dissymétrie Moléculaire*, *Revue Scientifique*, 1884, *13*, 2-6.
- [16] Van't Hoff, J.H., *La Chimie dans L'Espace*, Bazendijk: Rotterdam, The Netherlands, 1875, 13-14.
- [17] Le Bel, J.A., *Bull. Soc. Chim. Fr.*, 1874, [2], 22, 337.
- [18] Wagnière, G. H., *On Chirality and the Universal Asymmetry. Reflections on Image and Mirror Image*. Wiley-VCH, Weinheim, Germany, 2007.
- [19] Goesmann, F., Rosenbauer, H., Roll, R., Böhnhardt, H., *Astrobiology* 2005, *5*, 622-631.
- [20] Fietzek, C., Hermle, T., Rosenstiel, W., Schurig, V., *Fresenius J. Anal. Chem.* 2001, *371*, 58-63.
- [21] Schurig, V., Schleimer, M., Jung, M., Mayer, S., Glausch, A., in: *Progress in Flavour Precursor Studies* (Schreier, P., Winterhalter, P., eds.), Allured Publishing Corporation, Carol Stream, USA, 1993, 63-75.
- [22] Cahn, R.S., Ingold, C.K., Prelog, V., *Angew. Chem. Int. Ed.*, 1966, *5*, 385-415.
- [23] The impact of stereochemistry on drug development and use (Aboul-Enein, H.Y., Wainer, I. W., eds.), Vol. 142 in the Series on Chemical Analysis, John Wiley, New York, 1997.
- [24] Schoetz, G., Trapp, O., Schurig, V., *Electrophoresis*, 2001, *22*, 3185-3190.
- [25] De Camp, W. H., *Chirality*, 1989, *1*, 2-6.
- [26] Schurig, V., Lindner W., in: Houben-Weyl 'Methods of Organic Chemistry', Volume E21a (Stereoselective Synthesis), Thieme, Stuttgart, 1995, Chapter A.3.1., 147-224.

- [27] Senchenkova, E. M., Michael Tswett, the Creator of Chromatography, Russian Academy of Sciences, Scientific Council on Adsorption and Chromatography, Moscow, 2003.
- [28] Prelog, V., Wieland P., *Helv. Chim. Acta* 1944, 27, 1127-1134.
- [29] Gil-Av, E., Feibush, B., Charles-Sigler, R., *Tetrahedr. Lett.*, 1966, 1009-1015.

## Determination of Essential Elements in Milk and Urine of Camel And in *Nigella sativa* Seeds

Amirah S. Al-Attas

Department of Analytical Chemistry, Girls College of Education, Kingdom of Saudi Arabia,  
P.O.Box :16531, Jeddah: 21474

E-mail : [amirh-alattas@hotmail.com](mailto:amirh-alattas@hotmail.com)

### Abstract

Studies on milk and urine of camel and *Nigella sativa* seeds , whether with respect to concentration or bioavailability of major and trace essential elements from these milk, urine and *Nigella sativa* are limited and warrant further investigation . The objective of this study was to determine the concentration of minerals in milk and urine of camel as well as in *Nigella sativa* using neutron activation analysis .

Camel milk and urine have higher concentration of Na than *Nigella sativa* seeds, but K concentration in camel urine & *Nigella sativa* are higher than that of milk. The Ca and Mg concentrations in *Nigella sativa* are higher than that in milk and urine . Higher concentrations of iron and Zn are found in *Nigella sativa* . The concentration of Co and Cr in urine and in *Nigella sativa* are higher than in camel milk . The Se content was found only in camel's urine by this method . *Nigella sativa* seed contains more trace elements such as Sr, Al, Rb, Ba, and La.

**Keywords:** Essential Elements; Camel Milk; Camel Urine ; *Nigella sativa* neutron Activation Analysis.

### 1. Introduction

Camel milk is different from other ruminant milk; having low cholesterol, low sugar, high minerals (sodium, potassium, iron, copper, zinc and magnesium), high vitamin C, B<sub>2</sub>, A and E, low protein and high concentrations of insulin [1 , 2]. It has no allergic properties, and it can be consumed by lactase deficient persons and those with weak immune systems.

The milk is considered to have medicinal properties. In Sahara, fresh butter is often used as a base for medicines. The products developed also include cosmetics or pharmaceuticals [3]. A series of metabolic and autoimmune diseases are successfully being treated with camel milk. In India, camel milk is used therapeutically

against dropsy, jaundice, problems of the spleen, tuberculosis, asthma, anemia, piles and diabetes [4]. Beneficial role of raw camel milk in chronic pulmonary tuberculosis patients has been observed [5]. In repeated trials, it was observed that there was 30-35 percent reduction in daily doses of insulin in patients of type 1 diabetes receiving raw camel milk [6-8]. It is mentioned in Islam online that Camel's milk and urine have medical effects, so Islam encourages and permits the drinking of camel milk, and camel urine is permitted in case of necessary medical treatment [9,10] .

The unique composition of camel milk has been proved to fortify the immunity system, where it has a heavy chain of amino acids which makes the camel milk so unique. Such immunity components have proved to be



effective in killing microbial agents both viral and bacterial, and in protecting the human body against various diseases as well as treating some types of cancer[11].

*Nigella sativa* (L.) is a herbaceous plant, which is a member of the *Ramunculacea* family. *Nigella* seeds (the black cumin) or their oils are used by many people for many medical purposes. Nowadays, many reports have been written indicating the significant role of *Nigella* seed oil in increasing immunity and maintaining good health [12].

In the present work it is proposed to determine concentrations of essential elements in milk and urine of camel and in *Nigella sativa* seeds using neutron activation analysis.

## 2. Experimental

### Materials and Methods

Milk and urine of camel samples were collected from young camels in the morning before provender breakfast( food stuff and desert plants) at the autumn . Samples were collected from four representative animals in the same time , and composite samples were taken for analysis. 500 ml of samples were collected in white clean polyethylene bottles, previously washed with dil. nitric acid and de-ionized water. The samples were dried at 100°C till constant weight.

Al-Qaseem *Nigella sativa* seeds (the black cumin) were collected from Makkah. It was taken to determine the elements concentrations without any further treatment.

0.3 g dried samples was taken and irradiated with a biological reference material (i.e. Hay Powder) (IAEA – V-10), the samples and the reference material were irradiated in clean polyethylene vials short irradiation (4min) with neutron flux  $10^{11}$  n/cm<sup>2</sup>.s and a long irradiation (4h) in neutron flux  $10^3$  n/cm<sup>2</sup>.s.

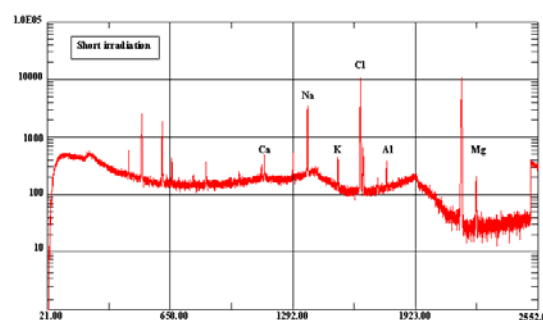
The gamma-ray measurements of irradiated samples as well as the standard were carried out by a hyper pure germanium (HPGe) gamma spectrometer (ORTEC). The type of detector: Ortec Coaxial HPGe , model: GEM-100210-P-Plus, Serial No.: 36-0611A, Relative Efficiency: 100%; Resolution: 2.4, Calibration source :point source at 7 cm

The accuracy and precision of the results have been checked by analyzing five replicates of the sample and standard reference material. Measurements were performed at nuclear research center – EAEA (Egyptian Atomic Energy Authority) –Egypt.

## 3. Results and Discussion

Essential Elements are those if removed from diet results inconsistent and reproducible impairment of physiological function [13]. The deficiency of these element results from a combination of poor availability and low intake [14].

The samples of camel urine, milk and *Nigella sativa* seeds were irradiated and the gamma spectra of irradiated samples are shown in Figs.(1- 3).



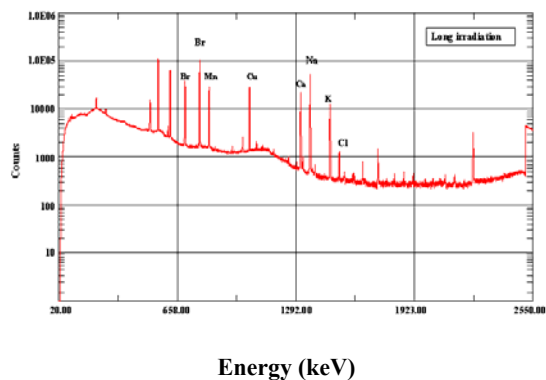


Fig.(1):  $\gamma$ -spectra of irradiated Camel Milk

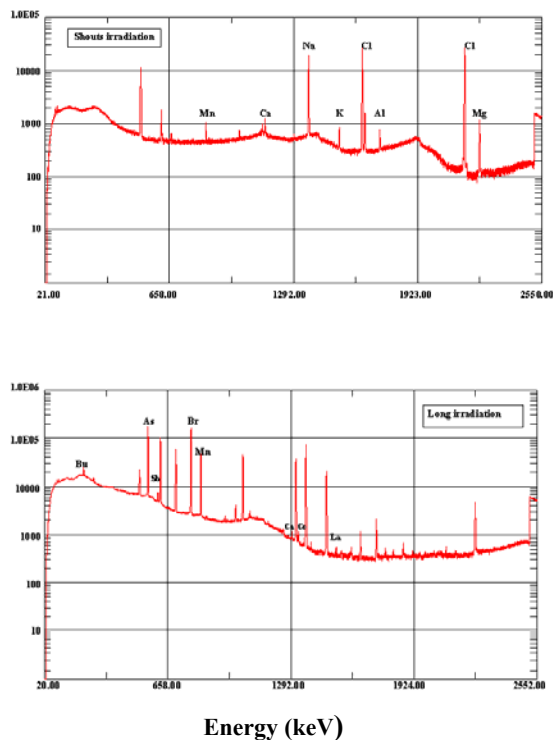


Fig.(2):  $\gamma$ -spectra of irradiated Camel Urine

The results of major elements concentration in addition to the standard deviation in the samples are shown in Table (1). From the table, it is clear that the camel urine has high level of K (7740 ppm) and Na (8478 ppm). Therefore, it could be considered a good source of K and Na which are

known as the principle cation in the extra and intra cellular fluid, respectively. They regulate nerve and muscle function[14].

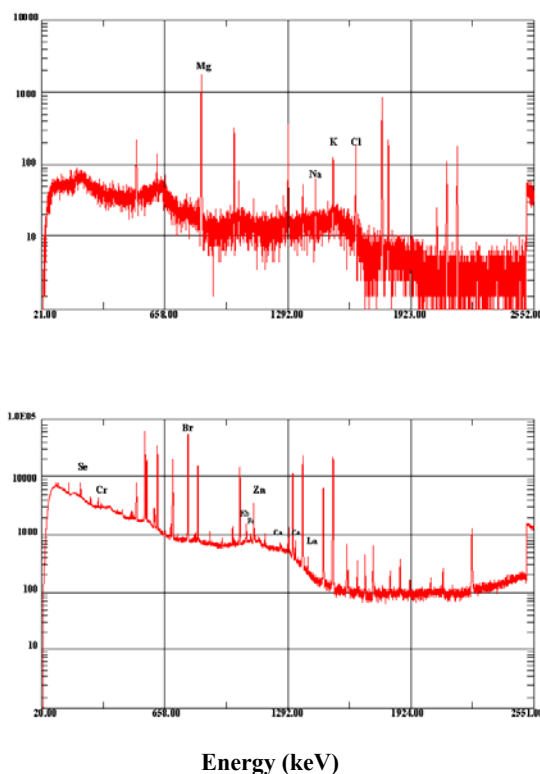


Fig.(3):  $\gamma$ -spectra of irradiated *Nigella sativa* seeds.

Table (1) Also, it can be seen in that *Nigella sativa* seeds have higher concentration of Mg. It is considered as a good source of Ca which plays a good role in the constituent of bone and teeth. It is also important in the hydrolysis and energy storage reaction of phosphate derivatives, and play an important role in enzymatic reaction catalyzed by certain kinase [15].

The highest Ca concentration was found in *Nigella sativa* seeds 4387  $\mu\text{g/g}$  while urine's camel shows the lowest one. *Nigella sativa* seeds and camel milk are good source of Ca which besides its constituent of bone and teeth, it plays a major regulatory role in numerous biochemical and physiological processes, it is involves in oxidative

phosphorylation, blood clotting, muscle contraction, cell division, transmission of nerve impulses, enzyme activity, cell membrane function and hormone secretion [14].

**Table (1) Shows some of major elements in ppm in camel milk, urine and in *Nigella sativa* seeds, with the mean values  $\pm$  S.D.**

Element	Milk	Urine	<i>Nigella sativa</i> seeds
Na	287 $\pm$ 11	8478 $\pm$ 323	39 $\pm$ 7
K	1004 $\pm$ 152	7740 $\pm$ 118	5379 $\pm$ 111
Mg	25 $\pm$ 9	476 $\pm$ 101	2294 $\pm$ 230
Ca	789 $\pm$ 35	204 $\pm$ 16	4387 $\pm$ 152
Cl	1204 $\pm$ 58	3871 $\pm$ 180	236 $\pm$ 16
Br	153 $\pm$ 12	9.25 $\pm$ 1.8	7.19 $\pm$ 0.89

On the other hand, the results show that the level of Al concentration was found to be 43.22 ppm in *Nigella sativa* seeds and 0.731 ppm in camel's milk (Table 1).

The presence of chlorine with high concentration in urine, milk and *Nigella sativa* seeds indicate that most of Na and K are present in chloride form. The bromine presents at high concentration in camel's milk and amounted to 153 ppm while urine and *Nigella sativa* show lower concentration. 9.25 and 7.19 ppm, respectively. The level of trace elements in ppm in camel milk and urine and in *Nigella sativa* are presented in (Table 2). Zinc enters in many physiological functions such as taste sensation, metabolism of skin, reproductive process, bone formation, wound healing, brain function and metabolism of carbohydrate, protein and nucleic acid. It enters in many metallo enzymes [13].

Regarding to Zn the highest concentration of this element were recorded in *Nigella sativa* seeds (42.27 ppm) and the lowest concentration was observed in milk and urine of camel. The concentration of Zn in milk and urine in this results are low comparing with the reported values in Saudi Arabia 4.79 & 6.4 ppm for milk and urine

respectively [16] and in Kuwait 4.9 ppm for milk [17]. This may be due to the independency of Zn concentration from the kind of diet food and desert plants. Also, it can be seen from Table (2) that it is clear that the concentration of Fe is higher in *Nigella sativa*. Therefore it is considered a good source of Fe, which plays many key roles in biological systems, including oxygen transport and storage, adenosine triphosphate (ATP) generation, DNA synthesis and chlorophyll synthesis [14].

*Nigella sativa* seeds contain moderate concentration of Mn (6.04 ppm) which plays an essential role in cellular metabolism where a number of enzymes require the presence of this element for their function. These include enzymes for the synthesis of mucopolysaccharides, for protein and energy metabolism and for cell protection from free radical damage [21].

It is noted from Table (2) that the concentration of Cr ranged between 0.008 to 0.324 ppm in camel's milk and urine respectively and 0.18 ppm in *Nigella sativa* seeds.

**Table (2) Shows some of trace elements in ppm in camel milk, urine and in *Nigella sativa* seeds, with the mean values  $\pm$  S.D.**

Element	Milk	Urine	<i>Nigella sativa</i> Seeds
Fe	2.152 $\pm$ 0.428	8.045 $\pm$ 3.24	77.460 $\pm$ 4.102
Mn	0.097 $\pm$ 0.002	ND	6.040 $\pm$ 0.390
Zn	1.516 $\pm$ 0.067	2.319 $\pm$ 0.259	42.270 $\pm$ 2.48
Cr	0.008 $\pm$ 0.003	0.324 $\pm$ 0.162	0.180 $\pm$ 0.048
Sr	ND	ND	52.010 $\pm$ 7.830
Al	0.731 $\pm$ 0.225	ND	43.220 $\pm$ 15.660
Sc	0.0003 $\pm$ 0.00008	ND	0.0111 $\pm$ 0.002
Rb	0.290 $\pm$ 0.021	5.255 $\pm$ 0.649	8.038 $\pm$ 0.405
Ba	ND	ND	11.074 $\pm$ 2.797
Se	ND	0.348 $\pm$ 0.057	---
Co	0.0015 $\pm$ 0.0005	0.227 $\pm$ 0.004	0.057 $\pm$ 0.007
Sb	ND	ND	0.038 $\pm$ 0.002
La	ND	ND	0.0379 $\pm$ 0.006

ND : Not Detected

In individuals who have low levels of chromium, symptoms of hyperglycemia or abnormal lipid levels may be corrected by providing supplementation designed to normalize chromium status[22 , 23].

Cobalt also like Zn, Mn, Fe & Cr which are now termed as essential trace metals present in *Nigella sativa* seeds with amount of 0.057  $\mu$ g/g, and in urine and milk are found with amount of 0.227 & 0.0015 ppm, respectively.

Selenium does function as an antioxidant and individuals may take supplements to enhance immune function or increase antioxidant activity [24]. The concentration of Se in milk's camel and in *Nigella sativa* seeds was not detected by this method. But urine's camel was found to contain a concentration of 0.384 ppm. On the

other hand, other studies in Kuwait proved that camel's milk contains Se[17].

The order of abundance of the studied metals follows the following sequence:

In *Nigella sativa* seeds: K > Ca > Mg > Fe > Sr > Al > Zn > Na > Ba > Rb > Mn > Cr > Co > Sb > La > Sc.

In camel's milk : K > Ca > Na > Mg > Fe > Zn > Al > Rb > Mn > Cr > Sc > Co.

In camel's Urine : Na > K > Mg > Ca > Fe > Rb > Zn > Cr > Se > Cr > Co.

### 3. Conclusion

*Nigella sativa* seeds contain most of elements needed and repair any damage in the biological cell. This confirm with

Hadeeth of the profit Mohamed that Black seed (*Nigella sativa* seeds) cure from all diseases except the death. Other Hadeeth said that : Camel urine is used as a medicine incase of diarrhea. This can be ascribed to the fact that it contains large amount of Na & K substituting the loss of such elements in case of diarrhea .Also it contains large amount of Zn which assists in cure the infection due to diarrhea.

### References

- [1] K. H. Knoess, IFS Symposium, Sudan; 201 (1979).
- [2] Z. Farah, R. Rettenmaier and D. Atkins; Intemat. J. Vit. Nutr. Res., 62, 30 (1992).
- [3] M. Gast, L. Mauboisj and J. Adda; Center Rech. Anthr. Prehist. Ethn. (1969).
- [4] M.B. Rao, R.C. Gupta and N.N. Dastur, Indian Journal of Dairy Science; 23, 71 (1970).
- [5] G. Mal, D.S. Sena, V.K. Jain M.S.Sahani; Livestock International, 4-8 (2001).
- [6] R. P. Agrawal, S.C. Swami , R. Beniwal, D. K. Kochar and R.P. Kothari; Int. J. of Diab. in Devel. Count., 22, 70 (2002).
- [7] R.P. Agrawal, S.C. Swami, D.K. Kochur and M.S. Sahani; Indian. J. of Animal Sci, 73 (10), 1105 (2003).
- [8] R.P. Agrawal, D.K. Kochar, M.S. Sahani, F.C. Tuteja and S.K. Ghorui; IN.T. J. Diab. Dev. Countries, 24 (2004).
- [9] Al Bukhari : The Prophet , Vol. 8 , Book 82 , No. 794.
- [10] Narrated Abu Huraira , Vol. 4, Book 54 , No. 537.
- [11] G. H. Gabry; Veterinary Medical Journal, Giza, 51 (1), 5 (2003).
- [12] O. A. R . Abu Zeid ; Zag. Vet. J. , 29 (1) 105 (2001).
- [13] E.J. Under and W. mertz; "Introduction in Trace Elements in Human and Animal Nutrition" , 5<sup>th</sup> ed., Academic Press , San Diego, USA, 1 (1987).
- [14] R.F. Owen; "Food Chemistry" , 3<sup>rd</sup> ed., Marcel Dekker Inc., New York, USA, 625 (1996).
- [15] K. Maureen, T.M. Michael, J.P. Martin and D.R. Kerry; Eds., "Metals in Biological Systems", Ellis Horwood London , UK, 64 (1992) .
- [16] N.S. Abu-Gabal, Bull of High Ins. of Publ. Health, 34 (2), 289 (2004).
- [17] F.M. Al-Awadi and T.S. Srikumar, Journal of Dairy Research, 68, 463 (2001).
- [18] A.R. Mceuen, "Manganese Metalloproteins and Manganese Activated Enzymes in Inorganic Biochemistry" Hill H.A.O.(Ed) Royal Society of Chemistry. Burtington House, London, UK, 249 (1981).
- [19] K.I. Young and P.N. Lee; International Studies on Cancer. Eur. J. Cancer Prev., 8, 91 (1999).
- [20] J.L. Burguera, M. Burguera, M. Galignani, O.M. Alarcon and J.A. Burguera; J. Trace Elementary Electrolytes Health Dis., 4, 73 (1990).
- [21] G.F. Combs , Jr. Clark L.C. and B.W. Turnbull, Biomed Environ. Sci. , 10, 227 (1997).

- -

.

.

.

.

.

.

**Determination of Indoleamine 2, 3- dioxygenase activity in tissues of Arabian Camel (*Camelus dromedarius*)**

**N. J. Siddiqi\* and A. S. Alhomida**

*Department of Biochemistry, College of Science, PO Box 2455, King Saud University, Riyadh – 11451, Saudi Arabia.*

**Abstract**

Indoleamine 2, 3-dioxygenase is a cytoplasmic, heme containing enzyme which catalyzes the oxidative cleavage of tryptophan. It catalyzes the initial and rate limiting step in the metabolism of L-tryptophan to kynurenine. Indoleamine 2, 3-dioxygenase is expressed in many tissues like lungs, intestine, placenta and stomach. In the present study various camel tissues including liver, kidneys, intestine, lungs and plasma were studied for the presence of indoleamine 2, 3-dioxygenase. Indoleamine 2, 3-dioxygenase activity was detected only in lungs and intestine. Lungs were found to have higher enzyme ( $18.00 \pm 2.45$  units protein  $\text{mg}^{-1}$ ) activity than intestine ( $12.08 \pm 3.412$  units protein  $\text{mg}^{-1}$ ). No enzyme activity was detected in liver, kidneys and plasma. This may be either due to the differences between species and therefore there is a need for more sensitive method to assay indoleamine 2, 3-dioxygenase in other camel tissues.

**Keywords:** Camel tissues, indoleamine 2, 3-dioxygenase, tryptophan.

---

\* Corresponding author; E-mail: [nikhat@ksu.edu.sa](mailto:nikhat@ksu.edu.sa) ; Fax +96614675791



## 1. Introduction

Indoleamine 2, 3-dioxygenase is a cytoplasmic, heme containing enzyme which catalyzes the oxidative cleavage of tryptophan (Trp). L- tryptophan is the least abundant of all essential amino acids. The major catabolic route of L – Trp is the kynurenine pathway that can ultimately lead to the biosynthesis of nicotamide adenine dinucleotide (NAD) [1] . The initial and the rate limiting reaction of kynurenine pathway is the oxidation of L – Trp to N-formyl-L-kynurenine, catalyzed by hepatic tryptophan 2, 3-dioxygenase (TDO EC 1.13.11.11) or the ubiquitous extra-hepatic, indoleamine 2, 3-dioxygenase (IDO or INDO, EC 1.13.11.17) [1] . Indoleamine 2, 3-dioxygenase is expressed in many tissues like lungs, intestine, placenta and stomach [2].

The functions of indoleamine 2, 3-dioxygenase include its role in protecting the foreign conceptus from maternal immune system, involvement in immunoregulation, regulation of tumor growth etc. [3]. Tryptophan is an indispensable constituent of all proteins. This amino acid represents a source for two main biochemical pathways viz., generation of 5-hydroxytryptamine (serotonin, a neurotransmitter and a vasoconstrictor is also degraded by Indoleamine 2, 3-dioxygenase) and Indoleamine 2, 3-dioxygenase catalyzed formation of kynurenines. Because of the crucial role of tryptophan catabolism in controlling the levels of such important regulatory molecules, indoleamine 2, 3-dioxygenase activity affects several pathological processes.

The Arabian camel (*Camelus dromedarius*) has adaptations to survive the hot and dry weather of the desert. It has remarkable ability to survive up to 20 days without food and water [4, 5]. Camels can tolerate high levels of blood glucose and urea and have the ability to adjust their body temperature with changes in the environmental temperature [5].

In the present study an attempt was made to standardize and determine the concentration of indoleamine 2, 3-dioxygenase in some tissues of the Arabian camels.

## 2. Experimental

### Materials and Methods

#### Chemicals

L-tryptophan, methylene blue, ascorbic acid, catalase, p-dimethylaminobenzaldehyde (Ehrlich's reagent), kynurenine, sodium hydroxide, potassium dihydrogen phosphate, trichloroacetic acid and bovine serum albumin were purchased from Sigma Chemical Company, St Louis, MO, USA. Glass distilled water was used throughout the study.

#### Sample Preparation

Camel tissues from animals (n=5) of same age (about 2-3 years) were bought from a local slaughter house. The tissues were dissected out, washed and frozen immediately in liquid nitrogen and stored at -80<sup>0</sup> C until processed. Tissues were homogenized in normal saline (10% W/V) using a stainless steel Omni-Mixer homogenizer (Omni International, Inc, Gainesville, VA, USA). The homogenate was centrifuged at 6000 rpm for 30 minutes and the supernatant was used for determination of IDO activity.

#### Measurement of Indoleamine 2, 3-dioxygenase activity

Indoleamine 2, 3-dioxygenase activity was measured using the method Kudo and Boyd, [6] with a slight modification. Briefly, to 0.4 ml of enzyme supernatant was added an equal amount of a solution containing 1mM L-tryptophan, 20  $\mu$ M methylene blue, 40 mM ascorbic acid, catalase (200 units/ml) and 100 mM potassium phosphate buffer, pH 6.5. The enzyme supernatant and the incubation mixture buffer were pre-heated to 37<sup>0</sup> C before mixing.

The mixture was further incubated for 20 minutes at 37<sup>0</sup> C. The reaction was stopped by adding 0.2 ml of 30% (w/v) trichloroacetic acid. The mixture was incubated at 50<sup>0</sup> C for 30 minutes to hydrolyze N-formylkynurenine produced by indoleamine 2, 3-dioxygenase to kynurenine. The mixture was then centrifuged at 6000 rpm at room temperature to remove the sediment. To 0.8 ml of the supernatant was added 0.8 ml of 1% (w/v) p-dimethylaminobenzaldehyde in acetic acid. Then, the absorbance was determined at 480 nm. The amount of kynurenine liberated was determined using standard graph of kynurenine. One unit of enzyme activity was expressed as nanomoles of kynurenine liberated/minute/mg protein.

### Determination of Protein

Protein concentration was determined by the modified method of Lowry [7] using bovine serum albumin as a standard.

### 3. Results

Figure 1 shows the standard curve of L-kynurenine. The absorbance of L-kynurenine at 480 nm was found to obey Beer-Lambert law and was linear up to a concentration of 100 µg of kynurenine.

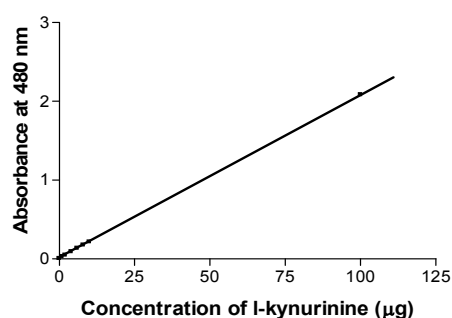


Figure 1: Standard curve of kynurenine

Figure 2 shows the protein concentration in various tissues of Arabian camel. Liver was found to have the highest concentration of protein followed by kidneys, intestine, plasma and lungs.

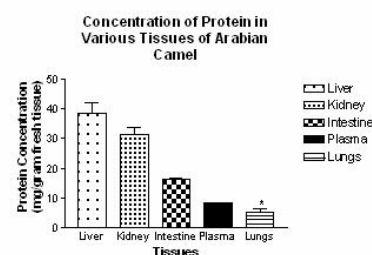


Figure 2: Concentration of protein in various tissues of Arabian camel. Values are expressed as  $\pm$  SD (n = 5 animals). \* P < 0.05 when compared to liver (Tukeys multiple comparison test).

Figure 3 shows the  $\pm$  SD activity of the enzyme indoleamine 2, 3-dioxygenase in two camel tissues viz., lungs and intestine. Of the different tissues studied for indoleamine 2, 3-dioxygenase activity, the activity was detected only in lungs and intestine. The activity of indoleamine 2, 3-dioxygenase in lungs and intestine was found to be  $18.00 \pm 2.45$  units protein mg<sup>-1</sup> and  $12.08 \pm 3.412$  units protein mg<sup>-1</sup>, respectively.

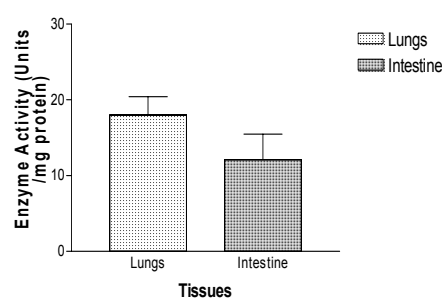


Figure 3: Indoleamine 2, 3-dioxygenase activity in tissues of Arabian camel. Values are expressed as  $\pm$  SD (n = 5 animals). The enzyme activity is expressed as

nanomoles of kynurenine liberated/minute/mg protein.

#### 4. Discussion

Indoleamine 2, 3-dioxygenase is a heme-containing dioxygenase which catalyzes the first and rate-limiting step in the major pathway of L-tryptophan catabolism in mammals. This enzyme has received much attention because of its diverse biological functions. These functions include the escape of malignant tumors from immune surveillance by immuno suppression caused by tryptophan depletion, involvement in several neurodegenerative disorders like Alzheimer's disease by aberrant production of neurotoxin, quinolinic acid and age- related cataract[8] .

A major part of dietary tryptophan is converted by kynurenine pathway leading to biosynthesis of NAD or complete oxidation of this amino acid. Indoleamine 2, 3-dioxygenase is expressed in many tissues like lungs, small and large intestine, colon, spleen, kidney, stomach and brain in rabbits[8].

Dromedary camels occupy arid regions of the Middle East through northern India and arid regions in Africa, most notably, the Sahara Desert. Dromedary camels have remarkable adaptations for their desert lifestyle. Their eyes are protected from blowing sand and dust by double row of eyelashes. During the sandstorm, these camels have the ability to close their nostrils to prevent sand from entering. Dromedary camels have the ability to conserve water in many ways and can tolerate greater than 30% water loss, a condition which is lethal in other mammals. These are some of unique features in camels not seen in other animals.

In the present study various camel tissues like liver, kidneys, lungs, intestine and plasma were analyzed to detect the activity of the enzyme indoleamine 2, 3-dioxygenase. The

enzyme activity was detected only in lungs and intestine. No enzyme activity was detected in liver, kidney and plasma. In other species like rabbits this enzyme has been reported to have extra hepatic distribution unlike tryptophan 2,3-dioxygenase a similar enzyme which is present in the liver [8].

Though this enzyme has been reported to be present in the kidneys of rabbit, it was not detected in camel kidneys. This may be either due to the fact that the enzyme is present in very low concentration which was not detected by the assay method used in this experiment or due to species variations.

Earlier studies have shown that most normal blood parameters of camels differed from those of other domestic animals and a lower activity and/or concentration of mixed function oxidase enzymes in kidneys and duodenum of camels than guinea pigs and rats [9] .

The activity of indoleamine 2, 3-dioxygenase was found to be higher in camel lungs than intestine. Lungs are one of the organs to be exposed to the pathogens which enter the body through the respiratory tract. Therefore in camel lungs this enzyme may catalyze the catabolism of Trp and thus deplete it in the vicinity. The depletion of L-Try may inhibit the growth of viruses, bacteria and parasites for whom it is most essential for their growth.

#### 5. Conclusion

Further studies are needed to measure the tissue distribution of indoleamine 2, 3-dioxygenase in all other camel organs using more sensitive methods and to investigate its role in this unique desert animal.

#### Acknowledgements

The authors are thankful to the Research Center, Sciences &

Medical Studies Department for Women Students, King

Saud University, Riyadh for financial support to NJS.

### References

- [1] King, N.J.C.; Thomas, S.R.; *Inter. J. Biochem. Cell Biol.* (2007), 39, 2167-2172.
- [2] Yamazaki, F.; Kuroiwa, T.; Takikawa, O.; Kido, R.; *Biochem. J.* (1985), 230, 635-638.
- [3] Travers, M.T.; Gow, I.F.; Barber, M.C.; Thomson, J.; Shennan, D.B.; *Biochim. Biophys. Acta.* 2004, 1661, 106-112.
- [4] Yagil, R.; *Comparative Animal Nutrition*, S. Karger, Switzerland, 1985, 10-42.
- [5] Elkhawad, A.O.; *Comp. Biochem. Physiol. Comp. Physiol.* 1992, 101 A, 195-201.
- [6] Kudo, Y.; Boyd, C.A.D.; *Biochem. Biophys. Acta.* 2000, 1500, 119-124.
- [7] Markwell, M.A.K.; Hass S.M.; Biebbber, L.L.; Tolbert, N.E.; *Anal. Biochem.* 1978, 87, 206-210.
- [8] Takikawa, O.; *Biochem. Biophys. Res. Commun.* 2005, 338, 12 -19.
- [9] Damanhour, Z.A.; 2002 *Com. Biochem. Physiol. Part C: Toxicol. Pharmacol.* 2002, 132, 445-450.

## **Application of Oxidative Coupling Reactions for the Estimation of Sildenafil Citrate in Bulk Sample and Dosage Forms**

**Safwan Ashour\*, Khalil Alkourdi**

*Department of Chemistry, Faculty of Sciences, University of Aleppo, Aleppo, Syria  
Tel: 00963-933-604016, e-mail: profashour@myway.com*

### **Abstract**

Sensitive and reliable spectrophotometric method by the application of oxidative coupling reaction for the assay of sildenafil citrate (SC) in pure form and pharmaceutical formulations has been developed. The method involves the oxidative coupling reaction of SC with 4-aminophenazone (4-AP) ( $\lambda_{\text{max}}$  526 nm) in the presence of periodate. The variable parameters in the method have been optimized and the chemical reactions involved are presented. Regression analysis of Beer's law plot showed good correlation in the concentration range of 3.33–98.0  $\mu\text{g mL}^{-1}$ . The molar absorptivity is  $7.5 \times 10^3 \text{ L mol}^{-1} \text{ cm}^{-1}$ . The method has been applied to the determination of the drug in commercial tablets. The results obtained in the method are statistically validated. The excipients present in the formulations do not interfere with the assay procedure.

**Keywords:** Oxidative coupling reactions, Sildenafil citrate, Dosage Forms.

### **1. Introduction**

Sildenafil citrate (SC) is an anti-impotent drug, a selective inhibitor of cyclic guanosine monophosphate (cGMP)-specific phosphodiesterase type 5 (PDE5). Sildenafil citrate is chemically designated as 1-[[3-(6,7-dihydro-1-methyl-7-oxo-3-propyl-1H-pyrazole [4,3-d] pyrimidin-5-yl)-4-ethoxyphenyl]sulfonyl]-4-methylpiperazine citrate [1].

Many workers [2-4] have reported the activity of SC as an efficacious, orally active agent for the treatment of male erectile dysfunction. No official (pharmacopoeial) method has been found for the assay of SC in its formulations. However, isocratic HPLC methods using

acetonitrile–phosphate buffer–water (28:4:68, v/v/v) with detection at 230 nm [5] and aqueous 60% acetonitrile with detection at 292 nm [6] were utilized as routine analysis of SC in pharmaceutical products. A reverse-phase high performance liquid chromatographic (RP-HPLC) methods were reported for the determination of SC in pure form and in pharmaceutical samples [7-10]. A Flow Injection Analysis (FIA) method was described for the determination of SC using UV detection [11]. HPLC method was reported for the determination of SC and related substances in the commercial products and tablet dosage form [12]. Also, SC was determined in pharmaceutical preparations

using voltammetric techniques [13], electrochemical oxidation on carbon electrodes [14], certain sigma and pi-acceptors for the spectrophotometric method [15] and extractive spectrophotometric methods [16]. Micellar electrokinetic chromatography was used for the determination of sildenafil citrate and its main metabolite [17].

The present paper presents a novel analytical method, based on the oxidative coupling reaction of SC with the reagent 4AP-KIO<sub>4</sub>. The method is applicable to the determination of SC in bulk form and in formulations and is found to be superior to some of the existing ones.

## 2. Experimental

### Instruments

A double-beam Biotech UV-visible spectrophotometer connected to a computer with UV-PC software was used for all absorbance measurements under the following operating conditions: scan speed medium (400 nm/min), scan range 450–650 nm and slit width 0.5 nm. The instrument has an automatic wavelength accuracy of 0.1 nm and matched quartz cells of 10 mm (1.0 cm) cell path length.

### Reagents

All reagents used were of analytical grade and all solutions were prepared with double distilled water. Freshly prepared solutions were always used. Aqueous solutions of  $1 \times 10^{-2}$  M 4-aminophenazone (Ferack) and  $1 \times 10^{-2}$  M KIO<sub>4</sub> (BDH), were prepared.

### Materials

1. Sildenafil citrate, working standard, ( $C_{22}H_{30}N_6O_4S \cdot C_6H_8O_7 = 666.701$  g/mole, obtained from Cipex Specialities Pvt Ltd, Mumbai, India). Its purity was found to be 99.8% according to the compendial method.
2. Vagran Tablets supplied by Barakat Pharmaceutical Industries, Aleppo, Syria, each tablet was labeled to contain sildenafil citrate 25, 50 or 100 mg.
3. Extra Tablets supplied by Alpha Pharmaceuticals Industries, Aleppo, Syria, each tablet was labeled to contain sildenafil citrate 50 mg.
4. Vega Tablets supplied by Asia Laboratories for Pharmaceutical Industries, Aleppo, Syria, each tablet was labeled to contain sildenafil citrate 50 mg.

### Standard drug solution

A stock standard solution of 0.001M was prepared by dissolving SC in doubly distilled water. Working standard solutions were then prepared by a suitable dilution of the stock standard solution with water.

### Recommended procedure

Aliquots of SC (0.05-1.47 mL, 0.001M) solution were transferred into a series of 10 mL volumetric flasks. Then 1.4 mL of 4-AP solution and 0.8 mL of KIO<sub>4</sub> solution were added and kept aside for 2 min. The volume was made up to the mark with distilled water. The absorbance of the solution was measured at 526 nm against a similar reagent

blank, prepared under identical conditions but the drug, within the stability period of 10 min after colour development. The amount of SC was determined from its Beer's law plot prepared with standard drug solution under identical conditions.

#### Procedure for formulations

Twenty tablets were weighed and finely powdered. An accurately weighed portion of the powder equivalent to 50 mg of SC was transferred into a 50 mL volumetric flask and dissolved in a doubly distilled water to achieve a

concentration of  $1 \text{ mg mL}^{-1}$ . The solution was shaken well and filtered. The solution was further diluted stepwise with distilled water to get working solutions and analysed under procedures described for bulk samples.

#### Validation

##### Linearity

To establish linearity of the proposed method, five separate series of solutions of SC ( $3.33\text{--}98.0 \text{ } \mu\text{g mL}^{-1}$ ) were prepared from the stock solution and analyzed. Least square regression analysis was done for the obtained data. (Table 1).

**Table 1. Optical and regression characteristics, precision and accuracy of the propose method.**

<i>Parameters</i>	<i>Method</i>
$\lambda_{\text{max}}$ (nm)	526
Beer's law range ( $\mu\text{g mL}^{-1}$ )	3.33–98.0
Molar absorptivity ( $\text{L.mol}^{-1}.\text{cm}^{-1}$ )	$7.5 \times 10^3$
Ringbom concentration range ( $\mu\text{g.mL}^{-1}$ )	16.0-73.0
Detection limits( $\mu\text{g.mL}^{-1}$ )	0.95
Sandell's sensitivity ( $\mu\text{g.cm}^{-2}$ per 0.001 absorbance unit)	0.0886
Regression equation <sup>a</sup>	$A = 0.0072 \text{ } C + 0.0726$
Correlation coefficient, r	0.9997
Range of error, %	$\pm 0.63$

<sup>a</sup> With respect to  $A = mC + b$ , where  $C$  is the concentration ( $\mu\text{g mL}^{-1}$ ) and  $A$  is absorbance.

##### Accuracy

To determine the accuracy of the proposed method, different levels of drug concentrations were prepared from independent stock solutions and analyzed (n= 6). Accuracy

was assessed as the percentage relative error and mean percentage recovery (Table 2).



**Table 2. Analysis of SC in bulk powder by the proposed method.**

$\mu\text{g.mL}^{-1}$		Relative error (%)	RSD (%)	Confidence limits (p = 0.05; n = 6)
Taken	Found*			
3.33	3.31	-0.60	1.76	3.31 $\pm$ 0.06
5.00	5.01	0.20	0.82	5.01 $\pm$ 0.04
10.00	10.03	0.30	0.64	10.03 $\pm$ 0.06
20.00	20.05	0.25	0.51	20.05 $\pm$ 0.11
40.00	40.11	0.27	0.43	40.11 $\pm$ 0.18
60.00	60.19	0.31	0.31	60.19 $\pm$ 0.20
80.00	80.23	0.28	0.11	80.23 $\pm$ 0.09

\*Average of six determinations.

**Precision**

Repeatability was determined by using different levels of drug concentrations (same concentration levels taken in accuracy study), prepared from independent stock solutions and analyzed (n = 6) (Table 2). The percent relative

standard deviation (% R.S.D.) of the predicted concentrations from the regression equation was taken as precision (Table 3). Precision studies were also carried out using the real samples of SC tablets in a similar way to standard solution to prove the useful of method.

**Table 3. Determination of sildenafil citrate in different pharmaceutical formulations by the proposed method and reference method.**

Drug	Labeled claim/tablet	%Recovery <sup>a</sup> $\pm$ SD	
		Proposed method	UV reference method [16]
Vaigran	25 mg	101.18 $\pm$ 0.21 $t=2.09$ $F=2.25$	100.81 $\pm$ 0.14 $t=1.62$
		102.08 $\pm$ 0.17 $t=1.96$ $F=1.71$	101.14 $\pm$ 0.13 $t=1.73$
	100 mg	100.84 $\pm$ 0.19 $t=1.61$ $F=1.41$	100.36 $\pm$ 0.16 $t=1.83$
Extra	50 mg	102.10 $\pm$ 0.23 $t=1.94$ $F=1.83$	100.53 $\pm$ 0.17 $t=1.55$
Vega	50 mg	101.27 $\pm$ 0.24 $t=1.59$ $F=1.59$	100.83 $\pm$ 0.19 $t=1.92$

### 3. Results and Discussion

#### Method development

The optimum conditions for the development of method were established by varying the parameters one at a time and keeping the others fixed and observing the effect produced on the absorbance of the coloured oxidative coupling product. The following experiments were conducted for this purpose and the conditions so obtained were incorporated in the recommended procedures.

In order to establish experimental conditions, the effect of various parameters such as volumes of 4-AP and  $\text{KIO}_4$ , waiting time, order of addition of reagents and the stability of coloured oxidative coupling product were studied at room temperature. The applicability of 4-AP in combination with various oxidising agents such as  $\text{Fe(III)}$ ,  $\text{Ce(IV)}$ ,  $\text{Cr(VI)}$ ,  $\text{IO}_4^-$ ,  $\text{Fe(CN)}_6^{3-}$  were examined.

Preliminary investigations revealed that the cationic oxidants [ $\text{Fe(III)}$ ,  $\text{Ce(IV)}$ ,  $\text{Cr(VI)}$ ] produced yellow colour with SC and enhanced the final colour. So further investigations were carried out with anionic oxidants as they do not produce any colour directly with SC.  $\text{IO}_4^-$  was found to be superior because of its sensitivity over  $\text{Fe(CN)}_6^{3-}$ . The laboratory temperature ( $25 \pm 0.5^\circ\text{C}$ ) anion was found to be optimal for all the experiments.

Addition of SC, 4-AP and  $\text{KIO}_4$  in that order gave maximum absorbance. Altering this order of addition (i.e.  $\text{SC} + \text{KIO}_4 + 4\text{-AP}$ ) resulted in a decrease in absorbance. Final colour was achieved with 5min. The coloured product was stable for further 10 min and was measured at 526 nm

(Fig. 1). A volume of 1.4 ml of  $1.0 \times 10^{-2}$  M 4-AP and 0.8 ml of  $1.0 \times 10^{-2}$  M  $\text{KIO}_4$  was found to be optimal for maximum colour development, since the absorbance was found to be maxima at the mentioned volumes (Fig 2).

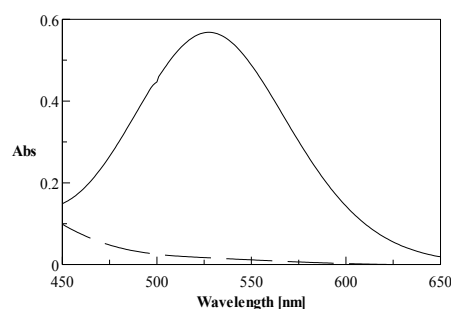


Figure1. Absorption spectra of SC-4AP- $\text{KIO}_4$  system (—) against reagent blank (---) vs. distilled water.  $[\text{SC}] = 66 \mu\text{g/mL} + 0.8 \text{ mL of } 10^{-2} \text{ M } \text{KIO}_4 + 1.4 \text{ mL of } 10^{-2} \text{ M } 4\text{-AP}$ .

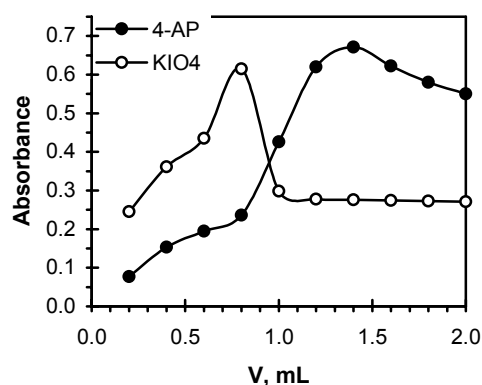


Figure2. Effect of concentration of (●) 4-AP in the presence of 0.8 mL of  $10^{-2}$  M  $\text{KIO}_4$  and (○)  $\text{KIO}_4$  in the presence of 1.4 mL of  $10^{-2}$  M 4-AP on the formation of SC-4AP- $\text{KIO}_4$  system.  $[\text{SC}] = 200 \mu\text{M}$ .

#### Stoichiometric relationship

The composition of the coloured oxidative coupling product was determined by Job's method using equimolar solution. The plot reached maximum at a mole fraction of

0.5, indicating the formation of 1:1 complex (Fig. 3). Also, the mole-ratio method showed that the formation of 1:1 complex (Fig.4).

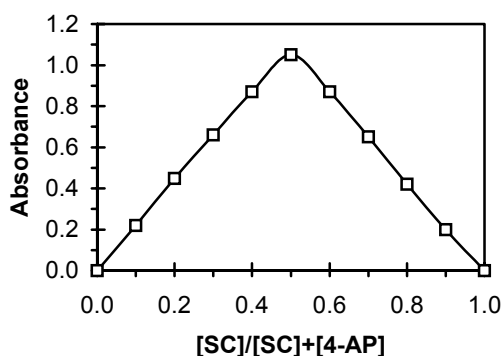


Figure 3. Job's method of continuous variations of drug-dye systems: SC+4-AP =  $2.0 \times 10^{-3}$  M.

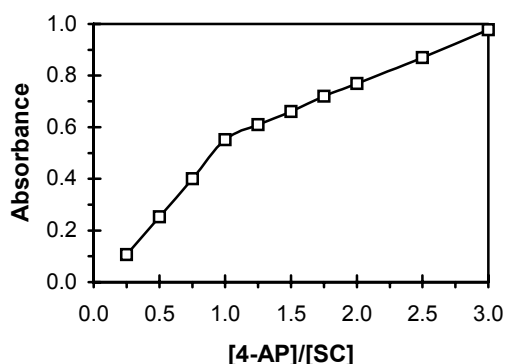


Figure 4. Mole-ratio method of SC-4AP system,  $[SC] = 5.10^{-3}$  M.

#### Linearity and range

In order to test whether the coloured oxidative coupling product formed in the above method adhere to Beer's law, the absorbance at appropriate length of a set of solutions containing varying amounts of SC and specified amounts of reagents (as given in the recommended procedure) were recorded against the corresponding reagent blank.

The Beer's law range, molar absorptivity, Sandell's sensitivity, regression equation, and correlation coefficient determined for the developed method are given in Table 1. A linear relationship was found between the absorbance at  $\lambda_{\max}$  and the concentration of the drug in the range  $3.33\text{--}98.0 \mu\text{g mL}^{-1}$ , in the final measured volume of 10 ml. Regression analysis of the Beer's law plots at  $\lambda_{\max}$  reveals a good correlation. The graph show negligible intercept and is described by the regression equation,  $A = mC + b$  (where  $A$  is the absorbance of 1 cm layer,  $m$  is the slope,  $b$  is the intercept and  $C$  is the concentration of the measured solution in  $\mu\text{g mL}^{-1}$ ) obtained by the least-squares method [18]. The high molar absorptivity of the resulting coloured oxidative coupling product indicates the high sensitivity of the method.

#### Validation of the method

The validity of the method for the analysis of SC in its pure state and in its formulations was examined by analyzing the samples using the proposed procedure. The results obtained for pure drug are given in Table 2. The precision and accuracy of the method were tested by analyzing six replicates of the drug. The low values of relative standard deviation (R.S.D.) indicate good precision and reproducibility of the method.

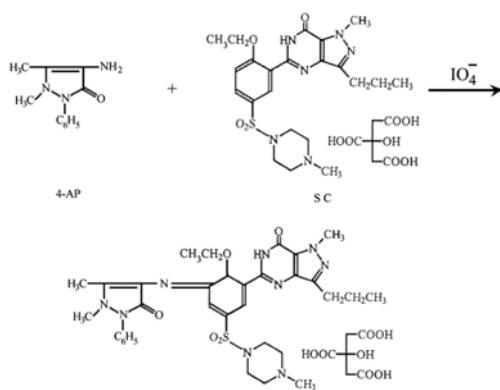
#### Application to the pharmaceutical dosage forms

The proposed technique was applied to the commercial formulations (tablets) containing SC. The values obtained

by the proposed and reference methods for formulations were compared statistically with *t*- and *F*-tests and found to be not to differ significantly. The results were summarised in Table 3. The average percent recoveries obtained were quantitative (100.84–102.10%), indicating good accuracy of the method. The ingredients in the tablets such as starch, lactose, glucose, sodium chloride and titanium dioxide do not interfere with the assay procedures.

### Chemistry of the coloured product

4-AP in the presence of periodate yields N-substituted quinone imine which in turn is known to spontaneously react with ethoxy compounds to yield a red coloured antipyrine dye. The coloured oxidative coupling product formation based on analogy is presented in Scheme 1.



**Scheme 1.**

### 4. Conclusion

As a conclusion, the method proposed in this study is simple, accurate, precise and rapid. Therefore, this approach could be considered for the analysis of sildenafil

citrate in the quality control laboratories. Proposed method makes use of simple reagents, which an ordinary analytical laboratory can afford. Method is sufficiently sensitive to permit determination even down to  $0.95 \mu\text{g mL}^{-1}$ .

The sensitivity in terms of molar absorptivity and the precision in terms of R.S.D. of the method are very suitable for the determination of sildenafil citrate in pure and dosage forms. The commonly used additives such as starch, lactose, glucose, sodium chloride and titanium dioxide do not interfere with the assay procedures.

### References

- [1] Terrett, N.K.; Bell, A.S.; Brown, D., Ellis P., Bioorg. Med. Chem. Lett. 1996, 6 (15), 1819-1824.
- [2] Chuang, A.T.; Strauss, J.D.; Murphy, R.A.; Steers, W.D., J. Urol. 1998, 160 (1), 257-261.
- [3] Turko, I.V.; Ballard, S.A.; Francis, S.H.; Corbin, J.D., Mol. Pharmacol. 1999, 56 (1), 124-130.
- [4] Umrani, D.N.; Goyal, R.K., Indian J. Physiol. Pharmacol. 1999, 43 (2), 160-164.
- [5] Cooper, J.D.H.; Muirhead, D.C.; Taylor, J.E.; Baker, P.R., J. Chromatogr. B 1997, 701 (1), 87-95.
- [6] Aboul-Enein, H.Y.; Hefnawy, M.M., J. Liq. Chromatogr. Relat. Technol., 2003, 26 (17), 2897-2908.
- [7] Dinesh, N.D.; Vishukumar, B.K.; Nagaraja, P.; Made Gowda, N.M.; Rangappa, K.S., J. Pharm. Biomed. Anal, 2002, 29 (4), 743-748.
- [8] Dong, F.T.; Liao, J.; Yuan, Z.; Liang, Y.Q.; Zhang, X., Fenxi Ceshi Xuebao, 2000, 19 (3), 53-54.

- [9] Liu, Y.M.; Yang, H.C.; Miao, J.R., Yaowu Fenxi Zazhi., 2000, 20(1), 61-62.
- [10] Segall, A.I.; Vitale, M.F.; Perez, V.L.; Palacios, M.L.; Pizzorno, M.T., J. Liq. Chromatogr. Relat. Technol., 2000, 23 (9), 1377-1386.
- [11] Altiokka, G.; Atkosar, Z.; Sener, E.; Tunçel, M., J. Pharm. Biomed. Anal., 2001, 25 (2), 339-342.
- [12] Daraghmech, N.; Al-Omari, M.; Badwan, A.A.; Jaber, A.M.Y., J. Pharm. Biomed. Anal., 2001, 25 (3-4), 483-492.
- [13] Berzas, J.J.; Rodríguez, J.; Castañeda, G.; Villaseñor, M.J., Anal. Chim. Acta, 2000, 417 (2), 143-148.
- [14] Özkan, S.A.; Uslu, B.; Zuman, P., Anal. Chim. Acta., 2004, 501 (2), 227-233.
- [15] Amin, A.S.; El-Beshbeshy, A.M., Mikrochim. Acta., 2001, 137 (1-2), 63-69.
- [16] Dinesh, N.D.; Nagaraja, P.; Made Gowda, N.M.; Rangappa, K.S., Talanta., 2002, 57 (4), 757-764.
- [17] Berzas Nevado, J.J.; Rodríguez Flores, J.; Castañeda Peñalvo, G.; Rodríguez Fariñas, N., J. Chromatogr. A, 2002, 953 (1-2), 279-286.
- [18] Miller, J.C.; Miller, J.N., Statistics in Analytical Chemistry, 3rd ed., Ellis Horwood, Chichester, 1993; pp 119.

## Use of Solid Superbase (Na/FAP) as Efficient Catalyst in Facile Construction of a Carbon-Carbon and Carbon-Hetero Atom Bonds

Mohamed Zahouily<sup>a,\*</sup>, Bahija Mounir<sup>a</sup>, Ahmed Rayadh<sup>a</sup>, M. Abdellah Bahlaoui<sup>b</sup>, Saïd Sebt<sup>c</sup>

### Abstract

The solid obtained by impregnation of fluorapatite with a solution of sodium nitrate. Followed by calcination at 900°C, is a strongly basic catalyst that is easily prepared from cheap precursors. The catalytic activity of this solid in the Michael addition of amine, thiol and active methylene to chalcone derivative was studied and high yields were obtained with a small amount of catalyst. Na/FAP is used as the catalyst for a facile synthesis of  $\beta$ -sulfur acid and 4*H*-chromene under heterogeneous conditions. The protocol is simple and potentially leads with use of Na/FAP. The catalyst can be easily recovered and efficiently reused.

**Keywords:** Fluorapatite; carbon-hetero atom bond;  $\beta$ -sulfur ester; 4*H*-chromene; heterogeneous catalyst.

---

<sup>a,\*</sup> *Laboratoire de Catalyse, Chimiométrie et Environnement, UFR de Chimie Appliquée, Université Hassan II, Faculté des Sciences et Techniques, B.P. 146, 20650, Mohammedia, Maroc*  
Tel. : + 212 61 62 80 76 ; Fax : + 212 23 31 53 53 ; e-mail : [mzahouily@yahoo.fr](mailto:mzahouily@yahoo.fr)

<sup>b</sup> *Laboratoire Génie Industriel et Métrologie de l'Environnement, UFR Biotechnologie et Génie de dépollution, Université Hassan II, Faculté des Sciences et Techniques, B.P. 146, 20650, Mohammedia, Maroc.*

<sup>c</sup> *Laboratoire de Chimie Organique, Catalyse et Environnement, Université Hassan II, Faculté des Sciences Ben M'Sik, B.P. 7955, Casablanca, Maroc*

## 1. Introduction

The replacement of liquid basic catalysts by solid bases in the synthesis of fine and intermediate organic chemicals allows one to avoid corrosion and environmental problems.

Solid basic catalysts are potentially favourable for organic syntheses involving carbon–carbon and carbon-hetero atom bonds formation such as addition and condensation reactions. The versatile Michael reactions have numerous applications in the elegant synthesis of fine chemicals [1] and are classically catalysed by bases or suitable combinations of amines and carboxylic or Lewis acids under homogeneous conditions. The employment of these bases/acids in these reactions, however, leads to two main problems affecting the environment; the necessity to dispose of huge amounts of organic waste due to formation of undesirable side products resulting from polymerisation, bis-addition and self condensation, and total dissolved salts formed following the neutralisation of soluble bases with acids or acids with bases [2].

There are a few reports concerning heterogeneous catalysis for Michael additions mediated particularly by  $\text{Zr}(\text{KPO}_4)_2$  [3], P-BEMP [4], K10 montmorillonite [5], alumina [6], KF/alumina [7], MCM-41 [8], synthetic phosphate ( $\text{Na}_2\text{CaP}_2\text{O}_7$ ) [9], fluoroapatite [10], and hydroxyapatite alone and doped with sodium nitrate [11] and

more recently, natural phosphate both alone and doped with potassium fluoride [12] or sodium nitrate [13] have been tested with success. Other researchers have increased the effect of the catalyst with addition of ultrasound [14], and microwave radiation [15].

Here, we present results related to the use of the fluorapatite (FAP) alone and activated by sodium nitrate (Na/FAP), in the Michael addition between  $\alpha,\beta$ -unsaturated carbonyl compounds and nucleophile including aliphatic and aromatic amines, thiol and active methylene.

## 2. Materials and methods

### 2.1. General comments

The molecular structure and catalytic activity of FAP and Na/FAP were studied by several techniques (electrochemistry, BET, BJH,  $^1\text{H}$ ,  $^{13}\text{C}$  NMR, X-ray, IR and MS spectroscopies).  $^1\text{H}$  and  $^{13}\text{C}$  NMR spectra were recorded on Bruker DRX-400 spectrometer at 400 and 100 MHz respectively and in  $\text{CDCl}_3$  as internal standard. The chemical shifts ( $\delta$ ) are expressed in ppm relative to  $\text{CDCl}_3$  and coupling constant ( $J$ ) in Hertz. Mass spectra were obtained on TRACE DSQ (Thermo electron) mass spectrometer. IR spectra were obtained on a FTIR (ATI Mattson-Genesis Series) and reported in wave numbers ( $\text{cm}^{-1}$ ). Surface area and pore size analysis were carried out at 77 K on a

Micromeritics ASAP2010 instrument using nitrogen as adsorbent. X-ray diffraction patterns of the catalysts were obtained on a Philips 1710 diffractometer using  $\text{CuK}\alpha$  radiation and SEM images were taken on a Hitachi S-2400 microscope. Melting points were determined with a “Thomas Hoover” melting (capillary method) apparatus and are uncorrected. Flash column chromatography was performed using Merck silica gel 60 (230-400 mesh ASTM).

All reactions were carried out under atmosphere air. Solvents and starting materials (Aldrich) were used without further purification.

## 2.2. Preparation and characterisation of fluorapatite (FAP).

The synthesis of FAP in powder state is carried out by means of reaction between diammonium phosphate, calcium nitrate and ammonium fluoride in the presence of ammonia (Figure 1).

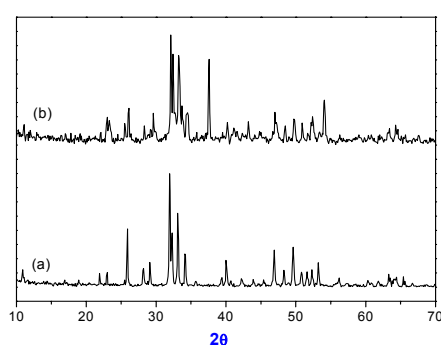


**Figure 1** : Synthesis reaction of fluorapatite (FAP).

FAP was obtained by co-precipitation, *i.e.*, 250 ml of a solution containing 7.92 g of diammonium hydrogen phosphate and 1 g of ammonium fluoride, maintained at pH greater than 12 by addition of ammonium hydroxide (15-20 ml), were dropped under constant stirring into 150 ml of a solution containing 23.6 g of calcium nitrate ( $\text{Ca}(\text{NO}_3)_2 \cdot 4\text{H}_2\text{O}$ ). The suspension was refluxed for 4h. Doubly distilled water (DDW) was used to prepare the solutions. The FAP crystallites were filtered, washed with DDW, dried overnight at 80 °C and calcined in air at 700 °C for 30 min before use.

The final product is identified by X-ray diffraction (space group hexagonal system;  $a = 9.364 \text{ \AA}$  and  $c = 6.893 \text{ \AA}$ ), infrared spectra IR and chemical analysis (Ca = 38.29 %, P = 17.78 % and Ca/P = 1.66). The BET specific surface area was found to be  $S = 15.4 \text{ m}^2/\text{g}$ . The total pore volume was calculated by the BJH method at  $P/P_0 = 0.98$  ( $V_t = 0.0576 \text{ cm}^3/\text{g}$ ).

## 2.3. Preparation and characterisation of Na/FAP

The modified FAP (Na/FAP = 1/2 w/w) was prepared by addition of FAP (10 g) to an aqueous sodium nitrate solution (50 ml, 1.17 M). The mixture was stirred at room temperature for 15 min and then the water evaporated under vacuum. The resulting solid was calcined under air at 900 °C. The XRD patterns of calcined Na/FAP showed the apparition of new



phases, so the CaO phase ( $2\theta = 32.2, 37.5$  and  $54.0$ ) is clearly identified (Figure 2). Two new phases ( $\text{CaNaPO}_4$  and  $\text{Na}_2\text{Ca}_4(\text{PO}_4)_3\text{F}$ ) are probably obtained by an exchange of sodium with calcium. No crystalline phases of  $\text{Na}_2\text{O}$  and  $\text{CaF}_2$  were observed. The surface area of the new catalyst Na/FAP was determined by the BET method as  $S = 5.4 \text{ m}^2/\text{g}$  and the total pore volume obtained by BJH method is  $0.0032 \text{ cm}^3/\text{g}$ .

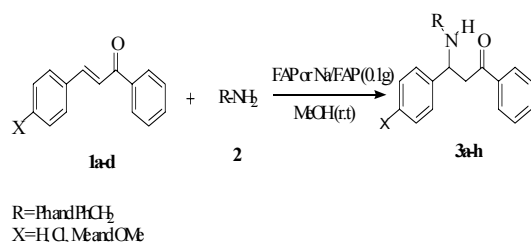


**Figure 2 :** The XRD pattern of FAP (a) and Na/FAP (b).

#### 2.4. Typical experimental procedure

To a flask containing an equimolar mixture (1.5 mmol) of nucleophile **2**, **12** or **18** and chalcone derivative **1** in methanol (1.5 ml), phosphate catalyst (Na/FAP) 0.1 g was added and the mixture was stirred at room temperature until completion of the reaction, as monitored by thin layer chromatography (TLC). The reaction mixture was filtered and the catalyst washed with dichloromethane. After concentration of the filtrate under reduced pressure, the residue was subjected to chromatography or recrystallization (*n*-hexane/ethyl acetate) leading to the Michael adduct. The product structure was

verified by  $^1\text{H}$ ,  $^{13}\text{C}$  NMR, IR spectrometry, melting points and mass spectrometer [16].

### 3. Results and Discussion.

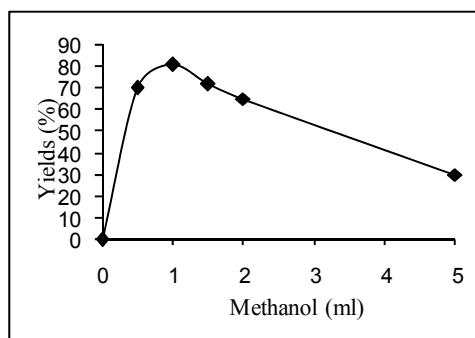
#### 3.1. Construction carbon-nitrogen bond in the presence of FAP and Na/FAP.

$\beta$ -amino derivatives such as  $\beta$ -amino esters,  $\beta$ -amino carbonyl and  $\beta$ -amino acids are of interest in the pharmaceutical chemistry because of their therapeutic applications. Among the different synthetic methodologies in the literature for the preparation of  $\beta$ -amino derivatives, one of the simplest and most widely used methods is the conjugate addition of amines to  $\alpha,\beta$ -unsaturated carbonyl derivatives. These reactions are generally performed using Lewis acid [17, 18], processes in which hazardous residues are formed.

In view of this, the aim of the present study is to investigate the effect of the heterogeneous catalyst on the construction of a carbon-nitrogen bond using the fluorapatite alone and fluorapatite doped with sodium nitrate.

Reaction of aniline and chalcone ( $\text{X} = \text{H}$ , Figure 3) was chosen as the model substrates to detect whether the use of FAP was to investigate the optimized conditions. Firstly, various solvents were tested. Thus, after 24 h of reaction the yields obtained of **3a** are 81, 48, 28 and 20 % in presence of methanol, ethanol, butanol and isopropanol, respectively. In

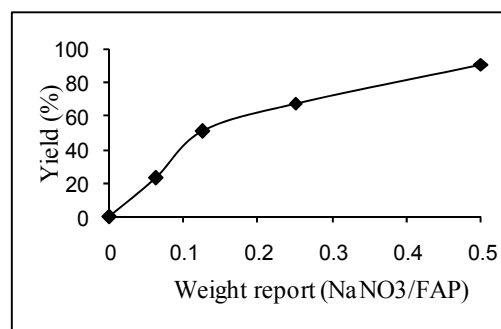
the cases of dioxane, THF, hexane or dichloromethane no **3a** was observed under reaction conditions, only the starting material was isolated.



**Figure 3 :** Reaction of aniline and chalcone in presence of FAF or Na/FAP.

Therefore, we carried out the reaction in various quantities of methanol. The best yield is obtained after 24 h with a volume of 0.5-1.5 ml. An increase in the volume up to 2 ml slightly decreases the reaction yield to 68 % and this drops further to 36 % when a volume of 5 ml is used (Figure 4). This behaviour indicates that some solvent is needed to facilities the contact between the reagents and the active sites,

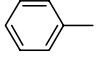
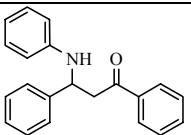
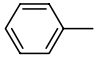
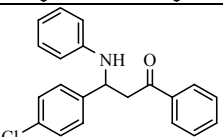
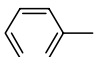
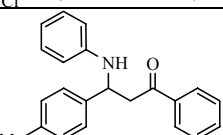
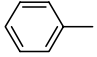
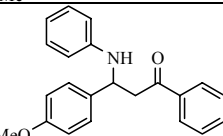
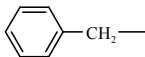
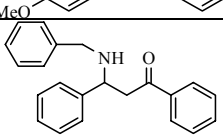
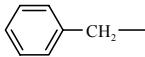
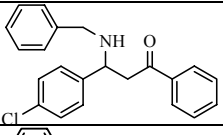
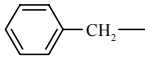
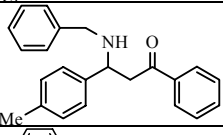
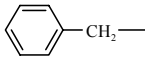
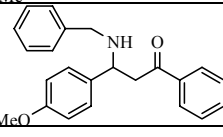
but a large volume reduces the concentration and, as a consequence, the reaction rate.



**Figure 4 :** Influence of methanol as solvent in the synthesis of the product **3a**.

To determine the scope and limitation of this reaction, the optimum conditions were applied to other substrates as shown in table 1. In general, the use of FAP alone as heterogeneous catalyst in the construction of a carbon-nitrogen bond has allowed the isolation of the  $\beta$ -amino carbonyl with modest yields (Table 1). The yields seem to be limited even if the time of the reaction is prolonged. However, for all cases the reaction rate is very long.

**Table 1** : Construction of a carbon-nitrogen bond by Michael addition using FAP and Na/FAP as catalysts.

R	X	Products	Yield in % [time (h)] <sup>a</sup>	
			FAP	Na/FAP
	H	<b>3a</b> 	58 (16) 81 (24)	96 (2,5)
	Cl	<b>3b</b> 	65 (24)	70 (8) 90 (16)
	Me	<b>3c</b> 	70 (24)	47 (8) 93 (16)
	OMe	<b>3d</b> 	75 (24)	98 (16)
	H	<b>3e</b> 	50 (48)	84 (18)
	Cl	<b>3f</b> 	80 (48)	90 (18)
	Me	<b>3g</b> 	53 (48)	54 (24) 73 (48)
	OMe	<b>3h</b> 	11 (48)	51 (48)

<sup>a</sup> Yields of pure products isolated by chromatography and recrystallized from *n*-hexane/ethyl acetate. The products were identified by <sup>1</sup>H, <sup>13</sup>C-NMR, IR spectroscopy and melting points.

To improve the reactivity of the FAP, we used sodium nitrate supported on FAP in different proportions. To determine the best weight report ( $r = \text{NaNO}_3/\text{FAP}$ ), we carried out the synthesis of **3a** at room temperature using the weight report of  $r = 1/16$ ,  $1/8$ ,  $1/4$  and  $1/2$ . The best yield in **3a** is obtained with  $r = 1/2$  (Figure 5). In the presence of 0.034 g of  $\text{NaNO}_3$  alone (the present quantity in  $\text{NaNO}_3/\text{FAP}$ :  $1/2$ ) has no activity in the Michael addition.

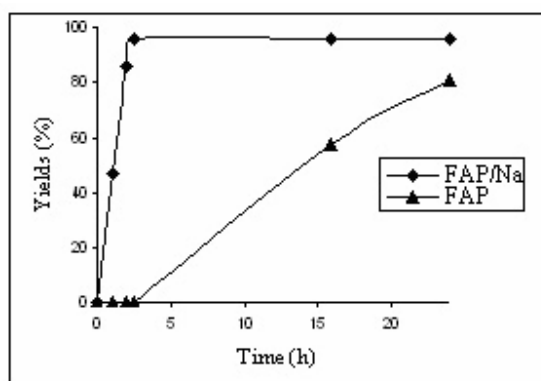


Figure 5 :.Influence of weight report  $\text{NaNO}_3$  on the yield in **3a** after 2.5 h of reaction.

Solid catalysts become particularly interesting when they can be regenerated. Indeed, in our case,  $\text{Na}/\text{FAP}$  was recovered quantitatively by simple filtration and regenerated by calcination for 15 min at  $700^\circ\text{C}$ . The recovered catalyst was reused several times without loss of activity. Even after the seventh cycles, product **3a** was obtained with some yield.

The use of  $\text{Na}/\text{FAP}$ , remarkably, increased the catalytic activity and decreased the reaction time of the Michael addition (Table 1 and Figure 6). The yields were very high (84 – 96 %), except, **3g** and **3h**, which afforded only a moderate yields (73 and 51%) of the 1,4 addition product.

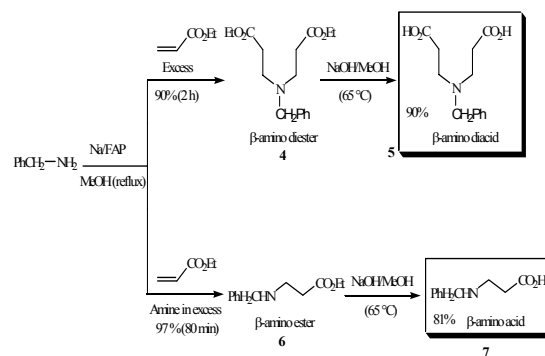


Figure 6 : Time of product **3a** synthesis in the presence of FAP and  $\text{Na}/\text{FAP}$  respectively.

### 3.2. Synthesis of $\beta$ -amino acid

The  $\beta$ -amino acids, in free form, show interesting pharmacological properties. For instance, hypoglycemic and antiketogenic activities were observed in rats after oral intake of emeramine. Functionalized  $\beta$ -amino acids are the key component of a variety of bioactive molecules such as taxol, which is one of the most active antitumor agents. During the past few years the synthesis of  $\beta$ -amino acid derivatives with different substitution patterns at the carbon

chain has become a field of increasing interest in organic synthetic [19].

The reaction of ethyl acrylate with an excess of benzylamine in the presence of Na/FAP furnished  $\beta$ -amino ester as the sole product due to a mono addition reaction (Figure 7). The reaction of benzylamine with an excess of

ethyl acrylate in the presence of Na/FAP gave bis-addition product **8** in excellent yield. While  $\beta$ -amino diester **4** is a direct precursor of  $\beta$ -amino diacid **5** has been used as a starting material for the synthesis of heterocyclic compounds and derivatives of nicotinic acids [20].

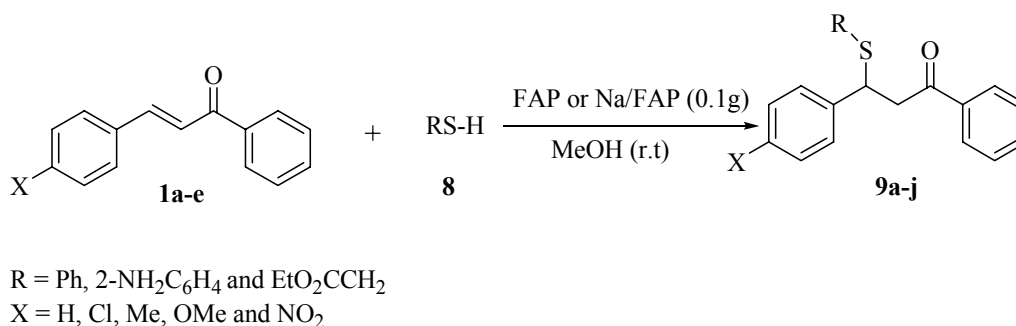


**Figure 7 :** Proposed catalytic reaction by Na/FAP for synthesis of  $\beta$ -amino acids.

### 3.3. Construction of carbon-sulfur bond in the presence of FAP and Na/FAP

Recently, conjugate addition of mercaptans to enones has attracted considerable interest [9-13, 21] as it leads to the synthesis of biologically active compounds [22] and corrosion inhibitors products [23]. Thus, a number of procedures either based on the activation of thiol by a base or activation of acceptor olefins with Lewis acids have

been developed [18, 24]. The optimized conditions for construction of a carbon-nitrogen bond are generalized to construction of a carbon-sulfur bond. Several  $\alpha,\beta$ -unsaturated carbonyl compounds such as *p*-methylchalcone as acceptors were subjected to this reaction with Na/FAP as catalyst and thiophenol, *m*-aminothiophenol or EtO<sub>2</sub>CCH<sub>2</sub>SH as the nucleophile thiol (Figure 8, Table 2).

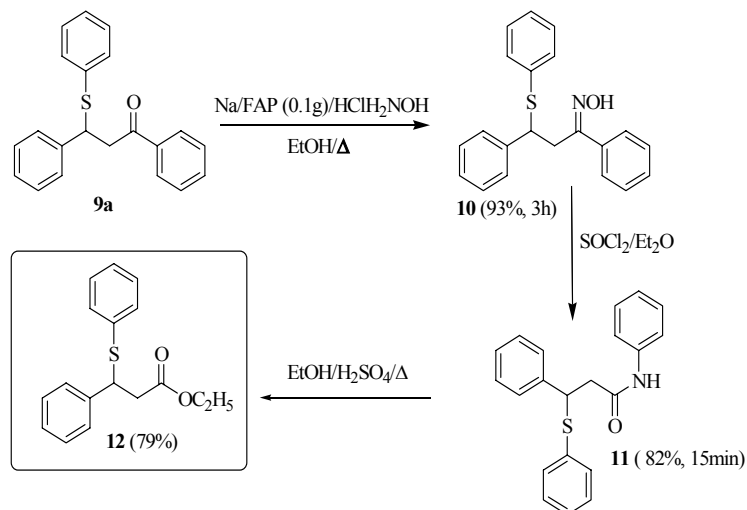
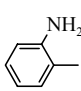
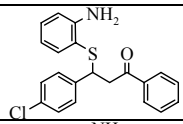
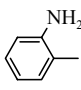
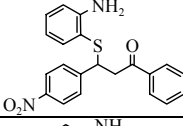
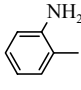
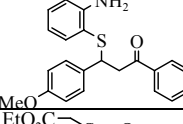
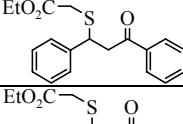
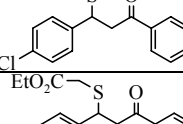
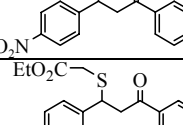
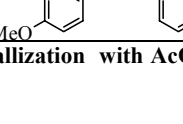


Figure 8 : Proposed catalytic reaction by Na/FAP for synthesis of product 9 (see table 2).

Table 2 : Construction of a carbon-sulfur bond by Michael addition using FAP and Na/FAP as catalysts.

R	X	Products	Yield in % [time (min)] <sup>a</sup>	
			FAP	Na/FAP
	H	<b>9a</b>	93 (25)	92 (1)
	Cl	<b>9b</b>	94 (15)	93 (1.5)
	NO <sub>2</sub>	<b>9c</b>	96 (12)	90 (1)
	OMe	<b>9d</b>	94 (105)	95 (5)
	H	<b>9e</b>	91 (8)	94 (0.45)

**Table 2 - Continued**

R	X		Products	Yield in % [time (min)] <sup>a</sup>	
				FAP	Na/FAP
	Cl	<b>9f</b>		95 (7)	91 (0.5)
	NO <sub>2</sub>	<b>9g</b>		93 (2)	92 (0.5)
	OMe	<b>9h</b>		94 (10)	93 (2.5)
EtO <sub>2</sub> C—CH <sub>2</sub> —	H	<b>9i</b>		72 (60)	91 (5)
EtO <sub>2</sub> C—CH <sub>2</sub> —	Cl	<b>9j</b>		82 (60)	93 (2)
EtO <sub>2</sub> C—CH <sub>2</sub> —	NO <sub>2</sub>	<b>9k</b>		93 (60)	92 (2)
EtO <sub>2</sub> C—CH <sub>2</sub> —	OMe	<b>9l</b>		57 (180)	92 (10)

<sup>a</sup> Yields in pure products isolated by recrystallization with AcOEt/CH<sub>2</sub>Cl<sub>2</sub> or distillation under vacuum and identified by <sup>1</sup>H, <sup>13</sup>C-NMR and IR spectroscopy.

In all cases the use of fluorapatite modified by sodium nitrate (Na/FAP) as heterogeneous in the construction of a carbon-sulfur bond has allowed the isolation of products **9** rapidly (1-10 min) and with excellent yields (91-95 %) ; (Table 2).

Except in one case, all the combination lead selectivity to the corresponding 1,4-adducts. No by-products resulting from the undesirable 1,2-addition and/or bis-addition side reactions (usually observed under classical conditions in some cases) were observed. However, reaction of 2-aminothiophenol with Michael acceptor bearing in *para*

position a nitro group ( $X = \text{NO}_2$ , Table 2) gives a 85/15 mixture of 1,4- and 1,3-addition products.

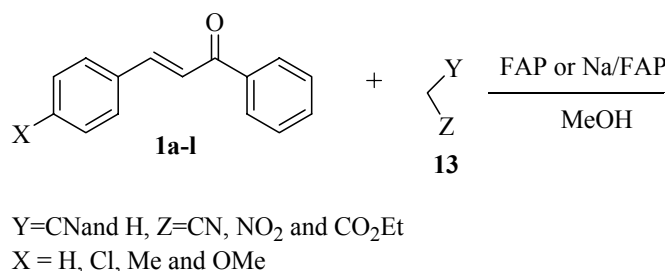


**Figure 9 : Proposed mechanism of conversion of product 9 to  $\beta$ -sulfur ester (12).**

#### 3.4. Construction carbon-carbon bond in the presence of FAP and Na/FAP

The Michael reaction is one of the efficient methods for effecting carbon-carbon bond formation and has wide synthetic applications in organic synthesis. Traditionally, these reactions are catalyzed by strong bases such as alkali metal alkoxides and hydroxides [25]. These limitations of the strong bases in these reactions are mainly the formation of undesirable side products by polymerization, bis-addition and self condensation. In recent years various

The product **9a** was converted to  $\beta$ -sulfur ester **12** (anilide of 3-phenyl-3-sulfinylpropanoic acid) by different steps (Figure 9).

solid base such as alumina [5], KF/alumina [6] and potassium modified  $\text{ZrO}_2$  [26] has been used to effect carbon-carbon bond formation. This encouraged us to investigate the reaction with FAP alone and Na/FAP.

The Michael addition is carried out between the chalcone **1** and the activated methylene **13** with FAP or Na/FAP at room temperature or 65 °C with 1ml of methanol (Figure 10). The yields obtained are grouped in table 3.



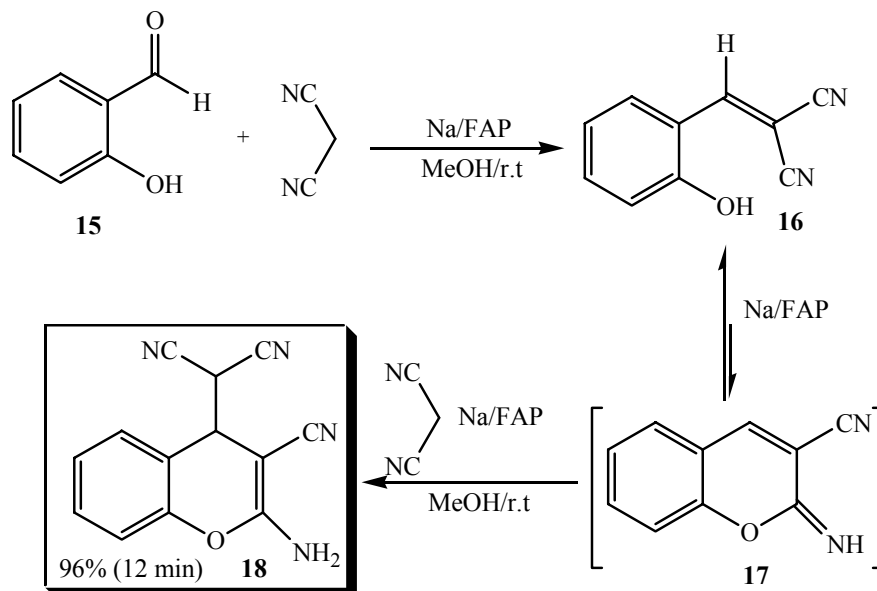
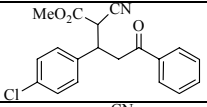
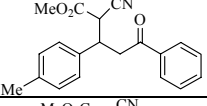
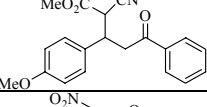
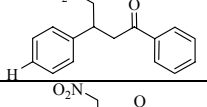
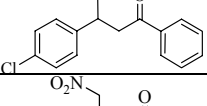
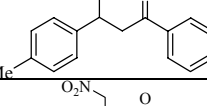
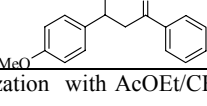


Figure 10 : Reaction chalcone and activated methylene in presence of FAF or Na/FAP.

Table 3 : Construction of a carbon-carbon bond by Michael addition using FAP and Na/FAP as catalysts.

X	Y	Z	Products	Yield in % [time] <sup>a</sup>	
				FAP (h)	Na/FAP (min)
H	CN	CN	<b>14a</b> 	92 (16)	93 (25)
Cl	CN	CN	<b>14b</b> 	81 (16)	96 (40)
Me	CN	CN	<b>14c</b> 	88 (20)	90 (50)
OMe	CN	CN	<b>14d</b> 	64 (20)	95 (60)
H	CN	CO <sub>2</sub> Me	<b>14e</b> 	83 (24)	96 (30)

Table 3 - Continued

X	Y	Z	Products	Yield in % [time] <sup>a</sup>	
				FAP (h)	Na/FAP (min)
Cl	CN	CO <sub>2</sub> Me	<b>14f</b> 	51 (24)	90 (50)
Me	CN	CO <sub>2</sub> Me	<b>14g</b> 	77 (41)	94 (60)
OMe	CN	CO <sub>2</sub> Me	<b>14h</b> 	67 (41)	90 (80)
H	NO <sub>2</sub>	H	<b>14i</b> 	46 (26) <sup>b</sup>	88 (55) <sup>b</sup>
Cl	H	NO <sub>2</sub>	<b>14j</b> 	30 (26) <sup>b</sup>	91 (120) <sup>b</sup>
Me	H	NO <sub>2</sub>	<b>14k</b> 	15 (26) <sup>b</sup>	90 (150) <sup>b</sup>
OMe	H	NO <sub>2</sub>	<b>14l</b> 	0 (26) <sup>b</sup>	87 (180) <sup>b</sup>

<sup>a</sup> Yields in pure products isolated by recrystallization with AcOEt/CH<sub>2</sub>Cl<sub>2</sub> or distillation under vacuum and identified by <sup>1</sup>H, <sup>13</sup>C-NMR and IR spectroscopy;

<sup>b</sup> The reaction mixture was stirred at 65 °C, traces of polymerization products were observed.

In all cases the use of Na/FAP as heterogeneous catalyst in the Michael addition allowed the isolation of products **14** rapidly and with excellent yields (87-96 % ; Table 3), except in the case where the nucleophile is nitromethane. In the presence of 0.0063 g of NaNO<sub>3</sub> alone (the present quantity in the NaNO<sub>3</sub>/FAP : 1/2 catalyst) no 1,4-addition product was observed under the reaction conditions, and

only the starting material was isolated. No by-product resulting from the undesirable 1,2-addition and/or bis-addition side reactions (usually observed under classical conditions in some cases) were observed. However, reaction of nitromethane with various  $\alpha,\beta$ -unsaturated carbonyl **1** at room temperature gives traces of polymerisation products (not isolated).

Reaction of salicylaldehydes **15** and malonitrile was investigated to establish conditions for the preparation of 4*H*-chromene **18** [12]. The reaction probably proceeds, in the first step, by a Knoevenagel condensation to give benzylidene derivatives **16** and then imino coumarin **17**. The intermediate **16** has been identified by  $^1\text{H}$  and  $^{13}\text{C}$

NMR spectra along with 4*H*-chromene **18**, when one equivalent of malonitrile is allowed to react with the salicylaldehydes **15**. The intermediate **16** is converted by Michael addition with excess of malonitrile present in the reaction mixture to the 4*H*-chromene **18** (Figure 11).

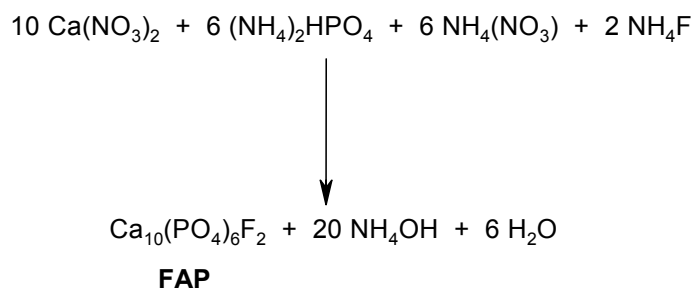


Figure 11 : Proposed mechanism of the synthese of 4 *H*-chromene.

In all cases, the use of fluorapatite doped by sodium nitrate (Na/FAP), remarkably, increases the catalytic activity and decreases the reaction time in the construction of a carbon-nitrogen, carbon-sulfur and carbon-carbon bonds (Table 1, 2 and 3). For the catalytic activity of Na/FAP in this Michael addition we speculate that the reaction occurs at the surface rather than inside tunnels of the catalyst. The dimensions of the tunnels in our catalyst are not large enough compared to those of zeolites [27]. Thus, we estimate that probably the surface of FAP presents multicatalytic active sites. The basic sites ( $\text{CaF}_2$  and

oxygen of  $\text{PO}_4$  group) enhance the thiol, nucleophilicity and the acidic sites ( $\text{Ca}^{2+}$  and phosphorus of  $\text{PO}_4$  group) probably increase the enone moiety polarization. Consequently, the S-C or C-C bond formation is accelerated and the final product is obtained after protonation of the resulting enolate. In the case of the construction of a carbon-nitrogen bond the basic sites deprotonate  $\text{RH}_2\text{N}^+\text{-C}$  after addition to the  $\text{C}=\text{C}$  bond.

#### 4. Conclusion

To sum up, the modified fluorapatite (Na/FAP) is a new inorganic reagent, which can represent an important breakthrough in the development of basic solid catalyst. The construction of a carbon-carbon, carbon-nitrogen and carbon sulphur bond have synthesised with high yields using catalytic amounts of Na/FAP. This phosphate is easily prepared from inexpensive precursors.

#### References

- [1] Choudary, B. M.; Lakshmi Kantam, M.; Neeraja, V.; Koteswara Rao, K.; Figueras, F.; Delmotte, L., *Green Chem.* 2001, 3, 257.
- [2] Martínez-Aranda, R. M.; Ortega-cantero, E.; Rojos-Cervantes, M. L.; Vicente-Rodríguez, M. A.; Bañares-Muñoz, M. A., *Catal. Lett.* 2002, 84, 201.
- [3] Costantino, U.; Marmottini, F., *Catal. Lett.* 1993, 22, 333.
- [4] Bensa, D.; Constantieux, T.; Rodriguez, J., *J. Síntesis* 2004, 6, 923.
- [5] Soriente, A.; Arienzo, R.; De Rosa, M.; Palombi, L.; Spinella, A.; Scettri, A., *Green Chem.* 1999, 9, 157.
- [6] Cheng, S.; Comer, D. D., *Tetrahedron Lett.* 2002, 43, 1179.
- [7] Xiang-Shan, W.; Da-Quing, S.; Shu-Jiang, T., *Chin. J. Chem.* 2004, 22, 122.
- [8] (a) Kloetstra, K. R.; Van Laren, M.; Van Bekkum, H., *J. Chem. Soc. Faraday Trans.* 1997, 93, 1211. ; (b) Corma, A.; Iborra, S.; Rodriguez, I.; Iglesias, M.; Sanchez, F., *Catal. Lett.* 2002, 82, 237.
- [9] Zahouily, M.; Abrouki, Y.; Rayadh, A., *Tetrahedron Lett.* 2002, 43, 7729.
- [10] Zahouily, M.; Abrouki, Y.; Rayadh, A.; Sebti, S.; Dhimane, H.; David, M., *Tetrahedron Lett.* 2003, 44, 2463.
- [11] (a) Zahouily, M.; Abrouki, Y.; Bahlaouan, B.; Rayadh, A.; Sebti, S., *Catal. Commun.* 2003, 4, 521. ; (b) Zahouily, M.; Bahlaouan, O.; Bahlaouan, B.; Rayadh, A.; Sebti, S., *Arkivoc* 2005, 13, 150.
- [12] (a) Zahouily, M.; Bahlaouan, B.; Aadil, M.; Rayadh, A.; Sebti, S., *Org. Process Research & Development* 2004, 8, 275. ; (b) Zahouily, M.; Bahlaouan, B.; Rayadh, A.; Sebti, S., *Tetrahedron Lett.* 2004, 45, 4135.
- [13] Zahouily, M.; Charki, H.; Abrouki, Y.; Mounir, B.; Bahlaouan, B.; Rayadh, A.; Sebti, S., *Lett. In Org. Chemistry* 2005, 2, 136.
- [14] Li, J.-T.; Chen, G.-F.; Xu, W.-Z.; Li, T.-S., *Ultrason Sonochem.* 2003, 10, 115.
- [15] (a) Sharma, U.; Bora, U.; Boruh, R. C.; Sandhu, J. S., *Tetrahedron Lett.* 2002, 43, 143. ; (b) Zahouily, M.;

- Elmakssoudi, A.; Mezdar, A.; Rayadh, A.; Sebti, S., J. Chem. Research 2005, 6, 324.
- [16] Zahouily, M.; Mounir, B.; Charki, H.; Mezdar, A.; Rayadh, A.; Sebti, S., ARKIVOC 2006, xiii, 178.
- [17] Shaikh, N. S.; Deshpande, V. H.; Bedekar, A. V., Tetrahedron 2001, 57, 9045.
- [18] Azizi, N.; Saidi, M. R., Tetrahedron 2004, 60, 383.
- [19] (a) Vicario, J. L.; Badia, D.; Carrillo, L., Org. Lett. 2001, 3, 773-??? ; (b) Gellman, S., Acc. Chem. Res. 1998, 31, 173.
- [20] Ali, F. E.; Bondinell, W. E.; Dandridge, P. A.; Frazee, J. S.; Garvey, E.; Girard, G. R.; Kaiser, C.; Ku, T. W.; Lafferty, J. J.; Moonsammy, G. I.; Oh, H.-J.; Rush, J.; Setler, P. E.; Stringer, O. D.; Venslavski, J. W.; Volpe, B. W.; Younger, L. M.; Zivkle, C. L., J. Med. Chem. 1985, 28, 653.
- [21] (a) Kamimura, A.; Murakami, N.; Yokota, K.; Shirai, M.; Okamoto, H., Tetrahedron Lett. 2002, 43, 7521. ; (b) McDaid, P.; Chen, Y.; Deng, L., Angew. Chem. Int. Ed. 2002, 41, 338. ; (c) Bandini, M.; Cozzi, P. G.; Giacomini, M.; Melchiorre, P.; Selva, S.; Ronchi, A. U., J. Org. Chem. 2002, 67, 3700. ; (d) Alam, M. M.; Varala, R. V.; Adapa, S. R., Tetrahedron Lett. 2003, 44, 5115. ; (e) Ranu, B. C.; Dey, S. S.; Hajra, A., Tetrahedron 2003, 59, 2417-??? ; (f) Ranu, B. C.; Dey, S. S., Tetrahedron 2004, 60, 4183.
- [22] Sheldon, R. A.; Chiretechnologies, Industrial synthesis of optically active compounds, Dekker, New York, 1993.
- [23] Hnini, K.; Chtaini, A.; Zahouily, M.; Outzourhit, A.; Elbouadili, A., ITE Lett. New Tech. and Medicine 2005, 6, 20.
- [24] (a) Emori, E.; Arai, T.; Sasai, H.; Shibasaki, M., J. Am. Chem. Soc. 1998, 120, 4043., and references cited therein ; Kanagasabapathy, S.; Sudalai, A.; Benicewicz, B. C., Tetrahedron Lett. 2001, 42, 3791., and references cited therein ; (c) Ahuja, P. R.; Natu, A. A.; Gogte, V. N., Tetrahedron Lett. 1980, 21, 4743.
- [25] Sreekumar, R.; Rugmini, P.; Padmakumar, R., Tetrahedron. Lett. 1997, 38, 6557.
- [26] Li, Z.-J.; Prescott, H. A.; Deutsch, J.; Trunschke, A.; Lieske, H.; Kemnitz, E., Catal. Lett. 2004, 92, 175.
- [27] Reddy, T. I.; Varma, R. S., Tetrahedron Lett. 1997, 38, 1721.

## Palladium(II)/diamine/phosphine and phosphine-free complexes as catalysts for Heck reactions

I. Warad<sup>\*</sup>, A. Al-Warthan, S. Al-Reseyes, N. Al-Zaqri, M. Fattoh and M. Al-Kahtani

*Department of Chemistry, Science of College, P.O. Box 2455, King Saud University, Riyadh-11451,  
Kingdom of Saudi Arabia*

### Abstract

The synthesis of neutral Pd [Cl<sub>2</sub>Pd(dp)] **2**, and [Cl<sub>2</sub>Pd(diamine)] **3** carried out starting from [PdCl<sub>2</sub>] **1** in dichloromethane at room temperature using dp (diphosphine Ph<sub>2</sub>PCH<sub>2</sub>CH<sub>2</sub>PPh<sub>2</sub>) and diamine H<sub>2</sub>NCH<sub>2</sub>CH(OH)CH<sub>2</sub>NH<sub>2</sub> ligands, respectively. Treatment of [Cl<sub>2</sub>Pd(dp)] **2** with two equivalent amount of AgBF<sub>4</sub> flowed directly by diamine ligand addition empowered us to prepare the dication complex [Pd(dp)diamine](BF<sub>4</sub>)<sub>2</sub> **4** in a highly yield for the first time, which can also be prepared by treatment of [Cl<sub>2</sub>Pd(diamine)] **3** with AgBF<sub>4</sub> reagent followed by dp ligand addition. The chemical behavior of the phosphine-contained these complexes has been investigated by <sup>31</sup>P{<sup>1</sup>H} NMR spectroscopy in all the reactions processes. These complexes showed good catalytic activity when it is subjected to C-C cross coupling process (Heck reaction).

**Keywords:** Palladium(II) catalysts, Heck reaction, cross-coupling, diphosphine and diamine ligands.

### 1. Introduction

Palladium-catalyzed coupling reactions have been recognized as extremely powerful tools in organic synthesis for the formation of carbon-carbon or carbon-heteroatom bonds [1-3]. The Heck reaction is among the most important ones due to its high tolerance of functional groups and general applicability [4-7]. The reaction generally proceeds in the presence of palladium catalysts associated with phosphine ligands which could stabilize the active palladium intermediates [6-11]. However, most of the phosphine ligands are air and moisture-sensitive. [12-15]. Considering the negative environmental effect, air-sensitivity, and cost of phosphine ligands, the development of phosphine-free catalysts for Heck reaction would be an important subject regarding academic and industrial application. Recently, some achievements have appeared in literature [6-17]. Among them, the low toxicity and

stability of nitrogen-based ligands such as diimine, dipyridine, hydrazone and imidazole [16-24] have attracted the interests of synthetic organic chemists. As examples, Hayashi et al. have reported the palladium-catalyzed Heck reaction that involved the simple catalytic system of PdCl<sub>2</sub>-imidazole [24].

To understand the chemical and structural behavior of the complexes containing phosphine ligand, <sup>31</sup>P{<sup>1</sup>H} NMR spectroscopy was used for investigation. Important parameters such as the chemical shift  $\delta$  (<sup>31</sup>P), and the coupling constant  $J_{PC}$  to an isotope active in NMR spectroscopy have been identified in this study.

In attempt to develop a new synthetic pathway towards palladium/phosphine palladium/diamine and palladium/phosphine/diamine complexes synthesis and test it as carbon-carbon cross coupling (Heck) catalysts. Here it

is reported a new facile promising method to synthesize series of neutral and dicationic (phosphine)<sub>2</sub>palladium(II) with and without different types of diamine.

## 2. Experimental

### 2.1 General remarks, materials, and instrumentations

Due to the air sensitivity of these compounds, all syntheses and other operations were carried out in an inert atmosphere (argon) with rigorous exclusion of dioxygen by using standard Schlenk tubes, vacuum line and catheter-tubing. Prior to use CH<sub>2</sub>Cl<sub>2</sub>, *n*-hexane, and Et<sub>2</sub>O were distilled from CaH<sub>2</sub>, LiAlH<sub>4</sub>, and from sodium / benzophenone, respectively.

The ethylenediphosphine (dp) ligand (Ph<sub>2</sub>PCH<sub>2</sub>CH<sub>2</sub>PPh<sub>2</sub>) was prepared according to some methods in the literature. The diamines were purchased from Acros, and Merck. Ph<sub>3</sub>P, BuLi, ClCH<sub>2</sub>CH<sub>2</sub>Cl, PdCl<sub>2</sub> and AgBF<sub>4</sub>, from Fluka, and used without purification. Elemental analyses were carried out on an Elementar Varrio EL analyzer. High-resolution <sup>1</sup>H, <sup>13</sup>C{<sup>1</sup>H}, DEPT 135, and <sup>31</sup>P{<sup>1</sup>H} NMR spectra were recorded on a Bruker DRX 250 spectrometer at 298 K. Frequencies are as follows: <sup>1</sup>H NMR 250.12 MHz, <sup>13</sup>C{<sup>1</sup>H} NMR 62.9 MHz, and <sup>31</sup>P{<sup>1</sup>H} NMR 101.25 MHz. Chemical shifts in the <sup>1</sup>H and <sup>13</sup>C{<sup>1</sup>H} NMR spectra were measured relative to partially deuterated solvent peaks which are reported relative to TMS. <sup>31</sup>P chemical shifts were measured relative to 85% H<sub>3</sub>PO<sub>4</sub> (δ<sub>p</sub> = 0). IR data were obtained on a Bruker IFS 48 FT-IR spectrometer. FAB-MS; Finnigan 711A (8kV), modified by AMD and reported as mass/charge (*m/z*).

### 2.2. General procedure for the preparation of 2 and 3

In 100 ml Schlenk tube excess of one equiv. amounts of the dp or diamine ligands in 20 ml of CH<sub>2</sub>Cl<sub>2</sub> was individually added dropwise to a stirred solution of 1 equiv. [PdCl<sub>2</sub>] **1** in 30 ml of CH<sub>2</sub>Cl<sub>2</sub>. Under vigorous stirring and at room temperature the color of reaction mixture was changed

from deep brown to light yellow within 60 min. <sup>31</sup>P{<sup>1</sup>H} NMR proved the formation of **2**. The volume of the solution was concentrated to a minimum volume under reduced pressure. Addition of 50 ml of *n*-hexane caused the precipitation of a solid which was filtered (P4) and well washed with diethyl ether and dried under vacuum.

### 2.3. General procedure for the preparation of 4 starting from 2

Complex **2** (500 mg, 0.973 mmol) in 50 ml of CH<sub>2</sub>Cl<sub>2</sub> was placed together with the AgBF<sub>4</sub> (400 mg, 2.062 mmol) followed by (90 mg, 1 mmol) of diamine ligand to prepare (530 mg, yield 90 %) of [Pd(dp)diamine](BF<sub>4</sub>)<sub>2</sub> **4**. The reaction mixture was stirred at room temperature in a sealed 150 ml Schlenk tube for 30 min, the mixture was filtrated (using P4) to remove any turbidity and the volume then was reduced under vacuum to about 5 ml. Addition of *n*-hexane caused a yellow solid, which was further washed three times with diethyl ether and dried in a vacuum.

### 2.4. Catalysis

PhI and methyl acrylate were used as received, while Et<sub>3</sub>N was distilled prior to use. The GC analyses were performed on a Dani HP 3800 flame-ionisation gas chromatograph (OV 101 on CHP column).

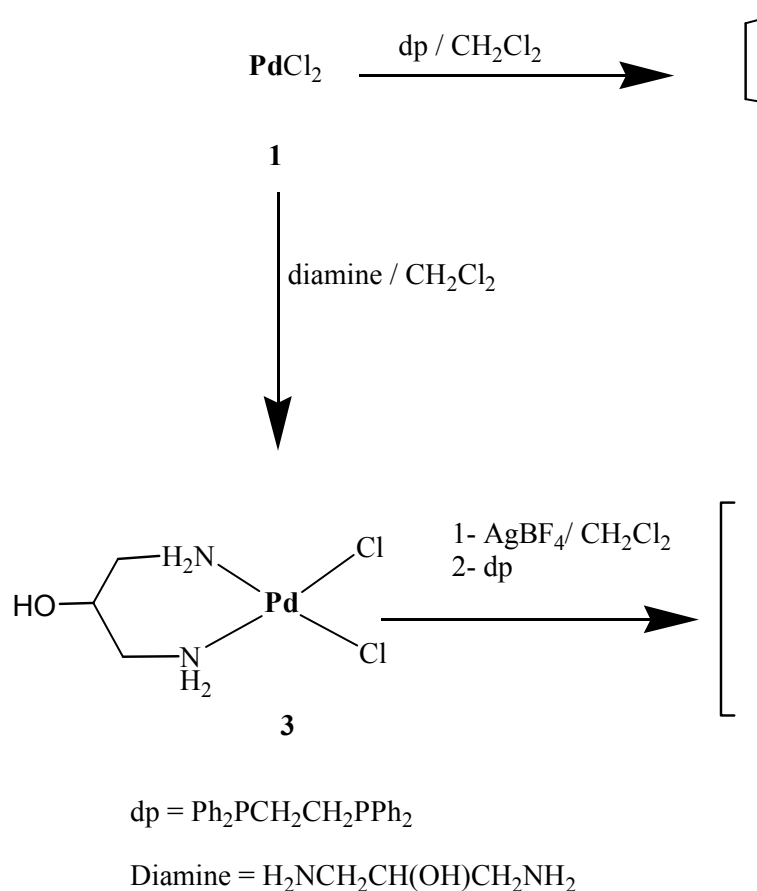
In a dry 100 ml capacity Schlenk tube equipped with a magnetic bar, iodobenzene, methyl acrylate, triethylamine and mesitilene (internal standard) were introduced; a 10 ml DMF solution containing 9×10<sup>-3</sup> mmol of complexes of Pd(II) was quantitatively transferred into the reactor and the solution thermostated at 80 °C using oil bath. Microvolumes of the reactant solutions were withdrawn, quenched with brine and extracted with dichloromethane. They were dried with anhydrous sodium sulphate and filtered, after that they were analysed by GC.

## 3. Results and Discussion

### 3.1 Synthesis and NMR investigations of the desired neutral and dicationic diamine-diphosphine/palladium(II)

The neutral Palladium(II) **2** and **3** were obtained in a quantitative yield, as yellow powder and colorless complexes by treatment of 1 equiv.  $[\text{PdCl}_2]$  **1** with 1 equiv. of the dp ( $\text{Ph}_2\text{PCH}_2\text{CH}_2\text{PPh}_2$ ) and diamine ( $\text{H}_2\text{NCH}_2\text{CHOHCH}_2\text{NH}_2$ ) ligands, respectively, at room temperature in  $\text{CH}_2\text{Cl}_2$ . The formations of these complexes were monitored by NMR, and the product was analyzed by NMR, FAB-mass spectra, IR and elemental analysis.

The NMR data are consistent with the coordination of the ligands in a static bidentate fashion. The  $^1\text{H}$ ,  $^{13}\text{C}$  and  $^{31}\text{P}$  NMR, Ms and IR spectra, as well as elemental analysis of the desired complexes are in agree very well with the proposed molecular formula corroborate the structures given in **Scheme 1** and Table 1.



**Scheme 1.** Synthesis of **1-4**.



**Table 1:** Characterization of Palladium(II) complexes.

Complex	Molecular Formula and Mol. Wt.	FAM-MS [M <sup>2+</sup> ]	Elemental Analysis			
			% C	% H	% N	% Cl
			Calcd. (Found)	Calcd. (Found)	Calcd. (Found)	Calcd. (Found)
<b>2</b>	C <sub>26</sub> H <sub>24</sub> Cl <sub>2</sub> P <sub>2</sub> d 514.56	514.2	43.05 (42.92)	3.61 (3.64)	-	18.15 (18.06)
<b>3</b>	C <sub>3</sub> H <sub>10</sub> Cl <sub>2</sub> N <sub>2</sub> OPd 267.45	267.2	13.47 (13.29)	3.77 (3.51)	10.47 (10.54)	26.51 (26.42)
<b>4</b>	C <sub>29</sub> H <sub>34</sub> N <sub>2</sub> OP <sub>2</sub> Pd 594.94	595.04	58.74 (58.49)	5.44 (5.72)	4.72 (4.54)	-

When complex **2** was treated with a slight excess of two equiv. of AgBF<sub>4</sub> in CH<sub>2</sub>Cl<sub>2</sub> followed directly by the diamine ligand in CH<sub>2</sub>Cl<sub>2</sub> complex **3** was formed in a very good yield. The two chloride atoms were abstracted from the backbone of the complexes, while diamine saturate the square planer required structure around the palladium(II) complex. This complex can be stored under argon at room temperature but is rather air-sensitive in solution.

<sup>31</sup>P{<sup>1</sup>H} NMR spectra of complex **3** is very simple and cleaned. they exhibit singlet which reveal that the phosphine groups are chemically equivalent in solution, due to the C<sub>2</sub> symmetry of the square planer coordination palladium(II) complexes. The phosphorus singlet and chemical shifts suggest that the diphosphine ligand is coordinated *trans* to the diamine chelate co-ligand, which confirmed the squar planer structure formation as in Figure 1.

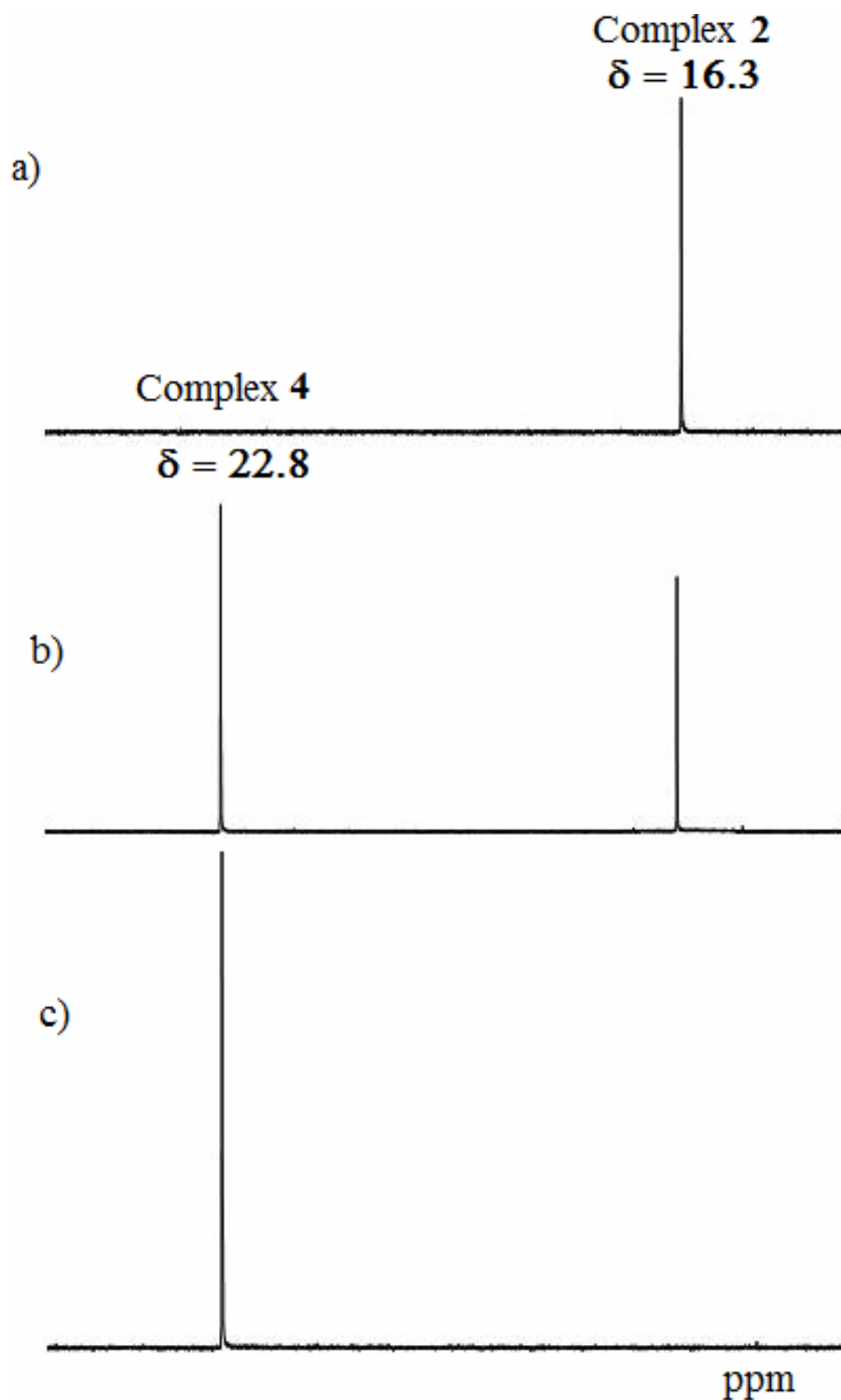


**Figure 1.** Time-dependent  $^{31}\text{P}\{^1\text{H}\}$  NMR spectroscopic control of the reaction between complex **2** mixed with  $[\text{AgBF}_4]$  and diamine] in  $\text{CH}_2\text{Cl}_2$  to produce complex **4** [ a) pure **2** before addition b) 30 min. and c) 2 h from the mixing (pure **4**)].

In the  $^1\text{H}$  NMR spectra of the new and dicationic diamine-bis(diphosphine)-palladium(II) complex characteristic sets of signals are observed, which are attributed to the phosphine ( $\text{CH}_2\text{P}$ ) as well as to the diamine ( $\text{H}_2\text{N}$ ,  $\text{CH}_2$ ,  $\text{CH}$  and  $\text{OH}$ ). Their assignment of signals were identified by the  $^{31}\text{P}\{^1\text{H}\}$ ,  $^{13}\text{C}\{^1\text{H}\}$ ,  $^1\text{H}$  NMR,  $^{13}\text{C}$  135 DEPT NMR and 2D H and H-COSY experiments which establish the connectivity between  $\text{NH}_2$  and  $\text{CH}_2$  functions as well as  $\text{CH}$  and  $\text{OH}$  in the diamine ligand, and  $\text{CH}_2\text{P}$  groups in the phosphine ligand. To differentiate between the C,  $\text{CH}$ ,  $\text{CH}_2$  and  $\text{CH}_3$  carbons types of dp and diamine binding in this complex, 135 DEPT  $^{13}\text{C}\{^1\text{H}\}$  NMR was investigated.

### 3.2 IR investigations

In order to study the binding mode of the diphosphine and diamine ligands to Palladium(II) in the new complexes. The IR spectra of the free ligands were compared with the spectra of the palladium complexes. The IR spectra of **2**, **3** and **4** in particular show three main sets of characteristic absorptions in the ranges  $3420\text{--}3305\text{ cm}^{-1}$ ,  $3267\text{--}3210\text{ cm}^{-1}$  and  $3181\text{--}3167\text{ cm}^{-1}$ , which can be attributed to stretching vibrations of the main functional group, [ $\text{NH}_2$  and  $\text{OH}$ ], [ $\text{Ph-H}$ ], and [ $\text{PCH}_2$ ,  $\text{NCH}_2$  CHO] of the dp and diamine ligands, respectively. All other characteristic bands due to the other functional groups are also present in the expected regions. The IR spectrum of complex **4** was represented in Figure 2 as typical example.

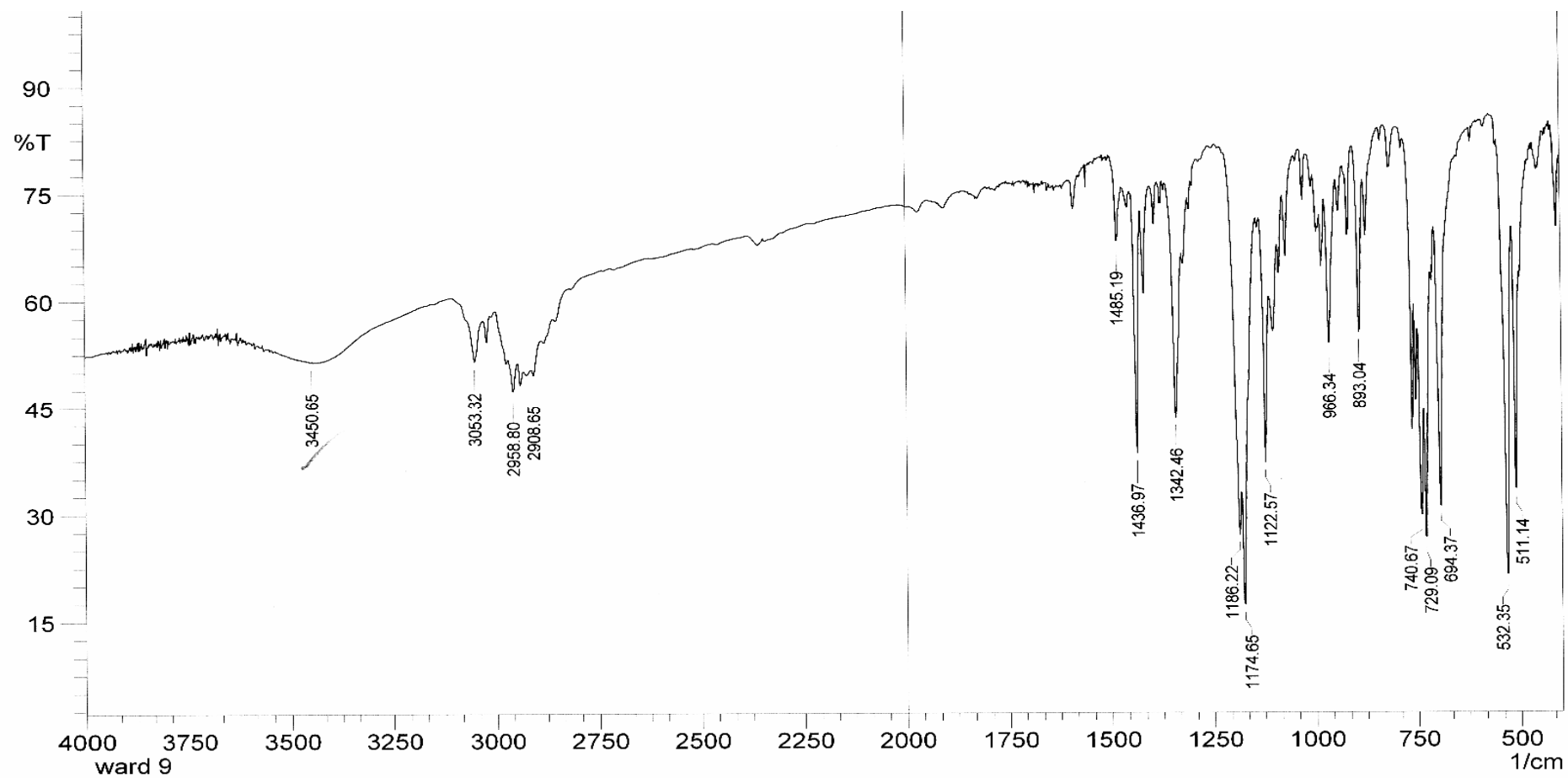
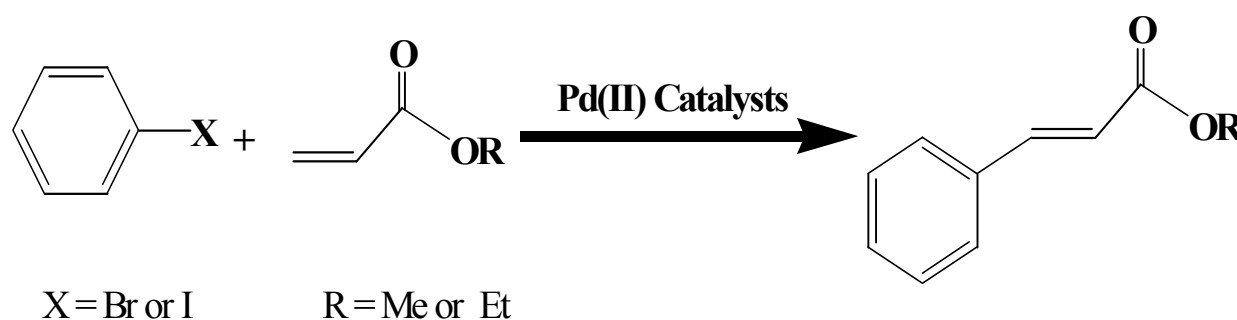


Figure. IR spectrum of complex 4.

### 3.3 Catalytic process toward Heck reaction

Primary and test study of catalytic activity was carried out in a basic medium; these complexes **1–4** have been tested as catalysts in the model coupling reaction of methyl acrylate (Meac) with iodobenzene, using DMF as

solvent, Et<sub>3</sub>N as base and a temperature of 80 °C. A Pd:PhI:Meac:Et<sub>3</sub>N= 1:1000:1100:1000 molar ratio has been kept constant at every catalytic experiment (Scheme 2).



**Scheme 1.** Heck cross-coupling reaction using Pd(II) complexes.

All the palladium complexes promote the complete conversion of iodobenzene into *trans*-methyl cynamate (unique product as established by <sup>1</sup>H NMR spectroscopy) within 2.5 h of reaction. On the basis of these data several type of parameters which could enhance the catalytic activity of cross-coupling reaction and promote both selectivity and yield will be studied in future step.

### 4. Conclusion

The presented investigation describe, a general, facile synthetic route to neutral and dicationic Palladium(II) complexes **2–4** was reported. the diamine/diphosphine/palladium(II) complex was successfully prepared for the first time, constructing a new promising method to prepare derivatives of such complexes by changing the diphosphine and diamine ligands. Primary study of catalytic activity, revealed that this simple palladium(II) complexes with such ligands promote the Heck coupling between iodobenzene and methyl acrylate.

### Acknowledgments

This project is supported by College of Science - Research Center project No (**Chem/2008/14**), for that Dr. I. Warad would like to thank the Research Center at King Saud University for financial support and use of some measurement facilities.

### References

- [1] A. de Meijere, F. Diederich (Eds.), Metal-catalyzed Crosscoupling Reactions, second ed., Wiley-VCH, Weinheim, 2004 (Chapter 5).
- [2] A.B. Donnay, L.E. Overman, Chem. Rev. 103 (2003) 2945.
- [3] G.C. Fu, S.T. Nguyen, R.H. Grubbs, J. Am. Chem. Soc. 115 (1993) 9856;
- [4] S.T. Nguyen, R.H. Grubbs, J.W. Ziller, J. Am. Chem. Soc. 115 (1993) 9858.
- [5] Y.C. Jung, R.K. Mishra, C.H. Yoon, K.W. Jung, Org. Lett. 5 (2003) 2231.

- [6] Y. Na, S. Park, S.B. Han, H. Han, S. Ko, S. Chang, J. Am. Chem. Soc. 126 (2004) 250.
- [7] A.E. Wang, J.H. Xie, L.X. Wang, Q.L. Zhou, Tetrahedron 61 (2005) 259.
- [8] T. Mino, Y. Shirae, Y. Sasai, M. Sakamoto, T. Fujita, J. Org. Chem. 71 (2006) 6834.
- [9] S. Li, Y.J. Lin, H.B. Xie, S.B. Zhang, J.N. Xu, Org. Lett. 8 (2006) 391.
- [10] B. Altava, M.I. Burguete, E.G. Verdugo, N. Karbass, S.V. Luis, A. Puzary, V. Sans, Tetrahedron Lett. 47 (2006) 2311.
- [11] M. Beller, H. Fischer, W.A. Herrmann, K. Ofele, C. Brossmer, Angew. Chem., Int. Ed. Engl. 34 (1995) 1844.
- [12] D.A. Alonso, C. Najera, M.C. Pacheco, Adv. Synth. Catal. 344 (2002) 172.
- [13] M.E. van der Boom, D. Milstein, Chem. Rev. 103 (2003) 1759.
- [14] D.E. Bergbreiter, P.L. Osburn, J.D. Frels, Adv. Synth. Catal. 347 (2005) 172.
- [15] W.A. Herrmann, V.P.W. Bohm, C.P. Reisinger, J. Organomet. Chem. 576 (1999) 23;
- [16] I.P. Beletskaya, A.V. Cheprakov, J. Organomet. Chem. 689 (2004) 4055.
- [17] J. Dupont, C.S. Consorti, J. Spencer, Chem. Rev. 105 (2005) 2427.
- [18] A.S. Gruber, D. Zim, G. Eberling, A.L. Monteiro, J. Dupont, Org. Lett. 2 (2000) 1287.
- [19] E. Peris, J. Mata, J.A. Loch, R.H. Crabtree, Chem. Commun. (2001) 201.
- [20] C.S. Consorti, M.L. Zanini, S. Leal, G. Ebeling, J. Dupont, Org. Lett. 5 (2003) 983.
- [21] M. Ohff, A. Ohff, D. Milstein, Chem. Commun. (1999) 357.
- [22] P.A. Gossage, H.A. Jenkins, P.N. Yadav, Tetrahedron Lett. 45 (2004) 7689.
- [23] M. Rosol, A. Moyano, J. Organomet. Chem. 690 (2005) 2291.
- [24] Y. Kawashita, C. Ueba, M. Hayashi, Tetrahedron Lett. 47 (2006) 4231.

## Catalytic Oxidation of CO pollutant over NiO induced by some transition metal oxides

*Mohammed A. Al-Omair*

*Chemistry Department, College of Science, King Faisal University, Al-Ahssa 31982, Saudi Arabia*

### Abstract

Binary systems of Cu-Ni-O-, Mn-Ni-O- and Co-Ni-O- having equimolar ratio of oxides were prepared. The samples were calcined at different temperatures [350-800 °C]. Surface area was determined from the low temperature adsorption of N<sub>2</sub> at 77 K. The structural characteristics were investigated by using thermal analysis [DTA and TGA] and powder X-ray diffraction [XRD] Techniques. The catalytic oxidation of CO by O<sub>2</sub> and their reaction kinetics were studied using the static method.

The surface area [ $S_{\text{BET}}$ ; m<sup>2</sup>/g] of individual oxides is greater than that of mixed oxides and the rise of calcinations temperature was associated with a decrease of  $S_{\text{BET}}$ . The structural analysis indicates a metal oxide-metal oxide interaction to form spinel, while the rise of calcinations temperatures leads to its decomposition.

The oxidation activity of CO by O<sub>2</sub> shows the promotion effect of cobalt, manganese and copper oxides to nickel oxide. Co-Ni-O- system has higher oxidation activity compared with the other examined systems and the oxidation process of CO at all conditions follows a first order kinetics.

**Keywords:** Cu-Ni-O-, Mn-Ni-O-, Co-Ni-O-, thermal analysis, XRD, CO, kinetics

### 1. Introduction

Carbon monoxide may build up in enclosed or semi-enclosed areas such as cars, houses, or buildings and becomes deadly. The vital effect of CO may be ranged from mild headache or stomachache without fever to severe signs of heart and brain damage, while the prolonged exposure for several days may result in death. The mechanism of carbon monoxide poisoning is caused by bonding of CO instead of oxygen with hemoglobin to form carboxy-hemoglobin. The delayed symptoms may include memory loss, changes in personality, disorientation, impaired reasoning ability, and behavioral or learning difficulties[1].

In recent years, the low temperature neutralization of hazard gases, e.g. NO<sub>x</sub>, SO<sub>x</sub> and CO, has been extensively studied. Catalytic oxidation of CO is incoming of environmental and industrial concerns, particularly the catalytic performance near room temperature. This would prevails a wide range of applications, e.g. closed cycle CO<sub>2</sub>

lasers and air purification devices [1-6]. However, noble metals, including Au, Sm, Pt, Pd, etc, have been approved as excellent catalyst for CO. The limited availability and high cost of such metal promoted the investigators to replace these precious metals with supported and/or unsupported transition metal oxides as more economical, commercial and active catalysts. Among of these oxides are Ag/MnO<sub>2</sub> [7], CuO and CeO<sub>2</sub> catalysts [8], NiO/Co<sub>3</sub>O<sub>4</sub> and Fe<sub>2</sub>O<sub>3</sub>/Co<sub>3</sub>O<sub>4</sub> [9], CuO/CeO<sub>2</sub> [10], NiMnO<sub>3</sub>-ilmenite and NiMn<sub>2</sub>O<sub>4</sub> [11]. Cobalt, copper and manganese oxides have received special attentions and widely used as catalysts because of their redox behaviors [12-14]. NiO is the least active catalysts for CO oxidation with O<sub>2</sub> compared with the other transition metals oxides [15]. Generally, the most reactive metal oxide catalysts to CO oxidation are those having p-type semi-conducting character. This may be attributed to the accommodation of excess oxygen in the lattice structure with the created vacancies [16, 17]. Haruta et al reported that the redox

behaviors of one oxide are strongly promoted when other ones are combined [18]. In particular, our interest was focused in; how to promote the activity of NiO towards the oxidation of CO via the incorporation of multivalent transition metals, e. g. copper, cobalt and manganese oxides, into NiO. In other words, the changes of redox property of the catalysts may be carried out on preparing binary and ternary oxides and therefore will be an effective factor in determining CO-oxidation activity. The combination of CuO, Co<sub>3</sub>O<sub>4</sub> and Mn<sub>3</sub>O<sub>4</sub> with NiO leads to creation of binary systems of new physicochemical and catalytic properties. Such properties of mixed oxide catalysts are dependent on the method of preparation, chemical composition and calcinations temperatures [15, 19-21]. The heat treatments of these systems are associated with spinel formation, showing distinguished changes in surface and catalytic performance of the examined catalysts [22, 23].

Herein, the present study concerned with the promoting effect of multivalent metal oxides, namely CuO, Co<sub>3</sub>O<sub>4</sub> and Mn<sub>3</sub>O<sub>4</sub> on CO-oxidation activity over NiO. Also, studying their effects on the physicochemical and catalytic properties of prepared catalysts subjected to pre-thermal treatments within the temperature range of 350-800°C.

## 2. Experimental

### Materials

All chemicals employed were of BDH analytical grade. Binary systems of Cu-Ni-O-, Co-Ni-O- and Mn-Ni-O- of equimolar ratio 1:1 were prepared by mechanical mixing of the corresponding powdered metal carbonates. The samples were calcined at 350, 550 and 800°C for 8 h.

### Techniques

The specific surface area of pre-calcined carbonates, both individual and mixed, were determined from the isothermal adsorption of N<sub>2</sub> at -196.8°C with an automatic Nova micrometric adsorption apparatus. Before undertaking the

adsorption measurements, the sample was degassed under a reduced pressure of 10<sup>-6</sup> torr for 3 hrs.

The X-ray diffractograms of all calcinations product were carried out using a Philips diffractometer [Type PW 1390]. The scans were followed with nickel-filtered copper radiation [ $\lambda = 1.5405$ ] and 36 kV and 16 mA with scanning rate 2° of 2 $\theta$  min<sup>-1</sup>. For phase identification, automatic JCPDS library search was used.

The thermal decomposition of pure and mixed carbonate precursors was studied with differential thermal analysis [DTA] and thermo gravimetric analysis [TGA], Shimadzu DT 50 H thermal analyzer.  $\alpha$ -Al<sub>2</sub>O<sub>3</sub> was used as a reference material, maintained the rate of heating at 10°C min<sup>-1</sup>.

The catalytic oxidation of CO by O<sub>2</sub> was performed at temperature of 225, 250 and 275°C using static method. A fresh activated oxide of 350 mg catalyst was used in each run and a stoichiometric mixture of CO and O<sub>2</sub> [CO + ½ O<sub>2</sub>] at a pressure of 2 Torr was admitted. CO<sub>2</sub>-oxidation product was driven off by freezing at liquid nitrogen temperature. The kinetics of the reaction was followed by measuring the pressure of the reaction mixture at different time intervals until no change in the pressure was observed. The percentage conversion was determined from the pressure drop of the reacting gases.

## 3. Results and discussion

### X-ray diffraction analysis

Figure (1) depicts the X-ray diffractograms of calcinations products of Co-Ni-O- systems at 350, 550 and 800°C. The obtained diffractograms shows that the sample being calcined at 350°C composes of Co<sub>3</sub>O<sub>4</sub>. It was reported that X-ray diffraction lines of NiCo<sub>2</sub>O<sub>4</sub> and Co<sub>3</sub>O<sub>4</sub> are assigned at the same 2 $\theta$ , so the distinguish of the two phase were being difficult [JCPDS files NiCo<sub>2</sub>O<sub>4</sub>; 20-781, Co<sub>3</sub>O<sub>4</sub>; 42-1467]. This may be supported by the absence of NiO



diffraction lines as a poorly crystalline phase and/or the dissolution of NiO in the lattice of  $\text{Co}_3\text{O}_4$  giving, therefore,  $\text{NiCo}_2\text{O}_4$  [24, 25] according to the following solid-solid interaction:

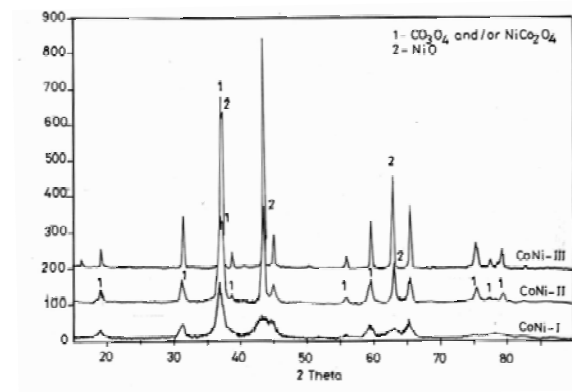
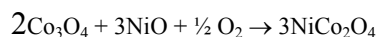


**Figure [1]: XRD patterns of Co-Ni-O- system calcined at different temperatures.**

The rise of calcinations temperatures within the temperature range of 550-800°C increases the relative intensities of X-ray diffraction lines of both NiO and  $\text{Co}_3\text{O}_4$ . The increase of the peaks intensities may be attributed to the preferential adsorption of Co(II) species on the top surface layers of Co-Ni-O- system. The formation of the latter phases was produced from the decomposition of nickel cobaltite according to:

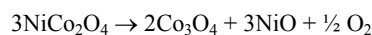
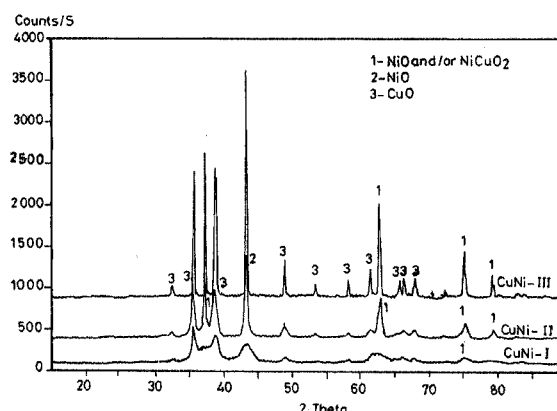
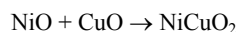


Figure (2) shows the X-ray diffraction patterns of calcined Cu-Ni-O- samples at 350, 550 and 800°C. The lower thermal treatments at 350-550°C produce CuO as major phase and NiO and/or  $\text{NiCuO}_2$  solid solution as minor phase according to:



**Figure [2]: XRD patterns of Cu-Ni-O- system calcined at different temperatures**

This may be explained from the preferential adsorption of Cu(II) species on the top surface of oxides layers. The elevation of thermal treatments up to 550°C promote the crystallization of NiO [minor] and/or  $\text{NiCuO}_2$  and CuO phases [major]. Inspection of X-ray diffraction patterns of 800°C calcinations products reveals that the peak height of the main diffraction lines which corresponds to CuO and NiO increase, indicating the abundance of both phases. It is worth mentioned that, the rise of calcinations temperature up to 800°C results in a decomposition of  $\text{NiCuO}_2$  to CuO and NiO phases.

Figure (3) represents X-ray diffractograms of the examined Mn-Ni-O- systems and received the same thermal treatments for Co-Ni-O- and Cu-Ni-O- systems. It is seen from this figure that the Mn-Ni-O- calcined at 350°C composed of a poorly crystalline  $\text{Mn}_2\text{O}_3$  phase. The traced NiO assigned at this calcinations temperature approved the dissolution of NiO in  $\text{Mn}_2\text{O}_3$  and or the formation of  $\text{NiMn}_2\text{O}_4$  spinel. The characteristic X-ray diffraction lines of  $\text{Mn}_2\text{O}_3$  and  $\text{NiMn}_2\text{O}_4$  having the same value of  $d$ -spacing, so that the presence of traces of NiO may be considered as an evidence for solid-solid interaction between NiO and  $\text{Mn}_2\text{O}_3$  [26]. The rise of calcinations temperature up to  $\geq 550^\circ\text{C}$  leads to the crystallization of NiO and  $\text{Mn}_2\text{O}_3$  as a separate phase. This finding reveals that  $\text{NiMn}_2\text{O}_4$  starts to decompose upon

heating at  $\geq 550^\circ\text{C}$  to NiO and  $\text{Mn}_2\text{O}_3$  [27]. The intensity of XRD lines of the latter two phases increase with the further elevation of calcinations temperature beyond  $550^\circ\text{C}$ .

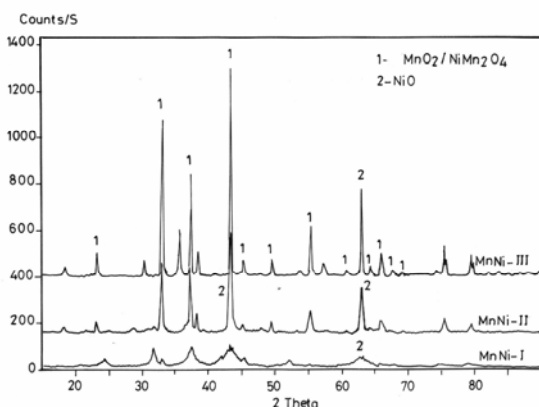


**Figure [3]: XRD patterns of Mn-Ni-O- system calcined at different temperatures**

### Thermal analysis

#### Thermal decomposition of pure metal carbonate

Figures (4-7) depict DTA-TGA curves of pure nickel carbonate as well as its mixture with cobalt, copper and manganese carbonates. DTA-TGA curves of individual cobalt, copper and manganese carbonates are not indicated. The TGA curve of pure basic nickel carbonate depicts two comparable sections, namely the partial dehydration of the precursor and decomposition of intermediate [28, 29]. The first section of DTA curve starts below and around the temperature of  $105^\circ\text{C}$  corresponds to a weight loss of 16.3 %. This earlier stage may be due to the partial dehydration of  $\text{NiCO}_3 \cdot \text{Ni}[\text{OH}]_2 \cdot 4\text{H}_2\text{O}$  to  $\text{NiCO}_3 \cdot \text{NiOOH}$ . The second weight loss of 17.67 % as shown by a sharp weight reduction indicates the formation of NiO at the temperature of  $286^\circ\text{C}$ . The DTA curve exhibits three endotherms corresponding to the weight losses within the temperature range  $41\text{--}286^\circ\text{C}$ .

The DTA-TGA curves of  $\text{CoCO}_3$  exhibit a loosely endotherms at  $137^\circ\text{C}$  and  $230^\circ\text{C}$ . These peaks represent the partial and complete thermal decomposition of  $\text{CoCO}_3$ , respectively. TGA curve of  $\text{CuCO}_3 \cdot \text{Cu}[\text{OH}]_2$  shows only

one decomposition stage. The DTA curve exhibits a strong and sharp endotherm at the temperature of  $297^\circ\text{C}$ . This endotherm may be attributed to the complete decomposition of basic copper carbonate to CuO [30].

TGA curve of  $\text{MnCO}_3$  comprises three stages of weight loss; the first corresponds to a weight loss of 6.7 %, the second of 6.94 % and the third of 19.17%. The first and the second weight losses correspond to two broad DTA-endotherms at temperature of  $141$  and  $405^\circ\text{C}$ . The third weight loss matches a sharp DTA-endotherm at  $486^\circ\text{C}$ . The endotherms at  $405$  and  $486^\circ\text{C}$  may be due to the decomposition of manganese carbonate to manganese dioxide, followed by the reduction of manganese dioxide to manganese trioxide, respectively [31-34].

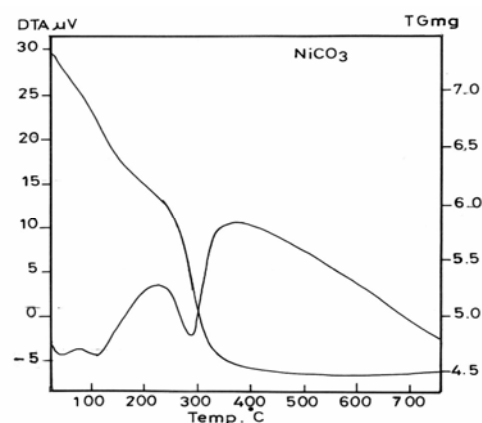


**Figure [4]: DTA-TGA curves of basic nickel carbonate**

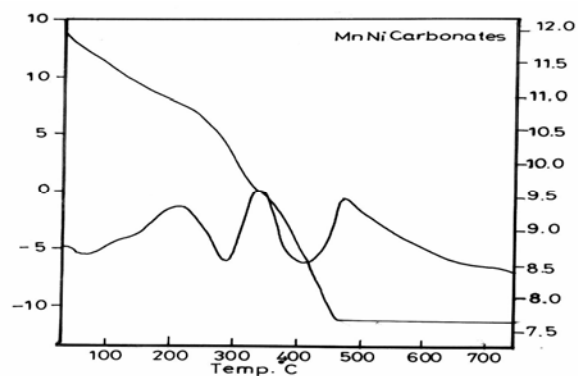


**Figure [5]: DTA-TGA curves of nickel-manganese carbonates**

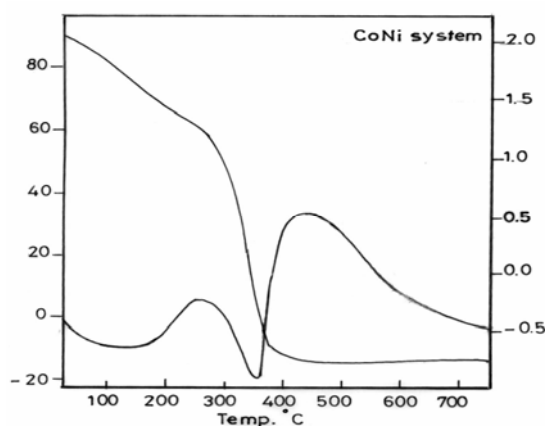


Figure [6]: DTA-TGA curves of nickel-cobalt carbonates

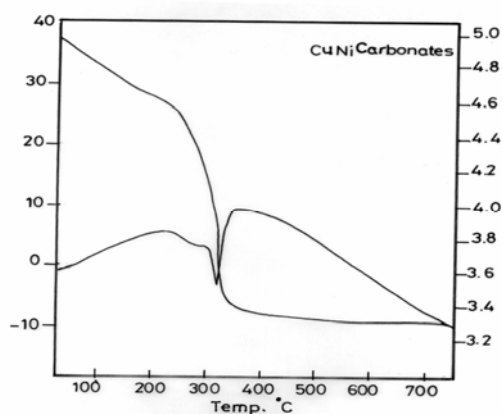


Figure [7]: DTA-TGA curves of nickel-copper carbonates

#### Thermal decomposition of Mixed metals carbonates

DTA-TG curves of Mn-Ni-O- systems exhibit mostly a similar endotherms to either pure  $\text{NiCO}_3$  or  $\text{MnCO}_3$ . The slight difference between the individual  $\text{NiCO}_3$ ,  $\text{MnCO}_3$  and their mixture is the appearance of broad endothermic peaks within the temperature of 381-461°C. These endotherms refer to the synchronous complete decomposition of the mixed carbonates into the corresponding metal oxides.

The mixing of cobalt carbonate with basic nickel carbonate increases the thermal stability of their carbonates and shifts the decomposition peaks to higher temperature,

i.e. to 350-400°C. The TGA curve includes two distinguishable sections; the first continued to 350°C, while the second extended to 400°C. The first section represents a weight loss of 36.4 %, while the second approaches 82.2 %.

The inspection of DTA curve of Cu-Ni-O- shows a couple of the DTA curves of individual copper and basic nickel carbonates. The first endothermic peak located at 283°C may be due to the complete decomposition of basic nickel carbonate into NiO [6.8 % weight loss]. The second endotherm at 320°C may be referred to the decomposition of copper carbonate into CuO [21.7 % weight loss]. The latter decomposition demands a higher thermal treatments of mixed carbonates compared with copper carbonate itself, indicating the higher thermal stability of copper carbonate in copper-nickel carbonates system.

The rise of calcinations temperature beyond 400°C was not associated with a weight loss. This may be indicated with the formation of solid solutions of binary oxides and/or solid-solid interaction of two oxides.

#### Surface area measurements

The specific surface areas [ $S_{\text{BET}}$ ;  $\text{m}^2/\text{g}$ ] of all calcinations products; 350-800°C; were measured as shown in Table 1. The inspection of these results shows that:

- (i) The individual oxides measure a higher specific surface area than the binary oxides; the measured surface areas are probably correlated with the thermal decomposition of carbonate precursors. The lower values of  $S_{\text{BET}}$  for binary system may be arisen from the transformation of single oxide lattices to binary system ones and/or the formation of spinel structure as indicated from XRD analyses.
- (ii) The rise of calcinations temperature is associated with a continuous decrease of specific surface area, attributing this to the sintering phenomena of investigated solids [22, 23].

**Table 1:** Specific surface area [ $S_{\text{BET}}$ ] of various calcinations products

Catalysts	Calcinations temperatures	[ $S_{\text{BET}}$ ; $\text{m}^2/\text{g}$ ]
NiO	350°C	88.2
Co-Ni-O	350°C	51.2
Cu-Ni-O	350°C	42.4
Mn-Ni-O	350°C	31.1
NiO	550°C	53.2
Co-Ni-O	550°C	27.3
Cu-Ni-O	550°C	19.8
Mn-Ni-O	550°C	11.2
NiO	800°C	29.5
Co-Ni-O	800°C	10.2
Cu-Ni-O	800°C	6.5
Mn-Ni-O	800°C	4.3

**Catalytic oxidation of CO**

The oxidation of CO by  $\text{O}_2$  was performed for all preparations, namely Ni-O-, Co-O-, Cu-O-, Mn-O-, Co-Ni-O-, Cu-Ni-O- and Mn-Ni-O- systems, pre-calcined at 350-800°C. At all reaction temperatures, the reaction follows a first order kinetics. Figure (8) depicts a representative first order linear plots of CO

oxidation with  $\text{O}_2$  carried out at 250°C. Listed in table (2) are the first order rate constant [ $k$ ] and the specific rate constant [ $k^-$ ; reaction rate per unit surface area] as readily determined from the slope of the first order plots.

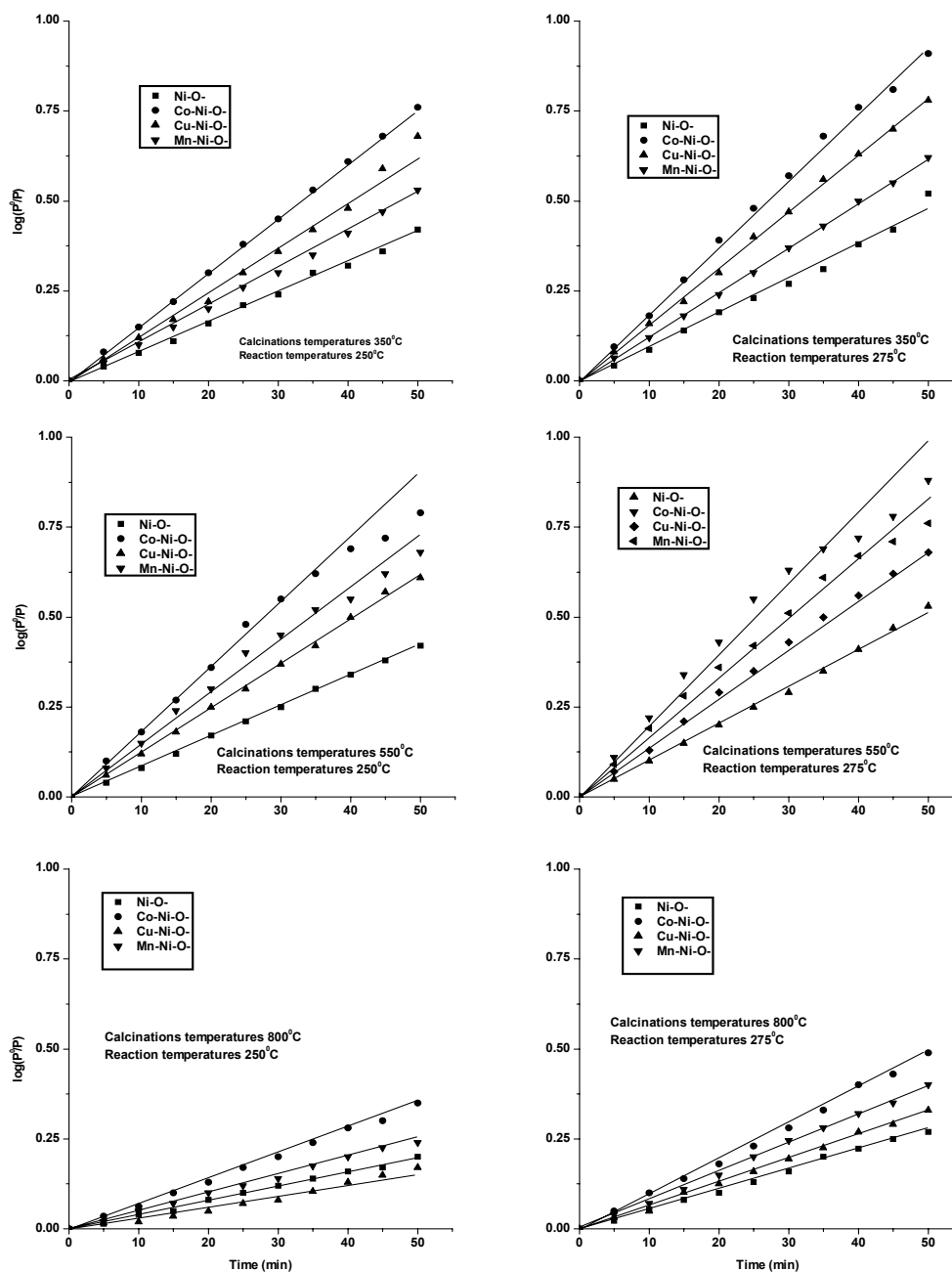


Figure [8]: First order plot of CO oxidation by O<sub>2</sub> over samples investigated

The data obtained in table (2) reveals that:

1. Ni-O- has a lower oxidation activity of CO by O<sub>2</sub>, compared with other binary oxides investigated [15]. In all cases, the activity increase with increasing the activation temperature. Figure (8) depicts the effect of calcinations temperatures on the specific rate constants of CO-oxidation.
2. The catalytic activity of Co-Ni-O- system, as being expressed with the rate constant, has the highest activity among the other catalysts investigated. The activity follows the order Co-Ni-O- > Cu-Ni-O- > Mn-Ni-O- > Ni-O-. The activity of the obtained samples calcined at higher temperatures follows the order: Co-Ni-O- > Mn-Ni-O- > Cu-Ni-O- > Ni-O-.
3. The activity of Co-Ni-O- system increases upon elevating the calcinations temperature from 350 to 550°C. The lowest oxidation activity of 350°C-calcinations products may be attributed to the presence of NiCo<sub>2</sub>O<sub>4</sub> as inactive catalytic phase. A good agreement with XRD analyses establishes the increase of oxidation activity of 550°C-calcinations products attributing to the thermal decomposition NiCo<sub>2</sub>O<sub>4</sub> to NiO and Co<sub>2</sub>O<sub>3</sub>. The further increase of calcinations temperature up to 800°C reduces the catalytic activity to an extent of 63.3 % at reaction temperature of 225°C.
4. The oxidation activity of Mn-Ni-O- prevail a similar behavior to that of Co-Ni-O- system. For all reaction temperatures, the calcined products at 350°C owe the lowest oxidation activity. The formation of NiMn<sub>2</sub>O<sub>4</sub> spinel as approved from XRD reduces the activity of Mn-Ni-O-. In addition, the higher calcinations temperatures of 550°C lead to the decomposition of pre-formed NiMn<sub>2</sub>O<sub>4</sub> into NiO and Mn<sub>2</sub>O<sub>3</sub> and therefore enhance CO-oxidation activities. The continuous increase of calcinations temperature beyond 550°C results in a significant decrease of catalytic activities.
5. In contrast with the Co-Ni-O- and Mn-Ni-O- systems, the catalytic activity of Cu-Ni-O- system continuously decreases with the rise of calcinations temperatures within the investigated intervals of temperatures. The higher oxidation activities of 350°C-calcinations products may be attributed to the formation NiCuO<sub>2</sub> as an active phase, The lowest values of  $k$  and  $k'$  at higher calcinations temperature of 550 and 800°C may be referred to the decomposition of NiCuO<sub>2</sub> into a less reactive species.

**Table 2:** Some kinetic parameters of CO oxidation by O<sub>2</sub> over catalysts investigated

Catalysts	Calcination temp [°C]	Reaction temp [°C]	$K \times 10^{-3} [\text{min}^{-1}]$	$k' \times 10^{-3} [\text{min}^{-1} \cdot \text{m}^{-2}]$	Catalysts	Calcination temp [°C]	Reaction temp [°C]	$K \times 10^{-3} [\text{min}^{-1}]$	$k' \times 10^{-3} [\text{min}^{-1} \cdot \text{m}^{-2}]$
NiO	350	225	7.5	0.085	Cu-Ni-O-	550	250	12.2	0.616
Co-Ni-O-	350	225	13.9	0.271	Mn-Ni-O-	550	250	13.3	1.188
Cu-Ni-O-	350	225	12.6	0.297	NiO	550	275	10.7	0.201
Mn-Ni-O-	350	225	9.3	0.299	Co-Ni-O-	550	275	17.1	0.626
NiO	350	250	8.4	0.095	Cu-Ni-O-	550	275	13.6	0.689
Co-Ni-O-	350	250	15.0	0.292	Mn-Ni-O-	550	275	14.9	1.330
Cu-Ni-O-	350	250	13.8	0.325	NiO	800	225	3.0	0.102
Mn-Ni-O-	350	250	10.7	0.344	Co-Ni-O-	800	225	5.7	0.559
NiO	350	275	10.6	0.120	Cu-Ni-O-	800	225	3.4	0.523
Co-Ni-O-	350	275	18.1	0.353	Mn-Ni-O-	800	225	4.0	0.930
Cu-Ni-O-	350	275	15.6	0.370	NiO	800	250	4.1	0.139
Mn-Ni-O-	350	275	12.4	0.399	Co-Ni-O-	800	250	7.0	0.686
NiO	550	225	6.6	0.124	Cu-Ni-O-	800	250	3.4	0.523
Co-Ni-O-	550	225	14.4	0.527	Mn-Ni-O-	800	250	4.9	1.140
Cu-Ni-O-	550	225	10.2	0.515	NiO	800	275	5.5	0.186
Mn-Ni-O-	550	225	12.9	0.963	Co-Ni-O-	800	275	9.8	0.961
NiO	550	250	8.4	0.158	Cu-Ni-O-	800	275	6.6	1.015
Co-Ni-O-	550	250	15.3	0.560	Mn-Ni-O-	800	275	8.0	1.860

The values of apparent activation energy [ $\Delta E$ ; J.mole<sup>-1</sup>] of CO oxidation by O<sub>2</sub> were calculated by applying the Arrhenius equation, using the values of the reaction rate constant k given in Table (2). The computed values of  $\Delta E$  are listed in Table (3).

The data obtained in table (3) reveals that:

(i) the values of  $\Delta E$  and lnA change in similar way for the different calcinations products,

(ii) the variation of  $\Delta E$  for the catalytic process over examined systems with the calcinations temperatures; followed generally the order: 800 > 550 > 350°C. These results coincide with the observed change of the catalytic activity towards CO oxidation. The slight fluctuation of lnA and  $\Delta E$  can be explained on the basis of dissipation function of active sites; i.e. the slight fluctuation of lnA indicates the surface heterogeneity of the catalysts examined.

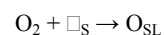
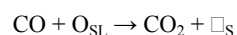
**Table 3:** Apparent activation energies [ $\Delta E$ ] and frequency factor [A] for the catalytic oxidation of CO by O<sub>2</sub> using catalysts investigated

Samples	Calcinations temperatures					
	350°C		550°C		800°C	
	Ln A	$\Delta E$	Ln A	$\Delta E$	Ln A	$\Delta E$
NiO	- 1.45	1730	- 0.17	2425	1.09	3448
Co-Ni-O-	- 5.31	1320	- 2.546	850	0.2568	2725
Cu-Ni-O-	- 2.239	1070	- 1.751	1410	0.961	3335
Mn-Ni-O-	- 1.799	1440	- 2.924	720	1.2685	3415

### Mechanism of CO oxidation by O<sub>2</sub>

It has been reported that the CO reduction of a metal oxide leads to the generation of reduced species and therefore the creation of surface heterogeneity. In the calcined nickel precursor the possible redox couples may be Ni<sup>0</sup>-Ni<sup>2+</sup>, Ni<sup>0</sup>-Ni<sup>+</sup> and Ni<sup>+</sup>-Ni<sup>2+</sup>. These ion pairs become more active in the presence of multi-valent cations of cobalt, copper and manganese because of their quick redox capability. In other words, the addition of multi-valent cations to Ni-O- system increases the concentration of ion pairs (Ni<sup>n+</sup>- M<sup>m+</sup>, where n is the oxidation state of Ni, m is the oxidation state of Co, Mn and Cu); promotes, therefore, the oxidation activities. Herein, one may consider different mechanisms of CO oxidation by O<sub>2</sub> over catalysts investigated:

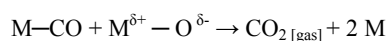
(i) Oxidation proceeds via oxidation-reduction cycle according to [35]:



Where O<sub>SL</sub> is the surface lattice oxygen and  $\square_{\text{S}}$  is a surface of oxygen vacancy on the metal oxide surface.

The first reaction is the slow one and appears to be the rate determining step. The rate of oxidation will be enhanced when a more lattice oxygen is withdrawn from the metal oxide.

- (ii) Reaction at the perimeter interface between the adsorbed CO and molecular oxygen at the active sites [ M] [36] according to:



- (iii) The adsorption of carbon monoxide at the active sites to form metal hydroxycarbonyl complexes [37-39], particularly for the lower temperatures calcinations products. These metal hydroxycarbonyl complexes is oxidized to bicarbonate, followed by de-carboxylation to CO<sub>2</sub> and regeneration of the active sites.

#### 4. Conclusion

- (i) S<sub>BET</sub> [m<sup>2</sup>/g] of individual oxides is higher than the binary oxides. The decrease of S<sub>BET</sub> values upon calcinating of mixed carbonates may be attributed to solid-solid interaction and sintering phenomena.
- (ii) The thermal treatments affect the structural characteristics of the catalysts examined. As illustrated from DTA-TGA and XRD analyses, the calcinations products of 350°C own spinel form, namely NiCo<sub>2</sub>O<sub>4</sub>, NiCuO<sub>2</sub> and NiMn<sub>2</sub>O<sub>4</sub>. The rise of calcinations temperatures to or beyond 550°C produces the individual metal oxides.
- (iii) NiO owns the lower oxidation activity of CO by O<sub>2</sub>, while the activity of the binary systems follows the order: Co-Ni-O- > Cu-Ni-O- > Mn-Ni-O- > Ni-O-. For Co-Ni-O- and Mn-Ni-O-, the rise of calcinations temperatures from 350°C to

550°C leads to an increase of the oxidation activities. In both systems, the increase of catalytic activities may be judged from the presence of binary metal oxides spinel. Moreover, for the mixed carbonates calcined at 800°C, the samples show a lower activity because of their presence as individual oxides.

- (iv) Cu-Ni-O- system shows a different behavior than that of Co-Ni-O- or Mn-Ni-O-. The oxidation of CO decreases gradually upon rising the calcinations temperature from 350 to 800°C. NiCuO<sub>2</sub> owns a higher oxidation activity compared with CuO or NiO.
- (v) In trial to correlate the oxidation activities with the measured surface areas, one can elucidate the dependence of CO oxidation on the concentration of metal ion pairs rather than the textural parameters.

#### References

- [1] Gardener, S. D.; Hofiund, G. B.; Upchurch, B. T.; Schryer, D. R.; Kielin E. J.; Schryer, J.; J. Catal.1991, 129,114.
- [2] Kobayashi, T.; Haruta M.; Sauno H.; Nakone, S. M.; Actuators Soc. Auto. Wng. 1988, 3, 339.
- [3] Kobayashi T.; Haruta M.; Sauno H.; Chem. Express 1989, 4, 217.
- [4] Harison P. G.; Willett M. J.; Nature 1988, 332, 337.
- [5] Stark D. S.; Crocher A.; Steward G. J.; J. Phys. E., Sci. Instrum. 1983, 16, 126.
- [6] Schryer D. R.; Upchurch B. I.; Van Norman J. D.; Brown K. G.; Schryer J.; J. Catal. 1990,122, 193.
- [7] Xu R.; Wang X.; Wang D.; Zhou K.; Li Y.; J. Catal. 2006, 237, 426.



- [8] G. Águila, F. Gracia, P. Araya, **Appl. Catal. A: In Press**, Available Online 19 March 2008
- [9] Natile M. M.; Glisenti A.; J. Mol. Catal. A: Chem. 2004, 217, 175.
- [10] X. Zheng, X. Zhang, X. Wang, S. Wang, S. Wu., Appl. Catal. A: 2005, 295, 142.
- [11] Mehandjiev D.; Naydenov A.; Ivanov G.; Appl. Catal. A: 2001, 206, 13.
- [12] Liotta L. F.; Pantaleo G.; Macaluso A.; Di Carlo G.; Deganello G.; Appl. Catal. A: 2003, 245, 167.
- [13] Wojciechowska M.; Przysajko W.; Zieliński M.; *Catal. Today*, 119, 2007, 338
- [14] Kang M.; Park E. D.; Mankim J.; Yie E.; Catal. Today 2006, 111, 236.
- [15] Youssef A. M.; El-Sharkawy E. A.; Adsorption Sci. & Technol. 1995, 12, 335.
- [16] Liqiang J.; Baifua X.; Fulonga Y.; Baiqib W.; Keyinga S.; Weiminb C.; Hongganga F.; Appl. Catal. A: 2004, 275, 49.
- [17] Yu Y.; Li W. Z.; Martin G. A.; Mirodatos C.; Appl. Catal. A: 1997, 158, 201.
- [18] Haruta M., Yamada N., Kobayashi T., Iijima S., J. Catal. 115, 1989, 301.
- [19] El-Sharkawy E. A., *MonatShefte für Chemie Chemical Monthly* 137, 2006, 1487.
- [20] Selim M.M., El-Aihy M.K., *Mater. Lett.* 21, 1994, 265.
- [21] Morales M. R., Barbero B. P., Cadús L. E., *Fuel*, 87, 2008, 1177.
- [22] El-Sharkawy E.A., Khder A.S., Ahmed A.I., *Microporous and Mesoporous Materials*, 102, 2007, 28.
- [23] El-Sharkawy E. A., Al-Shihry S. S., Ahmed A. I., *Adsorption Sci. & Technol.* 21, 2004, 863.
- [24] Fazle Kibria A.K.M., Tarafdar S.A., *Int. J. Hyd. Energy* 27, 2002, 879.
- [25] Bocca C., Barbucci A., Delucchi M., Cerisola G., *Int. J. Hyd. Energy* 24, 1999, 21.
- [26] XRPD files' Alphabetical Index for Inorganic Compounds' JCPDS International Center for Diffraction Data, 1978.
- [27] Csete de Györgyfalva G. D. C., Reaney I. M., *J. European Ceramic Soc.* 21, 2001, 2145.
- [28] Henmi H., Mori M., Hirayama T., Mizutani N., Kato M., *Thermochimica Acta* 104, 1986, 101.
- [29] Mansour S. A. A., *Thermochimica Acta* 228, 15, 1993, 155.
- [30] Hassan N.A., Shaheen W.M., Selim M.M., *International Conference on Chemistry and Its Role in Development*, Mansoura, Egypt, April 1997.
- [31] Selim M.M., Khalil L.B., *Revista de Qumica Teoricay Aplicada, AFINIDAD*, 48, 1991, 167.
- [32] Selim M.M., El-Aiashy M.K., *Materials Letters* 21, 1994, 265.
- [33] Edison I., *Handbook for Electricity metering*, 8<sup>th</sup> edn., Washington, DC, 1981.
- [34] Klup J.L., Kononov T., *Röntgen miner Syrya* 1, 1962, 120.
- [35] Borekov G. K., in: J. R. Anderson, M. Boudart [Eds.], *Catalysis: Sci., Technol.*, vol. 3, Springer-Verlag, Berlin/Heidelberg, 1982, p. 40.
- [36] Haruta M., Date M., *Appl. Catal. A*: 222, 2001, 427.
- [37] Ford P. C., Rokicki A., *Adv. Organomet. Chem.* 28, 1988, 139.
- [38] Gross D. F., Ford P. C., *J. Am. Chem. Soc.* 107, 1985, 585.
- [39] Costello C. K., Kung M. C., Oh H.-S., Wang Y., Kung H. H., *Appl. Catal. A*: 232, 2002, 159.

## Synthesis and Reactions of Some Novel Quinoxalines Derivatives

Haya A. Abubshait

Department of Chemistry, College of Medicine, King Faisal University, Dammam  
P.O.Box. 11718, Dammam 31463,  
Kingdome of Saudi Arabia; e-mail: [hAbubshait@kfu.edu.sa](mailto:hAbubshait@kfu.edu.sa)

### Abstract

Novel quinoxaline derivatives were synthesized by reactions of 4-methylphenylene-diamine **1** with  $\alpha$ -dicarbonyls, arylidene pyruvic acids and aryl pyruvates, to give compounds **3a-d** and **6a-c**, respectively. Quinoxalines **6a-c** were converted into dihydropyridazino[3,4-*b*]quinoxalines **8a-c**, thieno[2,3-*b*]quinoxalines **9a-c** and dichloroquinoxalines **10a-c**, by reactions with  $\text{NH}_2\text{-NH}_2$ ,  $\text{P}_2\text{S}_5$  and  $\text{POCl}_3$ , respectively. Compounds **10a-c** were converted into ethoxyquinoxalines **11a-c**, arylaminoquinoxalines **12a-c** and quinoxalino[2,1-*b*]quinazoline **13a-c**, on reactions with  $\text{CH}_3\text{CH}_2\text{Na}$ , aromatic amine and  $\text{POCl}_3$ , respectively. Reactions of **10a-c** with semicarbazide and sodium azide were also described.

**Keywords;** quinoxaline, *o*-phenylenediamine,  $\alpha$ -dicarbonyls, quinazoline, syntheses

### 1. Introduction

Among the various classes of nitrogen containing heterocyclic compounds, quinoxaline derivatives are important compounds with several pharmacological properties [1,2]. Although rarely found in nature, synthetic quinoxaline ring is a part of a number of antibiotics such as echinomycin, lermycin, and actinomycin, which inhibit the growth of gram positive bacteria, and are also active against various transplantable tumors [3]. Numerous publications have described of the synthesis of quinoxalines possessing a variety of pharmacological activities, such as, DNA cleaving agent [4], anti-HIV agent [5] and NMDA receptor antagonists [6].

A number of synthetic strategies have been described for the synthesis of substituted quinoxalines; the most common one is the condensation of an aryl 1,2-diamine with 1,2-dicarbonyl compounds [7-9]. However, many improved methods have been reported for the synthesis of quinoxalines using catalytic amounts of

various metal precursors, acids, and zeolites [10,11]. In addition reports were also available for with microwave [12,13] and solid phase synthesis of these compounds [14,15].

### 2. Experimental

4-methylphenylene-diamine, aromatic amines were purchased from Sigma-Aldrich Company and used without further purification. Compounds **2a-d** and **5a-c** were synthesized according to literature [16]. 6-methyl-3-styryl-1*H*-quinoxalin-2-one, and, **3a** 6-methyl-3-(2-oxo-2-phenylethyl)-1*H*-quinoxalin-2-one, **6a**, were synthesized as described previously [17,18]. Solvents were purified using the general methods.

### Material and Methods

Melting points (uncorrected) were recorded on *Buchi* 510 apparatus. IR spectra were recorded as KBr discs on

Perkin-Elmer 383 spectrometer and FTIR-spectrometer Nicolet, impact 400.  $^1\text{H}$ -NMR and  $^{13}\text{C}$ -NMR spectra were obtained on a Bruker Ac 200F and Ac 250, DRX 400 instrument at room temperature using TMS as internal standard in ( $\text{DMSO-d}_6$ ). Mass spectra were determined at 70 eV by using AEI MS 30 mass spectrometer. Elemental analyses were recorded on LECO-Analyser CHNS-932.

### Synthesis of 3-Styrylquinoxalines 3a-d

#### General Method

A mixture of **1** (0.01 mole) and the appropriate arylidenepyruvic acid **2a-d** (0.01 mole) in acetic acid (20 mL) was refluxed for 2 hr, and then cooled. The precipitate obtained was filtered and crystallized from ethanol:

6-Methyl-3-styryl-1*H*-quinoxalin-2-one, **3a** [17]

3-[2-(2-Chlorophenyl)-vinyl]-6-methyl-1*H*-quinoxalin-2-one, **3b**:  $^1\text{H}$  NMR  $\delta$  ppm, 2.6 (s, 3H,  $\text{CH}_3$ ), 7.54-7.60 (m,

7H, Ar), 7.95 (d, 1H, =CH), 8.03 (d, 1H, CH), 10.49 (s, 1H, NH);  $^{13}\text{C}$  NMR  $\delta$  ppm, 22.9 (1C,  $\text{CH}_3$ ), 118 (1C,  $\text{C}=\text{C}-\text{Cl}$ ), 128.5-140.3 (13C, Ar,  $\text{C}=\text{C}-\text{Cl}$ ,  $\text{C}-\text{Cl}$ ), 153 (1C,  $\text{C}=\text{N}$ ), 179.2 (1C,  $\text{C}=\text{O}$ ).

6-Methyl-3-[2-(3-nitrophenyl)-vinyl]-1*H*-quinoxalin-2-one, **3c**:  $^1\text{H}$  NMR  $\delta$  ppm, 2.6 (s, 3H,  $\text{CH}_3$ ), 7.32-8.50 (m, 7H, Ar), 7.95 (d, 1H, =CH), 8.05 (d, 1H, CH), 10.52 (s, 1H, NH);  $^{13}\text{C}$  NMR  $\delta$  ppm, 22 (1C,  $\text{CH}_3$ ), 121.5-135.8 (13C, Ar,  $\text{C}=\text{C}$ ), 152.6 (1C,  $\text{C}-\text{NO}_2$ ), 154 (1C,  $\text{C}=\text{N}$ ), 179.5 (1C,  $\text{C}=\text{O}$ ).

3-[2-(4-Dimethylaminophenyl)-vinyl]-6-methyl-1*H*-quinoxalin-2-one, **3d**:  $^1\text{H}$  NMR  $\delta$  ppm, 2.6, 3.01 (s, 9H,  $\text{CH}_3$ ), 6.54-7.5 (m, 7H, Ar), 7.94 (d, 1H, =CH), 8.03 (d, 1H, CH), 11.2 (s, 1H, NH);  $^{13}\text{C}$  NMR  $\delta$  ppm, 21.8 (1C,  $\text{CH}_3$ ), 45.1 (2C, N- $\text{CH}_3$ ), 121.6-141.25 (14C, Ar,  $\text{C}=\text{C}$ ), 155 (1C,  $\text{C}=\text{N}$ ), 180 (1C,  $\text{C}=\text{O}$ ). Physical, analytical and spectral data of the synthetic compounds **3b-d** are listed in Table 1.

**Table 1: Elemental, Spectral and Physical Properties of the Synthetic Compounds 3b-d.**

Compd.	Colour	Yield%	m.p [ $^{\circ}\text{C}$ ]	Formula (molecular mass)	Microanalysis Calcd./found			IR (Selected bands) $\text{cm}^{-1}$
					C%	H%	N%	
<b>3b</b>	Brown	92	234-235	$\text{C}_{17}\text{H}_{13}\text{N}_2\text{OCl}$ ( 296.75)	68.81 68.82	4.42 4.40	9.44 9.42	3161 (NH), 3062 (CH, Ar), 2923, 2854 (CH, Aliph.), 1681 (C=O), 1601 (C=N)
<b>3c</b>	Brown	89	250-251	$\text{C}_{17}\text{H}_{13}\text{N}_3\text{O}_3$ ( 307.30)	66.44 66.40	4.26 4.20	13.67 13.72	3162 (NH), 3062 (CH, Ar), 2925, 2850 (CH, Aliph.), 1662 (C=O), 1600 (C=N)
<b>3d</b>	Brown	84	+300	$\text{C}_{19}\text{H}_{19}\text{N}_3\text{O}$ ( 305.37)	74.73 74.80	6.27 6.27	13.67 13.85	3163 (NH), 3013 (CH, Ar), 2923, 2854 (CH, Aliph.), 1661 (C=O), 1609 (C=N)

### Synthesis of 3-Benzoylmethylquinoxalines 6a-c

#### General Method

A mixture of **1** (0.01 mole) and the appropriate ethylarylpypuvate **5a-c** (0.01 mole) in acetic acid (30 mL) was refluxed for 3 hr, and then cooled. The precipitate obtained was filtered and crystallized from ethanol:

6-Methyl-3-(2-oxo-2-phenylethyl)-1*H*-quinoxalin-2-one, **6a** [18].

3-[2-(4-Chlorophenyl)-2-oxoethyl]-6-methyl-1*H*-quinoxalin-2-one, **6b**:  $^1\text{H}$  NMR  $\delta$  ppm, 2.57 (s, 3H,  $\text{CH}_3$ ), 6.76 (s, 1H, CH), 7.02-7.96 (m, 7H, Ar), 12.00 (s, 1H, NH), 13.76 (s, 1H, OH);  $^{13}\text{C}$  NMR  $\delta$  ppm, 22.1 (1C,  $\text{CH}_3$ ),

121.6-136.5 (11C, Ar, C=C), 141 (1C, C-Cl), 144.5 (1C, C=C-OH), 154.7 (1C, C=N), 188 (2C, C=O).

6-Methyl-3-[2-(4-methylphenyl)-2-oxoethyl]-1*H*-quinoxalin-2-one, **6c**: <sup>1</sup>H NMR δ ppm, 2.36, 2.58 (s, 6H, CH<sub>3</sub>) 6.76 (s, 1H, CH), 6.95-7.87 (m, 7H, Ar), 11.96 (s,

1H, NH), 13.7 (s, 1H, OH); <sup>13</sup>C NMR δ ppm, 20.61, 22.5 (2C, CH<sub>3</sub>), 88.5 (1C, CH=C-OH), 121.6-136.5 (12C, Ar), 145.5 (1C, C=C-OH), 155.8 (1C, C=N), 188.2 (1C, C=O). Physical, analytical and spectral data of the synthetic compounds **6b-c** are listed in Table 2.

**Table 2: Elemental, Spectral and Physical Properties of the Synthetic Compounds 6b-c.**

Compd	Colour	Yield%	m.p [°C]	Formula (molecular mass)	Microanalysis Calcd./found			IR (Selected bands) cm <sup>-1</sup>
					C%	H%	N%	
<b>6b</b>	Orange	89	275-376	C <sub>17</sub> H <sub>13</sub> N <sub>2</sub> O <sub>2</sub> Cl (312.75)	65.29 65.25	4.19 4.20	8.96 9.01	3420 (OH), 3167 (NH), 3062 (CH, Ar), 2918, 2853 (CH, Aliph.), 1677 (C=O), 1597 (C=N)
<b>6c</b>	Yellow	80	245-247	C <sub>18</sub> H <sub>16</sub> N <sub>2</sub> O <sub>2</sub> (292.33)	73.95 74.02	5.52 5.49	9.58 9.61	3411 (OH), 3161(NH), 3054 (CH, Ar), 2918, 2851 (CH, Aliph.), 1677 (C=O), 1599 (C=N)

### Synthesis of 1,2-Dihydropyridazino[3,4-*b*]quinoxalines **8a-c**

#### General Method

A mixture of hydrazine hydrate (0.01 mole) and the appropriate of compounds **6a-c** (0.01 mole) in ethanol (25 mL) was refluxed for 3hr. The precipitate obtained upon cooling and pouring into ice cooled water was collected by filtration and crystallized from ethanol:

6-Methyl-3-phenyl-1,2-dihydropyridazo[3,4-*b*]quinoxaline, **8a**: <sup>1</sup>H NMR δ ppm, 2.61 (s, 3H, CH<sub>3</sub>), 2.99 (d, 1H, NH), 3.89 (d, 1H, NH), 6.5 (s, 1H, CH), 6.7-7.8 (m, 8H, Ar); <sup>13</sup>C NMR δ ppm, 21.9 (1C, CH<sub>3</sub>), 96.8 (1C, CH=C), 126.2-140.1 (12C, Ar), 144.6 (1C, C=N), 151.8 (1C, C=C-N), 157.5 (1C, N-C=N).

3-(4-Chlorophenyl)-6-methyl-1,2-dihydropyridazo[3,4-*b*]quinoxaline, **8b**: <sup>1</sup>H NMR δ ppm, 2.60 (s, 3H, CH<sub>3</sub>), 3.01, 3.91 (br, 2H, NH), 6.5 (s, 1H, CH), 6.67-7.78 (m, 7H, Ar); <sup>13</sup>C NMR δ ppm, 21.9 (1C, CH<sub>3</sub>), 96.8 (1C, CH=C), 126.2-140.1 (12C, Ar, C-Cl), 144.6 (1C, C=N), 151.8 (1C, C=C-N), 157.5 (1C, N-C=N).

3-(4-Methylphenyl)-6-methyl-1,2-dihydropyridazo[3,4-*b*]quinoxaline, **8c**: <sup>1</sup>H NMR δ ppm, 2.40, 2.61 (s, 6H, CH<sub>3</sub>), 3.00, 3.79 (br, 2H, NH), 6.5 (s, 1H, CH), 6.52-7.79 (m, 7H, Ar); <sup>13</sup>C NMR δ ppm, 21.8, 23.1 (2C, CH<sub>3</sub>), 96.8 (1C, CH=C), 126.2-136.9 (12C, Ar), 144.6 (1C, C=N), 151.8 (1C, C=C-N), 157.5 (1C, N-C=N). Physical, analytical and spectral data of the synthetic compounds **8a-c** are listed in Table 3.

**Table 3: Elemental, Spectral and Physical Properties of the Synthetic Compounds 8a-c.**

Compd	Colour	Yield%	m.p [°C]	Formula (molecular mass)	Microanalysis Calcd./found			IR (Selected bands) cm <sup>-1</sup>
					C%	H%	N%	
<b>8a</b>	Pink	65	190-192	C <sub>17</sub> H <sub>14</sub> N <sub>4</sub> ( 274.32)	74.43 74.50	5.14 5.19	20.42 20.50	3307, 3263 (NH), 3028 (CH, Ar), 2917, 2851 (CH, Aliph.), 1659 (C=N)
<b>8b</b>	Red	71	212-214	C <sub>17</sub> H <sub>13</sub> N <sub>4</sub> Cl ( 308.76)	66.13 66.20	4.24 4.21	18.15 18.20	3316, 3253 (NH), 3029 (CH, Ar), 2917, 2848 (CH, Aliph.), 1660 (C=N)
<b>8c</b>	Red	69	224-225	C <sub>18</sub> H <sub>16</sub> N <sub>4</sub> ( 288.35)	74.98 75.01	5.59 5.60	19.43 19.49	3309, 3261 (NH), 3031 (CH, Ar), 2915, 2850 (CH, Aliph.), 1662 (C=N)

**Synthesis of Thieno[2, 3-*b*]quinoxalines 9a-c****General Method**

A mixture of P<sub>2</sub>S<sub>5</sub> (0.01 mole) and the appropriate quinoxalines **6a-c** (0.01mole) in dry pyridine (30 mL) was refluxed for 3 hr. The precipitate obtained upon cooling and acidification with HCl (10 mL, 20%) was collected and crystallized from methanol:

6-Methyl-2-phenylthieno[2,3-*b*]quinoxaline, **9a**: <sup>1</sup>H NMR δ ppm, 2.41 (s, 3H, CH<sub>3</sub>), 6.92 (s, 1H, CH), 6.98-8.07 (m, 8H, Ar); <sup>13</sup>C NMR δ ppm, 20.1 (1C, CH<sub>3</sub>), 122.8-140.7 (13C, Ar), 142.6 (1C, C=C-S), 143.7 (1C, N=C-S), 144.6 (1C, C=N).

2-(4-Chlorophenyl)-6-methylthieno[2,3-*b*]quinoxaline, **9b**:

<sup>1</sup>H NMR δ ppm, 2.40 (s, 3H, CH<sub>3</sub>), 6.89 (s, 1H, CH), 7.50-8.07 (m, 7H, Ar); <sup>13</sup>C NMR δ ppm, 20.2 (1C, CH<sub>3</sub>), 122.7-139.2 (13C, Ar, C-Cl), 142.4 (1C, C=C-S), 144.7 (1C, N=C-S), 146.6 (1C, C=N).

2-(4-Methylphenyl)-6-methylthieno[2,3-*b*]quinoxaline, **9c**:

<sup>1</sup>H NMR δ ppm, 2.26, 2.44 (s, 6H, CH<sub>3</sub>), 7.3 (s, 1H, CH), 7.50-8.07 (m, 7H, Ar); <sup>13</sup>C NMR δ ppm, 20.2, 21.8 (2C, CH<sub>3</sub>), 122.8-140.7 (13C, Ar, C-Cl), 142.4 (1C, C=C-S), 144.7 (1C, N=C-S), 146.6 (1C, C=N). Physical, analytical and spectral data of the synthetic compounds **9a-c** are listed in Table 4.

**Table 4: Elemental, Spectral and Physical Properties of the Synthetic Compounds 9a-c.**

Compd	Colour	Yield%	m.p [°C]	Formula (molecular mass)	Microanalysis Calcd./found			IR (Selected bands) cm <sup>-1</sup>
					C%	H%	N%	
<b>9a</b>	Red	67	208-210	C <sub>17</sub> H <sub>12</sub> N <sub>2</sub> S (276.36)	73.88 73.98	4.38 4.35	10.14 10.20	3055 (CH, Ar), 2919, 2851 (CH, Aliph.), 1599 (C=N)
<b>9b</b>	Red	61	203-205	C <sub>17</sub> H <sub>11</sub> N <sub>2</sub> SCl (310.80)	65.70 65.50	3.57 3.59	9.01 8.98	3091 (CH, Ar), 2917, 2847 (CH, Aliph.), 1603 (C=N)
<b>9c</b>	Red	63	174-175	C <sub>18</sub> H <sub>14</sub> N <sub>2</sub> S (290.38)	74.45 74.50	4.86 4.90	9.65 9.77	3049 (CH, Ar), 2923, 2850 (CH, Aliph.), 1596 (C=N)

**Synthesis of Dichloroquinoxalines 10a-c****General Method**

A mixture of appropriate quinoxalines **6a-c** (0.01mole) and POCl<sub>3</sub> (0.03 mole) was refluxed for 4hr. The precipitate obtained upon cooling and pouring into ice cooled water was collected by filtration and crystallized from benzene:

2-Chloro-3-(2-chloro-2-phenyl-vinyl)-6-ethylquinoxaline, **10a**: <sup>1</sup>H NMR δ ppm, 2.59 (s, 3H, CH<sub>3</sub>), 6.89 (s, 1H, CH), 7.53-8.11 (m, 8H, Ar); <sup>13</sup>C NMR δ ppm, 21.91 (1C, CH<sub>3</sub>), 118.7 (1C, CH=C), 126.4-140.5 (13C, Ar, C=C-Cl), 146.5 (1C, N=C-Cl), 154.3 (1C, C=C-N).

2-Chloro-3-[2-chloro-2-(4-chlorophenyl)-vinyl]-6-methylquinoxaline, **10b**: <sup>1</sup>H NMR δ ppm, 2.59 (s, 3H, CH<sub>3</sub>), 7.33 (s, 1H, CH), 7.55-8.11 (m, 7H, Ar); <sup>13</sup>C NMR δ ppm, 21.8 (1C, CH<sub>3</sub>), 118.7 (1C, CH=C), 127.3-139.1

(13C, Ar, C=C-Cl), 146.5 (1C, N=C-Cl), 154.3 (1C, C=C-N).

2-Chloro-3-[2-chloro-2-(4-methylphenyl)-vinyl]-6-methylquinoxaline, **10c**: <sup>1</sup>H NMR δ ppm, 2.35, 2.59 (s, 6H, CH<sub>3</sub>), 7.33 (s, 1H, CH), 7.53-8.21 (m, 7H, Ar); <sup>13</sup>C NMR δ ppm, 21.4, 22.3 (2C, CH<sub>3</sub>), 118.5 (1C, CH=C), 126.5-139.1 (13C, Ar, C=C-Cl), 146.5 (1C, N=C-Cl), 154.3 (1C, C=C-N). Physical, analytical and spectral data of the synthetic compounds **10a-c** are listed in Table 5.

**Table 5: Elemental, Spectral and Physical Properties of the Synthetic Compounds 10a-c**

Compd	Colour	Yield%	m.p [°C]	Formula (molecular mass)	Microanalysis Calcd./found			IR (Selected bands) cm <sup>-1</sup>
					C%	H%	N%	
<b>10a</b>	Green	90	115-116	C <sub>17</sub> H <sub>12</sub> N <sub>2</sub> Cl <sub>2</sub> (315.20)	64.78 64.81	3.84 3.90	8.89 9.00	3056 (CH, Ar), 2918, 2854 (CH, Aliph.), 1614 (C=N)
<b>10b</b>	Green	91	118-120	C <sub>17</sub> H <sub>11</sub> N <sub>2</sub> Cl <sub>3</sub> (349.64)	58.40 58.31	3.17 3.20	8.01 7.79	3024 (CH, Ar), 2915, 2853 (CH, Aliph.), 1604 (C=N)
<b>10c</b>	Green	89	117-119	C <sub>18</sub> H <sub>14</sub> N <sub>2</sub> Cl <sub>2</sub> (329.22)	65.67 66.61	4.29 4.30	8.51 8.45	3059 (CH, Ar), 2918, 2853 (CH, Aliph.), 1605 (C=N)

**Synthesis of 2-Ethoxyquinoxalines 11a-c****General Method**

A mixture of the appropriate **10a-c** (0.01mole) and sodium ethoxide (0.03 mole) was refluxed for 8hr. The precipitate obtained upon dilution was collected by filtration and crystallized from ethanol:

3-(2-Chloro-2-phenyl-vinyl)-2-ethoxy-6-

methylquinoxaline, **11a**:  $^1\text{H}$  NMR  $\delta$  ppm, 1.46 (t, 3H,  $\text{CH}_3$ ), 2.59 (s, 3H,  $\text{CH}_3$ ), 4.54 (q, 2H,  $\text{CH}_2$ ), 7.32 (s, 1H, CH), 7.50-7.99 (m, 8H, Ar);  $^{13}\text{C}$  NMR  $\delta$  ppm, 14.3, 21.1 (2C,  $\underline{\text{CH}_3}$ ), 70.2 (1C,  $\underline{\text{CH}_2\text{-O}}$ ) 118.7 (1C,  $\underline{\text{CH}=\text{C}}$ ), 126.2-138.2 (13C, Ar,  $\text{C}=\underline{\text{C}}\text{-Cl}$ ), 146.4 (1C,  $\underline{\text{C}=\text{N}}$ ), 172.6 (1C,  $\text{N}=\underline{\text{C}}\text{-O}$ ).

3-[2-Chloro-2-(4-chlorophenyl)-vinyl]-2-ethoxy-6-

methylquinoxaline, **11b**:  $^1\text{H}$  NMR  $\delta$  ppm, 1.45 (t, 3H,  $\text{CH}_3$ ), 2.60 (s, 3H,  $\text{CH}_3$ ), 4.53 (q, 2H,  $\text{CH}_2$ ), 7.32 (s, 1H, CH), 7.50-7.99 (m, 7H, Ar);  $^{13}\text{C}$  NMR  $\delta$  ppm, 14.3, 20.8 (2C,  $\underline{\text{CH}_3}$ ), 70.2 (1C,  $\underline{\text{CH}_2\text{-O}}$ ) 118.7 (1C,  $\underline{\text{CH}=\text{C}}$ ), 126.2-

138.2 (13C, Ar,  $\text{C}=\underline{\text{C}}\text{-Cl}$ ,  $\underline{\text{C}}\text{-Cl}$ ), 146.4 (1C,  $\underline{\text{C}=\text{N}}$ ), 172.6 (1C,  $\text{N}=\underline{\text{C}}\text{-O}$ ).

3-[2-Chloro-2-(4-methylphenyl)-vinyl]-2-ethoxy-6-

methylquinoxaline, **11c**:  $^1\text{H}$  NMR  $\delta$  ppm, 1.46 (t, 3H,  $\text{CH}_3$ ), 2.35 (s, 3H,  $\text{CH}_3$ ), 2.61 (s, 3H,  $\text{CH}_3$ ), 4.54 (q, 2H,  $\text{CH}_2$ ), 7.32 (s, 1H, CH), 7.50-8 (m, 7H, Ar);  $^{13}\text{C}$  NMR  $\delta$  ppm, 14.3, 20.9 (3C,  $\underline{\text{CH}_3}$ ), 70.2 (1C,  $\underline{\text{CH}_2\text{-O}}$ ) 118.7 (1C,  $\underline{\text{CH}=\text{C}}$ ), 126.1-137.6 (13C, Ar,  $\text{C}=\underline{\text{C}}\text{-Cl}$ ), 172.6 (1C,  $\text{N}=\underline{\text{C}}\text{-O}$ ), 146.4 (1C,  $\underline{\text{C}=\text{N}}$ ). Physical, analytical and spectral data of the synthetic compounds **11a-c** are listed in Table 6.

**Table 6: Elemental, Spectral and Physical Properties of the Synthetic Compounds 11a-c.**

Compd	Colour	Yield%	m.p [°C]	Formula (molecular mass)	Microanalysis			IR (Selected bands) cm <sup>-1</sup>
					Calcd./found			
					C%	H%	N%	
11a	Yellow	80	190-191	C <sub>19</sub> H <sub>17</sub> N <sub>2</sub> OCl (324.80 )	70.26	5.28	8.62	3055 (CH, Ar), 2922, 2850 (CH, Aliph.), 1614 (C=N)
					70.32	5.29	8.60	
11b	Yellow	86	195-196	C <sub>19</sub> H <sub>16</sub> N <sub>2</sub> OCl <sub>2</sub> (359.25)	63.52	4.49	7.80	3026 (CH, Ar), 2920, 2854 (CH, Aliph.), 1603 (C=N)
					63.49	4.42	7.84	
11c	Yellow	77	205-207	C <sub>20</sub> H <sub>19</sub> N <sub>2</sub> OCl (338.83)	70.90	5.65	8.27	3051(CH, Ar), 2919,2853 (CH, Aliph.), 1619 (C=N)
					70.87	5.55	8.34	

### Synthesis of 2-Arylaminoquinoxalines **12a-f**

#### General Method

A mixture of appropriate **10a-c** and the appropriate aromatic amine namely; aniline, anthranilic acid (0.01mole) and triethylamine (TEA) in ethanol (25 mL) was refluxed for 8hr. The precipitate obtained upon cooling and pouring into ice cooled water was collected by filtration and crystallized from toluene:

[3-(2-Chloro-2-phenyl-vinyl)-6-methylquinoxalin-2-yl]-phenylamine, **12a**:  $^1\text{H}$  NMR  $\delta$  ppm, 2.59 (s, 3H,  $\text{CH}_3$ ), 6.77 (s, 1H, CH), 7.01-8.85 (m, 13H, Ar), 11.99 (s, 1H, NH);  $^{13}\text{C}$  NMR  $\delta$  ppm, 20.9 (1C,  $\underline{\text{CH}}_3$ ), 118.7 (1C,  $\underline{\text{CH}}=\text{C}$ ), 126.2-140.1 (18C, Ar,  $\text{C}=\underline{\text{C}}\text{-Cl}$ ), 144.6 (1C,  $\underline{\text{C}}=\text{N}$ ), 146.7 (1C,  $\text{C}=\underline{\text{C}}\text{-NH}$ ), 157.5 (1C,  $\text{N}=\underline{\text{C}}\text{-N}$ ).

{3-{3-[2-Chloro-2-(4-chlorophenyl)-vinyl]-6-methylquinoxalin-2-yl}-phenylamine, **12b**:  $^1\text{H}$  NMR  $\delta$  ppm, 2.59 (s, 3H,  $\text{CH}_3$ ), 6.55 (s, 1H, CH), 6.76-8.56 (m, 12H, Ar), 11.99 (s, 1H, NH);  $^{13}\text{C}$  NMR  $\delta$  ppm, 20.8 (1C,  $\underline{\text{CH}}_3$ ), 118.7 (1C,  $\underline{\text{CH}}=\text{C}$ ), 126.2-140 (18C, Ar,  $\text{C}=\underline{\text{C}}\text{-Cl}$ ), 144.6 (1C,  $\underline{\text{C}}=\text{N}$ ), 146.6 (1C,  $\text{C}=\underline{\text{C}}\text{-NH}$ ), 157.5 (1C,  $\text{N}=\underline{\text{C}}\text{-N}$ ).

{3-[2-Chloro-2-(4-methylphenyl)-vinyl]-6-methylquinoxalin-2-yl}-phenylamine, **12c**:  $^1\text{H}$  NMR  $\delta$  ppm, 2.35, 2.58 (s, 6H,  $\text{CH}_3$ ), 6.55 (s, 1H, CH), 6.75-8.56 (m, 12H, Ar), 11.99 (s, 1H, NH);  $^{13}\text{C}$  NMR  $\delta$  ppm, 21, 23.4 (2C,  $\underline{\text{CH}}_3$ ), 118.7 (1C,  $\underline{\text{CH}}=\text{C}$ ), 126.2-140 (18C, Ar,  $\text{C}=\underline{\text{C}}\text{-Cl}$ ), 144.6 (1C,  $\underline{\text{C}}=\text{N}$ ), 146.6 (1C,  $\text{C}=\underline{\text{C}}\text{-NH}$ ), 157.5 (1C,  $\text{N}=\underline{\text{C}}\text{-N}$ ).

2-[3-(2-Chloro-2-phenyl-vinyl)-6-methylquinoxalin-2-yl]-phenylamino]-benzoic acid, **12d**:  $^1\text{H}$  NMR  $\delta$  ppm, 2.6 (s,

3H,  $\text{CH}_3$ ), 6.57 (s, 1H, CH), 6.96-8.75 (m, 12H, Ar), 11.98 (s, 1H, NH), 13.78 (s, 1H, OH);  $^{13}\text{C}$  NMR  $\delta$  ppm, 20.9 (1C,  $\underline{\text{CH}}_3$ ), 116.9 (1C,  $\underline{\text{C}}\text{-C}=\text{O}$ ), 118.7 (1C,  $\underline{\text{CH}}=\text{C}$ ), 125.2-138.4 (17C, Ar,  $\text{C}=\underline{\text{C}}\text{-Cl}$ ), 144.6 (1C,  $\underline{\text{C}}=\text{N}$ ), 148.3 (1C,  $\text{C}=\underline{\text{C}}\text{-NH}$ ), 157.5 (1C,  $\text{N}=\underline{\text{C}}\text{-N}$ ), 172 (1C,  $\underline{\text{C}}=\text{O}$ ).

2-{3-[2-Chloro-2-(4-chlorophenyl)-vinyl]-6-methylquinoxalin-2-yl}-phenylamino}-benzoic acid, **12e**:  $^1\text{H}$  NMR  $\delta$  ppm, 2.6 (s, 3H,  $\text{CH}_3$ ), 6.75 (s, 1H, CH), 7.01-8.85 (m, 11H, Ar), 11.99 (s, 1H, NH), 13.76 (s, 1H, OH);  $^{13}\text{C}$  NMR  $\delta$  ppm, 20.9 (1C,  $\underline{\text{CH}}_3$ ), 116.9 (1C,  $\underline{\text{C}}\text{-C}=\text{O}$ ), 118.7 (1C,  $\underline{\text{CH}}=\text{C}$ ), 125.2-138.4 (17C, Ar,  $\text{C}=\underline{\text{C}}\text{-Cl}$ ,  $\underline{\text{C}}\text{-Cl}$ ), 144.6 (1C,  $\underline{\text{C}}=\text{N}$ ), 148.3 (1C,  $\text{C}=\underline{\text{C}}\text{-NH}$ ), 157.5 (1C,  $\text{N}=\underline{\text{C}}\text{-N}$ ), 172 (1C,  $\underline{\text{C}}=\text{O}$ ).

2-{3-[2-Chloro-2-(4-methylphenyl)-vinyl]-6-methylquinoxalin-2-yl}-phenylamino}-benzoic acid, **12f**:  $^1\text{H}$  NMR  $\delta$  ppm, 2.36, 2.59 (s, 6H,  $\text{CH}_3$ ), 6.56 (s, 1H, CH), 7.01-8.85 (m, 11H, Ar), 11.99 (s, 1H, NH), 13.50 (s, 1H, OH);  $^{13}\text{C}$  NMR  $\delta$  ppm, 20.9, 22.9 (2C,  $\underline{\text{CH}}_3$ ), 116.9 (1C,  $\underline{\text{C}}\text{-C}=\text{O}$ ), 118.7 (1C,  $\underline{\text{CH}}=\text{C}$ ), 125.2-138.4 (17C, Ar,  $\text{C}=\underline{\text{C}}\text{-Cl}$ ), 144.6 (1C,  $\underline{\text{C}}=\text{N}$ ), 148.3 (1C,  $\text{C}=\underline{\text{C}}\text{-NH}$ ), 157.5 (1C,  $\text{N}=\underline{\text{C}}\text{-N}$ ), 172 (1C,  $\underline{\text{C}}=\text{O}$ ). Physical, analytical and spectral data of the synthetic compounds **12a-f** are listed Table 7.



**Table 7: Elemental, Spectral and Physical Properties of the Synthetic Compounds 12a-f.**

Compd	Colour	Yield%	m.p [°C]	Formula (molecular mass)	Microanalysis Calcd./found			IR (Selected bands) cm <sup>-1</sup>
					C%	H%	N%	
<b>12a</b>	Yellow	76	176-178	C <sub>23</sub> H <sub>18</sub> N <sub>3</sub> Cl (371.86)	74.29 75.20	3.57 3.48	11.46 11.52	3120 (NH), 3065 (CH, Ar), 2920, 2851 (CH, Aliph.), 1687 (C=N)
<b>12b</b>	Yellow	78	165-166	C <sub>23</sub> H <sub>17</sub> N <sub>3</sub> Cl <sub>2</sub> (406.31)	68.84 68.90	3.02 2.89	10.47 10.30	3119 (NH), 3026 (CH, Ar), 2920, 2852 (CH, Aliph.), 1678 (C=N)
<b>12c</b>	Yellow	70	172-173	C <sub>24</sub> H <sub>20</sub> N <sub>3</sub> Cl (385.89)	75.69 76.00	3.97 4.01	11.03 10.92	3129 (NH), 3055 (CH, Ar), 2919, 2854 (CH, Aliph.), 1677 (C=N)
<b>12d</b>	Yellow	68	198-200	C <sub>24</sub> H <sub>18</sub> N <sub>3</sub> O <sub>2</sub> Cl (415.87)	69.31 69.20	4.36 4.40	10.10 10.27	3433 (OH), 3121 (NH), 3055 (CH, Ar), 2919, 2851 (CH, Aliph.), 1679 (C=O), 1617 (C=N)
<b>12e</b>	Yellow	71	180-182	C <sub>24</sub> H <sub>17</sub> N <sub>3</sub> O <sub>2</sub> Cl <sub>2</sub> (450.32)	64.01 63.94	3.81 3.70	9.33 9.24	3416 (OH), 3112 (NH), 3025 (CH, Ar), 2918, 2852 (CH, Aliph.), 1678 (C=O), 1602 (C=N)
<b>12f</b>	Yellow	68	195-196	C <sub>25</sub> H <sub>20</sub> N <sub>3</sub> O <sub>2</sub> Cl (429.90)	69.85 70.02	4.69 4.43	9.77 9.90	3424 (OH), 3132 (NH), 3058 (CH, Ar), 2920, 2851 (CH, Aliph.), 1682 (C=O), 1607 (C=N)

**Synthesis of Quinazolinquinoxalines 13a-c****General Method**

A mixture of appropriate **12d-f** (0.01mole) and POCl<sub>3</sub> (15 mL) was refluxed for 2hr. The precipitate obtained upon cooling and pouring into ice cooled water was collected by filtration and crystallized from dichloromethane:

6-(2-Chloro-2-phenyl-vinyl)-3-methylquinoxalino[2,1-*b*]quinazolin-12-one, **13a**: <sup>1</sup>H NMR δ ppm, 2.58 (s, 3H, CH<sub>3</sub>), 7.17 (s, 1H, CH), 7.29-8.05 (m, 12H, Ar); <sup>13</sup>C NMR δ ppm, 20.9 (1C, CH<sub>3</sub>), 118.5 (1C, CH=C), 121.6-134.6 (18C, Ar, C=C-Cl, C-C=O, C-Cl), 143.9 (1C, C=N), 147.8 (1C, C=C-N), 156.6 (1C, N=C-N), 168 (1C, C=O).

6-[2-Chloro-2-(4-chlorophenyl)-vinyl]-3-methylquinoxalino[2,1-*b*]quinazolin-12-one, **13b**: <sup>1</sup>H NMR δ ppm, 2.59 (s, 3H, CH<sub>3</sub>), 7.15 (s, 1H, CH), 7.17- 8.01 (m,

11H, Ar); <sup>13</sup>C NMR δ ppm, 20.9 (1C, CH<sub>3</sub>), 118.5 (1C, CH=C), 121.6-134.6 (18C, Ar, C=C-Cl, C-C=O, C-Cl), 143.9 (1C, C=N), 147.8 (1C, C=C-N), 156.6 (1C, N=C-N), 168 (1C, C=O).

6-[2-Chloro-2-(4-methylphenyl)-vinyl]-3-

methylquinoxalino[2,1-*b*]quinazolin-12-one, **13c**: <sup>1</sup>H NMR δ ppm, 2.35, 2.58 (s, 6H, CH<sub>3</sub>), 7.15 (s, 1H, CH), 7.2- 8.01 (m, 11H, Ar); <sup>13</sup>C NMR δ ppm, 20.9, 22.9 (2C, CH<sub>3</sub>), 118.5 (1C, CH=C), 121.6-134.6 (18C, Ar, C=C-Cl), 143.9 (1C, C=N), 147.8 (1C, C=C-N), 156.6 (1C, N=C-N), 168 (1C, C=O). Physical, analytical and spectral data of the synthetic compounds **13a-c** are listed in Table 8.

**Table 8: Elemental, Spectral and Physical Properties of the Synthetic Compounds 13a-c**

Compd	Colour	Yield%	m.p [°C]	Formula (molecular mass)	Microanalysis Calcd./found			IR (Selected bands) cm <sup>-1</sup>
					C%	H%	N%	
<b>13a</b>	Red	80	160- 162	C <sub>24</sub> H <sub>16</sub> N <sub>3</sub> OCl (397.86)	72.45 72.39	4.05 3.96	10.56 10.45	3075 (CH, Ar), 2921, 2851 (CH, Aliph.), 1662 (C=O), 1623 (C=N)
<b>13b</b>	Red	76	155- 157	C <sub>24</sub> H <sub>15</sub> N <sub>3</sub> OCl (432.30)	66.68 66.60	3.50 3.43	9.72 9.80	3057 (CH, Ar), 2922, 2852 (CH, Aliph.), 1663 (C=O), 1621 (C=N)
<b>13c</b>	Red	69	150- 152	C <sub>25</sub> H <sub>18</sub> N <sub>3</sub> OCl (411.88)	72.90 73.02	4.40 4.39	10.20 9.99	3027 (CH, Ar), 2919, 2852 (CH, Aliph.), 1666 (C=O), 1563 (C=N)

**Synthesis of Quinoxalin-2-yl semicarbazide 14a-c****General Method**

A mixture of appropriate **10a-c** (0.01mole) and semicarbazide hydrochloride (0.01 mole), TEA (4 drops) in ethanol (30 mL) was refluxed for 8hr. The precipitate obtained upon cooling was collected by filtration and crystallized from benzene:

2-[3-(2-Chloro-2-phenyl-vinyl)-6-methylquinoxalin-2-yl]-semicarbazide, **14a**: <sup>1</sup>H NMR δ ppm, 2.59 (s, 3H, CH<sub>3</sub>), 5.36 (s, 2H, NH<sub>2</sub>), 7.09 (s, 1H, CH), 7.11-8.08 (m, 8H, Ar), 9.8 (s, 1H, NH), 10.10 (s, 1H, NH); <sup>13</sup>C NMR δ ppm, 21.1 (1C, CH<sub>3</sub>), 117.1 (1C, CH=C), 124.9-139.8 (13C, Ar, C=C-Cl), 145.1 (1C, C=N), 156.7 (1C, N=C-N), 158 (1C, HN-C=O).

2-{3-[2-Chloro-2-(4-chlorophenyl)-vinyl]-6-methylquinoxalin-2-yl}-semicarbazide, **14b**: <sup>1</sup>H NMR δ ppm, 2.59 (s, 3H, CH<sub>3</sub>), 5.36 (s, 2H, NH<sub>2</sub>), 7.10 (s, 1H,

CH), 7.19-8.07 (m, 7H, Ar), 9.9 (s, 1H, NH), 10.14 (s, 1H, NH); <sup>13</sup>C NMR δ ppm, 21.8 (1C, CH<sub>3</sub>), 118.2 (1C, CH=C), 124.8-140.1 (13C, Ar, C=C-Cl, C-Cl), 144.9 (1C, C=N), 156.5 (1C, N=C-N), 158.3 (1C, HN-C=O).

{2-[3-(2-Chloro-2-(4-methylphenyl)-vinyl)-6-

methylquinoxalin-2-yl]-semicarbazide, **14c**: <sup>1</sup>H NMR δ ppm, 2.38, 2.61 (s, 6H, CH<sub>3</sub>), 5.36 (s, 2H, NH<sub>2</sub>), 7.09 (s, 1H, CH), 6.98-7.65 (m, 7H, Ar), 9.8 (s, 1H, NH), 10.13 (s, 1H, NH); <sup>13</sup>C NMR δ ppm, 21.9, 23 (2C, CH<sub>3</sub>), 118.2 (1C, CH=C), 124.8-139.9 (13C, Ar, C=C-Cl), 144.9 (1C, C=N), 156.5 (1C, N=C-N), 158.3 (1C, HN-C=O). Physical, analytical and spectral data of the synthetic compounds

**14a-c** are listed in Table 9.

**Table 9: Elemental, Spectral and Physical Properties of the Synthetic Compounds 14a-c.**

Compd	Colour	Yield%	m.p [°C]	Formula (molecular mass)	Microanalysis			IR (Selected bands) cm <sup>-1</sup>
					Calcd./found			
					C%	H%	N%	
14a	Yellow	65	+300	C <sub>18</sub> H <sub>16</sub> N <sub>5</sub> OCl ( 353.81)	61.10	4.56	19.79	3424, 3310 (NH <sub>2</sub> ), 3256, 3186 (NH), 3064 (CH, Ar), 2920, 2874 (CH, Aliph.), 1686 (C=O), 1642 (C=N)
					61.00	4.55	19.98	
14b	Yellow	62	170- 172	C <sub>18</sub> H <sub>15</sub> N <sub>5</sub> OCl <sub>2</sub> (388.25 )	55.68	3.89	18.04	3462, 3370 (NH <sub>2</sub> ), 3279, 3118 (NH), 3029 (CH, Ar), 2921, 2853 (CH, Aliph.), 1673 (C=O), 1612 (C=N)
					55.61	3.90	17.87	
14c	Yellow	60	180- 182	C <sub>19</sub> H <sub>18</sub> N <sub>5</sub> OCl (367.83 )	62.04	4.93	19.04	3461, 3373 (NH <sub>2</sub> ), 3261, 3119 (NH), 3030 (CH, Ar), 2921, 2852 (CH, Aliph.), 1677 (C=O),1639 (C=N)
					61.93	5.01	19.20	

**Synthesis of 2-Azidoquinoxalines 15a-c:****General Method**

A mixture of appropriate **10a-c** (0.01mole) and sodium azide (0.01 mole) in acetic acid (20 mL) and n-butanol (20 mL) was stirred for 3hr, at room temperature. The precipitate obtained upon pouring into ice cooled water was collected by filtration and crystallized from ethanol:

2-Azido-3-(2-chloro-2-phenyl-vinyl)-6-methylquinoxaline, **15a**: <sup>1</sup>H NMR δ ppm, 2.59 (s, 3H, CH<sub>3</sub>), 6.91 (s, 1H, CH), 7.12-7.99 (m, 8H, Ar); <sup>13</sup>C NMR δ ppm, 21.8 (1C, CH<sub>3</sub>), 118.7 (1C, CH=C), 123.4-140.1 (13C, Ar, C=C-Cl), 144.3 (1C, C=N), 156.5 (1C, N=C-N).

2-Azido-3-[2-chloro-2-(4-chlorophenyl)-vinyl]-6-methylquinoxaline, **15b**: <sup>1</sup>H NMR δ ppm, 2.61 (s, 3H, CH<sub>3</sub>), 7.01 (s, 1H, CH), 7.13-7.94 (m, 7H, Ar); <sup>13</sup>C NMR δ ppm, 21 (1C, CH<sub>3</sub>), 118.1 (1C, CH=C), 124.1-139.8 (13C, Ar, C=C-Cl, C-Cl), 145.3 (1C, C=N), 155.4 (1C, N=C-N).

2-Azido-3-[2-chloro-2-(4-methylphenyl)-vinyl]-6-methylquinoxaline, **15c**: <sup>1</sup>H NMR δ ppm, 2.35, 2.61 (s, 6H, CH<sub>3</sub>), 6.83 (s, 1H, CH), 6.94-7.56 (m, 7H, Ar); <sup>13</sup>C NMR δ ppm, 20.8, 22.9 (2C, CH<sub>3</sub>), 118.7 (1C, CH=C), 123.4-140.1 (13C, Ar, C=C-Cl), 144.3 (1C, C=N), 156.5 (1C, N=C-N).

Physical, analytical and spectral data of the synthetic compounds **15a-c** are listed in Table 10.

**Table 10: Elemental, Spectral and Physical Properties of the Synthetic Compounds 15a-c.**

Compd	Colour	Yield%	m.p [°C]	Formula (molecular mass)	Microanalysis			IR (Selected bands) cm <sup>-1</sup>
					Calcd./found			
					C%	H%	N%	
<b>15a</b>	Brown	71	125- 126	C <sub>17</sub> H <sub>12</sub> N <sub>5</sub> Cl (321.76 )	63.46	3.76	21.77	3058 (CH, Ar), 2919, 2854 (CH, Aliph.), 2122 (N <sub>3</sub> ), 1603 (C=N)
					63.46	3.70	21.88	
<b>15b</b>	Brown	68	133- 135	C <sub>17</sub> H <sub>11</sub> N <sub>5</sub> Cl <sub>2</sub> (356.21 )	57.32	3.11	19.66	3027 (CH, Ar), 2919, 2853 (CH, Aliph.), 2129 (N <sub>3</sub> ), 1607 (C=N)
					57.40	3.15	19.70	
<b>15c</b>	Brown	65	165- 166	C <sub>18</sub> H <sub>14</sub> N <sub>5</sub> Cl (335.79 )	64.38	4.20	20.86	3091 (CH, Ar), 2920, 2853 (CH, Aliph.), 2131 (N <sub>3</sub> ), 1602 (C=N)
					64.37	4.07	20.81	

### Synthesis of Tetra-azoloquinoxalines 16a-c

#### General Method

A mixture of appropriate **10a-c** (0.01mole) and sodium azide (0.01 mole) in acetic acid (20 mL) and n-butanol (20 mL) was refluxed for 6hr. The precipitate obtained upon pouring into ice-cooled water was collected by filtration and crystallized from ethanol:

4-(2-Chloro-2-phenyl-vinyl)-7-methyl-tetrazolo[1,5-*a*]quinoxaline, **16a**:  $^1\text{H}$  NMR  $\delta$  ppm, 2.59 (s, 3H,  $\text{CH}_3$ ), 7.50 (s, 1H, CH), 7.54-8.12 (m, 8H, Ar);  $^{13}\text{C}$  NMR  $\delta$  ppm, 21 (1C,  $\underline{\text{CH}}_3$ ), 117.5 (1C,  $\underline{\text{CH}}=\text{C}$ ), 126.6-138.9 (13C, Ar,  $\text{C}=\underline{\text{C}}\text{-Cl}$ ), 140.3 (1C,  $\underline{\text{C}}=\text{N}$ ), 150.4 (1C,  $\text{N}=\underline{\text{C}}\text{-N}$ ).

4-[2-Chloro-2-(4-chlorophenyl)-vinyl]-7-methyl-tetrazolo[1,5-*a*]quinoxaline, **16b**:  $^1\text{H}$  NMR  $\delta$  ppm, 2.59 (s, 3H,  $\text{CH}_3$ ), 7.49 (s, 1H, CH), 7.53-8.10 (m, 7H, Ar);  $^{13}\text{C}$

NMR  $\delta$  ppm, 21 (1C,  $\underline{\text{CH}}_3$ ), 117.5 (1C,  $\underline{\text{CH}}=\text{C}$ ), 127.6-139 (13C, Ar,  $\text{C}=\underline{\text{C}}\text{-Cl}$ ,  $\underline{\text{C}}\text{-Cl}$ ), 140.3 (1C,  $\underline{\text{C}}=\text{N}$ ), 150.4 (1C,  $\text{N}=\underline{\text{C}}\text{-N}$ ).

4-[2-Chloro-2-(4-methylphenyl)-vinyl]-7-methyl-tetrazolo[1,5-*a*]quinoxaline, **16c**:  $^1\text{H}$  NMR  $\delta$  ppm, 2.38, 2.50 (s, 6H,  $\text{CH}_3$ ), 7.50 (s, 1H, CH), 7.52-8.10 (m, 7H, Ar);  $^{13}\text{C}$  NMR  $\delta$  ppm, 21, 23.1 (2C,  $\underline{\text{CH}}_3$ ), 117.5 (1C,  $\underline{\text{CH}}=\text{C}$ ), 126.6-138.9 (13C, Ar,  $\text{C}=\underline{\text{C}}\text{-Cl}$ ), 140.3 (1C,  $\underline{\text{C}}=\text{N}$ ), 150.4 (1C,  $\text{N}=\underline{\text{C}}\text{-N}$ ). Physical, analytical and spectral data of the synthetic compounds **16a-c** are listed in Table 11.

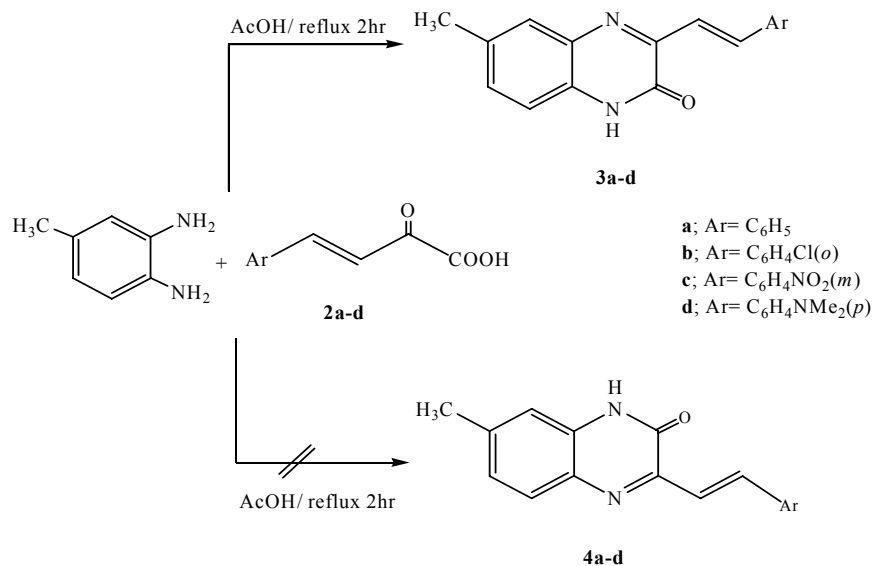
**Table 11: Elemental, Spectral and Physical Properties of the Synthetic Compounds 16a-c.**

Compd	Colour	Yield%	m.p [°C]	Formula (molecular mass)	Microanalysis Calcd./found			IR (Selected bands) $\text{cm}^{-1}$
					C%	H%	N%	
<b>16a</b>	Dark	60	180-	$\text{C}_{17}\text{H}_{12}\text{N}_5\text{Cl}$ ( 321.76)	63.46	3.76	21.77	3061 (CH, Ar), 2918, 2854 (CH, Aliph.), 1602 (C=N)
	Brown		181		63.50	3.80	21.62	
<b>16b</b>	Dark	59	140-	$\text{C}_{17}\text{H}_{11}\text{N}_5\text{Cl}_2$ ( 356.21)	57.32	3.11	19.66	3027 (CH, Ar), 2918, 2853 (CH, Aliph.), 1610 (C=N)
	Brown		141		57.40	3.01	19.57	
<b>16c</b>	Dark	63	186-	$\text{C}_{18}\text{H}_{14}\text{N}_5\text{Cl}$ ( 335.79)	64.38	4.20	20.86	3091 (CH, Ar), 2921, 2851 (CH, Aliph.), 1603 (C=N)
	Brown		188		64.35	4.21	20.90	

### 3. Results and Discussions

It was reported in the literature that 4-methylphenyldiamine **1** reacts with asymmetric  $\alpha$ -dicarbonyl to give 6-methylquinoxaline as a major product and the other isomer as minor product [19]. In the present study, following the

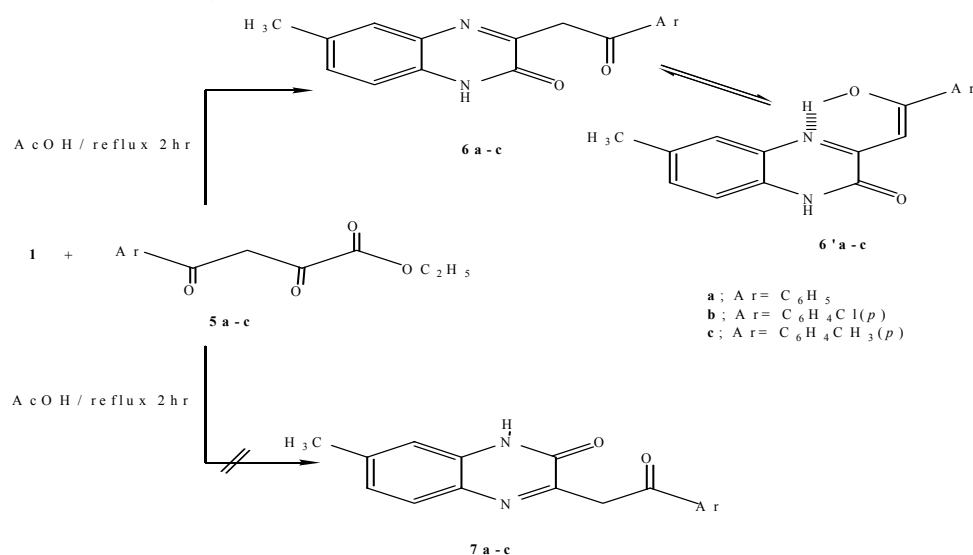
techniques [20-23]<sup>1</sup>, it was found that cyclo-condensation of arylidenepyruvic acids **2a-d** with **1** gave the corresponding 6-methylquinoxalines **3a-d**, not the other isomer **4a-d** (Scheme 1).



Scheme 1

The reaction of **1** with aryl-pyruvate **5a-c** resulted in cyclocondensation [24] to give corresponding 6-methylquinoxaline derivatives **6a-c**, not 7-methylquinoxaline derivatives **7a-c** (Scheme 2). The quinoxalines **6a-c** exist in **6'a-c** (ketonic form could not be

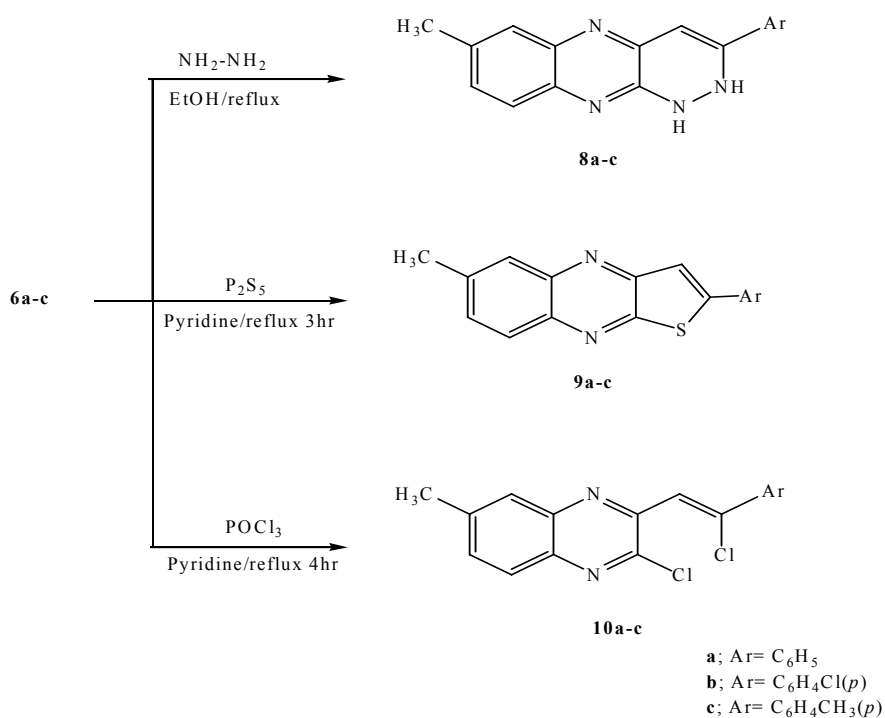
detected). Thus, the compounds **6a-c**, were confirmed by <sup>1</sup>HNMR spectrum, which lack signal for -CH<sub>2</sub>CO- in the range 3.5 and 4.5 ppm, while one proton singlet is observed at 6.76 ppm.



Scheme 2

Reaction of **6 a-c** with hydrazine hydrate<sup>[25]</sup> in ethanolic solution gave correspondingly 1,2-dihydropyridazino[3,4-*b*]quinoxaline **8a-c**, (**Scheme 3**). Reaction of quinoxaline, **6a-c** with P<sub>2</sub>S<sub>5</sub> in dry pyridine, resulted in thiation followed

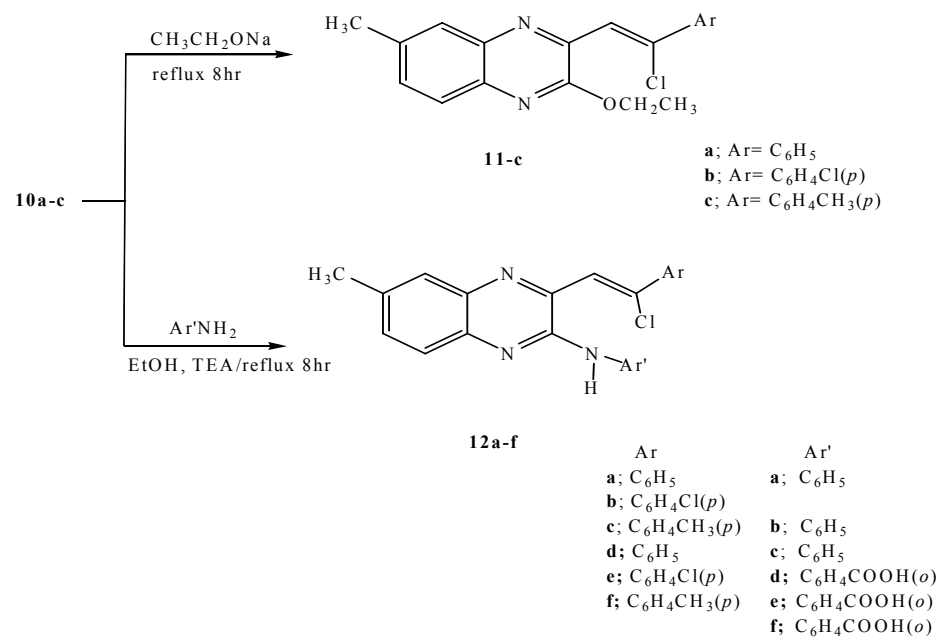
by cyclization giving thieno[2,3-*b*]quinoxaline, **9a-c** (**Scheme 3**). Reactions of **6a-c** with POCl<sub>3</sub> [26,27] gave the corresponding dichloroquinoxaline derivatives, **10a-c** (**Scheme 3**).



**Scheme 3**

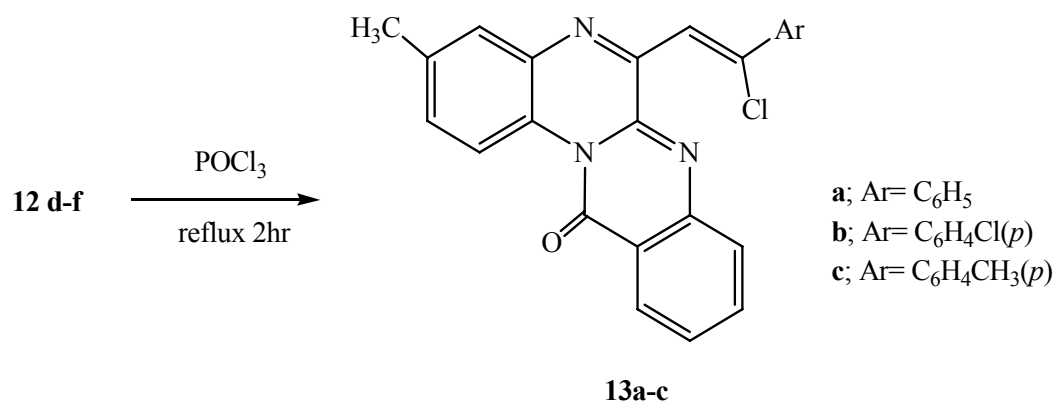
2-Chloroquinoxaline **10a-c** appears to be versatile starting compound for further functionlization and annulation of the quinoxaline ring. Thus, refluxing of 2-chloroquinoxaline, **10a-c** with sodium ethoxide [28] gave 2-ethoxyquinoxalines **11a-c** (**Scheme 4**).

Aminolysis [25] of chloroquinoxalines **10a-c** with aryl amines namely; aniline and anthranilic acid by refluxing in ethanol gave arylaminoquinoxalines, **12a-f** (**Scheme 4**).



Scheme 4

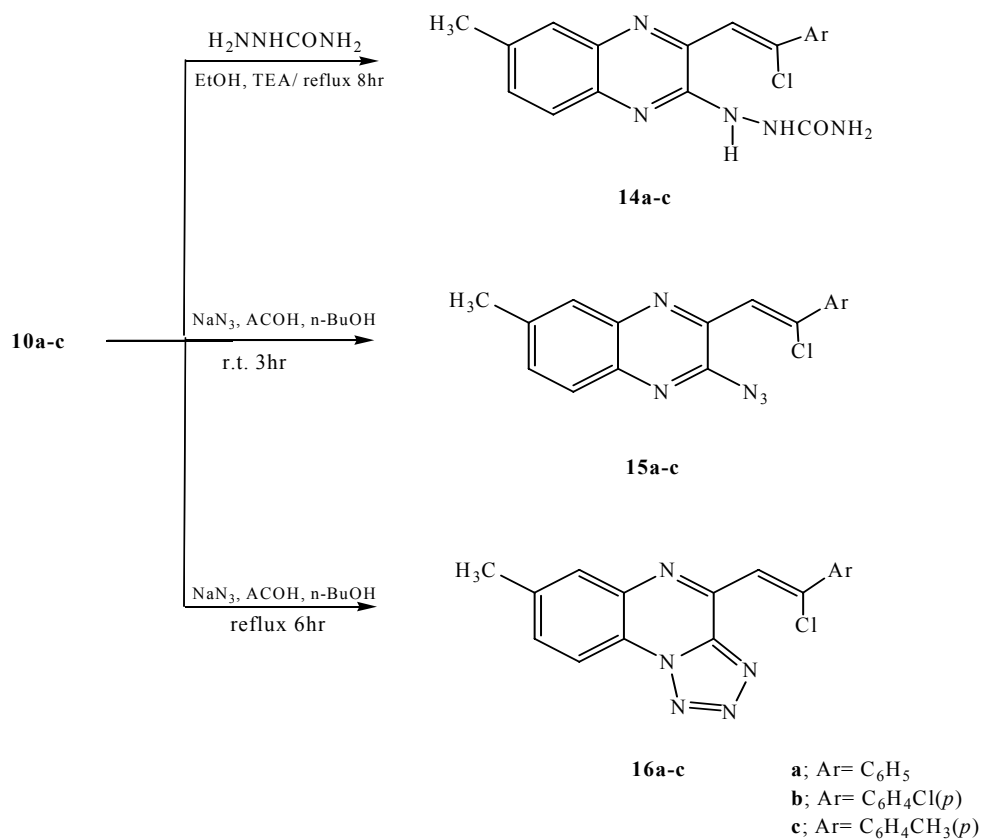
When compounds **12d-f** was allowed to react with POCl<sub>3</sub> [26] there resulted quinoxalino[2,1-*b*]quinazoline, **13a-c** (Scheme 5).



Scheme 5

The semi-carbazones, **14a-c** were obtained by the reaction of **10a-c** with semi-carbazide [25,26] (**Scheme 6**). Compounds **10a-c**, were reacted with sodium azide [29] at room temperature gave the corresponding azido derivatives, **15a-c**. Upon refluxing the compounds, **10a-c**

with sodium azide [30,31] corresponding tetra-azolo[1,5-*a*]quinoxaline derivatives, **16a-c** were formed, presumably *via* the formation of azido derivatives, **15a-c** (**Scheme 6**). The structures of **16a-c** were proved by the disappearance of azido group in IR.



**Scheme 6**

#### 4. Conclusions

Novel quinoxaline derivatives were synthesized by reactions of 4-methylphenylene-diamine **1** with  $\alpha$ -dicarbonyls to give **3a-d** and **6a-c** respectively. Quinoxalines **6a-c** were converted into dihydropyridazino[3,4-*b*]quinoxalines **8a-c**, thieno[2,3-*b*]quinoxalines **9a-c**, and dichloroquinoxalines **10a-c**, respectively. Compounds **10a-c** were converted into ethoxyquinoxalines **11a-c**, arylaminoquinoxalines **12a-c** and quinoxalino[2,1-*b*]quinazoline **13a-c** respectively. The

reaction of **10a-c** with semicarbazide and sodium azide was also described.

#### Acknowledgment

The author would like to thank Prof. H. M. Al-Hazimi, from King Saud University in Riyadh, department of chemistry, for his helpful in spectral analysis, and King Faisal University, college of Medicine, department of chemistry for special help, equipment and technical supports.



### References

- [1]. Arthur, G.; Elor, K. B.; Robert, G. S.; Guo, Z. Z.; Richard, J. P.; Stanley, D.; John, R. K.; Sean, T., J. Med. Chem. 2005, 48, 744.
- [2]. Andres, J.; Belen, Z.; Ilnacio, A.; Antonio, M., J. Med. Chem. 2005, 48, 2019.
- [3]. Bailly, C.; Echeparre, S.; Gago, F.; Waring, M., Anti-Cancer Drug Des. 1999, 15, 291.
- [4]. Louis, S.; Marc, M. G.; Jory, J. W.; Joseph, P. B., J. Org. Chem. 2003, 68, 4179.
- [5]. Keeble, J.; Al-Swayeh, O. A.; Moore, P. K., Br. J. Pharmacol. 2001, 133, 1023.
- [6]. Lin, S. K., Molecules. 1996, 1, 37.
- [7]. Vogel's Textbook of Practical Organic Chemistry, 5<sup>th</sup> ed., p1190.
- [8]. Brown, D. J.; Quinoxalines; supplement. II. The Chemistry of Heterocyclic Compound; Taylor, E. C.; Wipt, P., Eds.; John Wiley and Sons; New Jersey, 2004.
- [9]. El-Bahaie, S.; Assy, M. G.; Ibrahim, Y. A.; Kadry, A. M., Collet., Czech. Chem. Commun. 1990, 55, 1949.
- [10]. Shyamaprosad, G.; Avijit, K. A., Tetrahedron Lett. 2005, 46, 221.
- [11]. Shivaji, V.; More, M. N. V.; Sastry, M.; Chieh-Chieh, W.; Ching- Fa, Y., Tetrahedron Lett. 2005, 46, 6345.
- [12]. Wolkenberg, S. E.; Wisnoski, D. D.; Leister, W. H.; Leister, W. H.; Wang, Y.; Zhao, Z.; Lindsley, C. W., Organic Lett. 2004, 6(9), 1453.
- [13]. Zhao, Z.; Wisnoski, D. D.; Wolkenberg, S. E.; Wisnoski; Leister, W. H.; Wang, Y.; Lindsley, C. W., Tetrahedron Lett. 2004, 45, 4873.
- [14]. Orazio, A. A.; Lucia, D. C.; Paolino, F.; Fabio, M.; Stefania, S., Syn. Lett. 2003, 1183.
- [15]. Sanjay, K. S.; Priya, G.; Srinavas, D.; Bijoy, K., Syn. Lett. 2003, 2147.
- [16]. Annan, N.; Paris, R.; Jordan, F., J. Am. Chem. Soc. 1999, 111, 8895.
- [17]. Badforss, S., Univ. Lund, Swed. Ann. 1957, 609,103.
- [18]. Kamisaka, N.; Raku, N.; Ueno, K.; Nomoto, Y.; Takasaki, K.; Suda, M.; Kusaka, H.; Yano, H.; Nakanishi, S.; Matsuda, Y.; Jpn. Kokai Tokkyo Koho 2000, 74.
- [19]. Wolf, F. J.; Pfister, K.; Beutel, R. H.; Wilson, R. M.; Robinson, C. A.; Stevens, J. R., J. Am. Chem. Soc. 1949, 71, 6.
- [20]. Chebanov, V. A.; Desenko, S. M.; Sakhno, Y. I.; Panchenko, E. S.; Saraev, V. E.; Musatov, V. I.; Konev, V. F., Fiziol. Akt. Rechovini 2002, 33, 10.
- [21]. Abdel-Haby, S. A. L.; Badway, M. A.; Kadry, A. M.; Mosselhi, M. A. N., J. Heterocycl. Chem. 1987, 24, 1587.
- [22]. Abdel-Megid, M., Pharmazie. 2000, 55, 263.
- [23]. El- Maati, T. M. A., Boll. Chim. Farm. 1999, 138, 272.
- [24]. Chebanov, V. A.; Sakhno, Y. I.; Desenko, S. M.; Chernenko, V. N.; Musatov, V. I.; Shishkina, S. V.;

- Shishkin, O. V.; Kappe, C. O., *Tetrahedron* 2007, 63, 1229.
- [25]. Kim, H. S.; Jeong, W. Y.; Choi, K. O.; Lee, S. U.; Kwag, S. T.; Lee, M. K., *J. Korean Chem. Soc.* 2002, 46(1), 37.
- [26]. Banekovich, C.; Mereiter, K.; Matuszczak, B., *Tetrahedron. Lett.* 2003, 44, 9161.
- [27]. Matuszczak, B.; Pekala, E.; Muller, C. E., *Arch. Pharm. Pharm. Med. Chem.* 1998, 331, 163.
- [28]. Jeon, M. K.; Kim, D. S.; La, H. J.; Gong, Y. D., *Tetrahedron Lett.* 2005, 46, 4979.
- [29]. McManus, J. M.; Herbst, R. M., *J. Org. Chem.* 1959, 24, 1462.
- [30]. Duncia, J. V.; Pierce, M. E.; Santella, J. B., III, J. *Org. Chem.* 1991, 56, 2395.
- [31]. Wittenberg, S. J.; Donner, B. G., *J. Org. Chem.* 1993, 58, 4139.

## Synthesis and Characterization of the Gallosilicate Mesoporous Molecular sieve Ga-SBA-15

**L. CHERIF\*, R. BOURI\*, K. SAIDI\*, A. BENGUEDDACH\*\*, J. FRAISSARD\*\*\***

*\* Laboratoire de Catalyse et Synthèse en Chimie Organique, Université de Tlemcen BP 119, Algérie*

*E-mail : [cherifleila@hotmail.com](mailto:cherifleila@hotmail.com)*

*\*\*Laboratoire de Chimie des Matériaux, Université d'Oran, Algérie*

*\*\*\*Laboratoire de Chimie des Surfaces, Université P. et M. Curie, Paris VI, France*

### Abstract

Our research is a contribution to the study of mesoporous materials SBA-15 (nanostructure) and their modifications during the direct synthesis or post-synthesis in order to modify their acidity for their applications in catalysis. We have studied the incorporation of gallium in mesoporous silica SBA-15 via two ways: direct synthesis and post-synthesis. Characterization by X-ray diffraction, nitrogen adsorption, FT-IR spectroscopy and thermogravimetry analysis has been carried out to evaluate the efficiency of the incorporation of gallium by these procedures. Structural and textural evolution of Ga-SBA-15 material prepared were studied according to the extraction method of the structure-directing agent.

**Keywords:** Mesoporous materials, SBA-15, Ga-SBA-15, direct synthesis, post-synthesis.

### 1. Introduction

According to the definition of the IUPAC [1] relating to porosity, the materials can be classified in three groups: the microporous materials whose porous diameter is lower than 20Å, the mesoporous materials whose porous diameter is between 20Å and 500Å and the macroporous materials whose porous diameter is higher than 500Å.

In catalysis, the catalytic reactions implying microporous materials might be limited to the transformation of molecules having kinetic diameters lower than approximately 15Å. With bulky molecules such as those encountered in the refining industry, the limitations related to the diffusion inside the pores will restrict the possibilities of chemical reactions. In order to stage this inconvenient, researchers' efforts are thus directed towards

the material synthesis having more important sizes of pores, in particular in the mesoporous range [1].

Since mesoporous molecular sieves such as hexagonally ordered MCM41 were discovered by Mobil Corporation scientists in 1992 [2,3], there has been an extensive study of mesoporous materials. The unique characteristics of mesoporous molecular sieves, such as high surface area up to 1000 m<sup>2</sup>/g, large pore volume and well defined pore size of 15 to 100Å, make the material potential in catalysis, adsorption, nanoelectronics, etc. However, early reported mesoporous molecular sieves suffer low thermal and hydrothermal stabilities, which limit their applications.

In 1998, a new synthesis of ordered hexagonal mesoporous silica was proposed by Zhao and co-workers [4]. They have prepared a material named SBA-15 (for Santa Barbara Amorphous number 15) by using triblock

copolymers possessing several chains of alkylene polyoxide; these materials are similar to the MCM-41 (the most significant branch of the family of mesoporous materials designed by M41S) but they have thicker walls. What confer to them thermal and hydrothermal stabilities higher than those of the MCM 41 materials [4].

In order to generate catalytic activity, elements such as aluminium [5,6], chromium [7], titanium [8], ruthenium [9] and iron [10] were incorporated into the framework of mesoporous SBA-15 molecular sieve.

Aromatisation of the C<sub>3</sub> and C<sub>4</sub> alkanes and of the liquefied petroleum gas is an important industrial process. The introduction of gallium into silicates or aluminosilicates results in high selectivity to aromatics in the catalytic conversion of olefins and paraffins.

Reports on Gallium substituted mesoporous molecular sieve are relatively insufficient. Gallium element has been already incorporated into mesoporous MCM-41 molecular sieve [11-15]. The direct synthesis of Ga-MCM-41 with different ratio Si/Ga has been studied [12]. The quality of the products is very sensitive to the pH value. The NMR of <sup>29</sup>Si and <sup>71</sup>Ga show that gallium is in tetrahedral coordination and is introduced into MCM-41 materials structure. After calcination, the behavior of the gallio-MCM-41 depends on the Si/Ga ratio. The distribution of porous size showed that the Ga-MCM-41 structure (with Si/Ga = 20) is partially destroyed after calcination and the macropores are formed.

SBA-15 materials having thermal and hydrothermal stabilities higher than those of the MCM-41 materials, it is appeared interesting to us to prepare the material gallium-SBA-15 with various ratio Si/Ga and to follow its structural and textural evolution according to two preparation modes:

- introduction of gallium by direct synthesis
- introduction of gallium by post-synthesis.

By using X-ray diffraction, nitrogen adsorption, FT-IR spectroscopy and thermogravimetry analysis, the structural and textural evolution of these materials were studied.

## 2. Experimental

### Sample preparation

A detailed synthesis procedure for mesoporous Silica SBA-15 has been reported elsewhere [4]. In a typical synthesis in this work, 4 g of amphiphilic triblock copolymer poly(ethylene oxide)-poly(propylene oxide)-poly(ethylene oxide) (average molecular weight 5800, from Aldrich) was dispersed in 120 g of water and 8.64 g of 2M HCl solution at 40°C while stirring followed by the addition of 8.64 g of tetraethyl-orthosilicate (from Aldrich) to the homogenous solution with stirring. This gel mixture was continuously stirred at 40°C for 24h, and finally crystallized in a Teflon-lined autoclave at 100°C for 2 days. After cooling to room temperature the solid product was filtered and dried at room temperature in air. Template removal was achieved either by calcination in air at 500°C for 4h (heating rate: 1°C/min) or by solvent extraction. The solvent extraction was performed by stirring 1g of the product in 150 ml at 45°C for 1h. The extraction was repeated three times with pure ethanol and the final product was air dried over night.

Gallium – substituted mesoporous SBA-15 molecular sieve has been prepared by direct synthesis and post synthesis procedures using gallium nitrate as a source of Gallium.

Direct synthesis (DS) : 9 ml of tetraethyl-orthosilicate and the calculated amount of gallium nitrate, in order to obtain a well defined Si / Ga ratio equal to 20 and 60, were added to 10 ml of HCl aqueous solution at pH=1.5. This solution was stirred for over 3h and then added to a second solution containing 4 g of amphiphilic triblock copolymer poly(ethylene oxide)-poly(propyleneoxide)-poly(ethyleneoxide) (EO<sub>20</sub>PO<sub>70</sub>EO<sub>20</sub> (Pluronic 123 from

Aldrich) in 150ml of HCl aqueous solution at pH=1.5 at 40°C. The mixture was stirred for another 1h and finally crystallized in a Teflon-lined autoclave at 100°C for 2 days.

The solid product was filtered, dried at 100°C. Template removal was achieved by calcinations in air at 500°C for 4h (heating rate: 1°C/min).

Post-synthesis (PS) : Silica SBA-15 (0.5 g) prepared by solvent extraction of the template (SBA-15extr.) or by calcination (SBA-15 calc.) was dispersed in 50 ml of deionised water containing various amounts of gallium nitrate, in order to obtain a well defined Si/Ga ratio equal to 20 and 60. The resulting mixture was stirred at room temperature for 12 h and the powder was filtered, washed with deionised water and dried at room temperature in air.

### Characterization

Elemental Analysis: : the contents of Si and La were determined by inductively coupled plasma-atomic emission spectrometry (ICP-AES)

X-Ray Diffraction (XRD): spectra were performed on a D5000 Siemens powder diffractometer (Cu K $\alpha$ ) in the angle range of 0.5-3° 2 $\theta$  with the steps of 0.02° and a step time of 8 s.

The N<sub>2</sub> adsorption/desorption isotherms were measured on a Micromeritics SAP2010 at liquid N<sub>2</sub> temperature. Specific surface areas of the samples were calculated from the adsorption isotherms by the BET method and pore size distribution from the desorption isotherms by the BJH method.

Infrared spectra were acquired from KBr pellets in the 4000-400 cm<sup>-1</sup> range using a

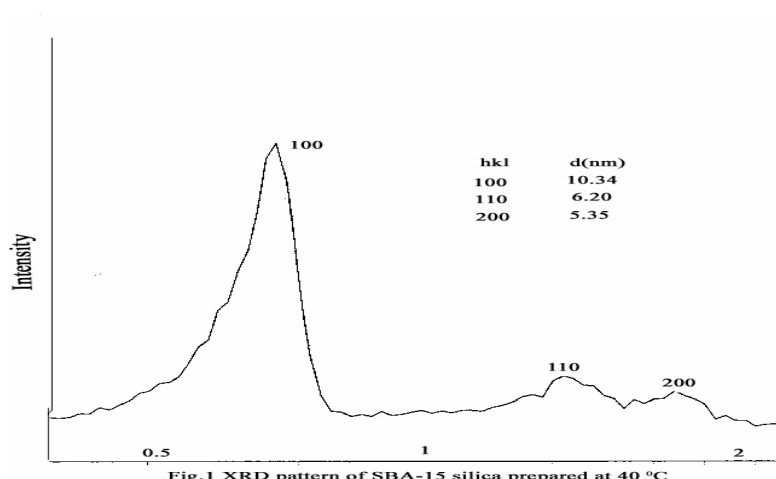
Perkin Elmer FT-IR spectrophotometer.

Thermogravimetry and derivative thermogravimetry spectra were obtained by using a SETTARAM TG DSC 111 scanning calorimeter.

## 3. Results and discussion

### 3.1. Mesoporous materials SBA-15

**3.1.1. XRD:** the XRD pattern of SBA-15 parent material synthesized at 40°C for 24 h and pH = 0.83 is shown in figure 1. It exhibits three well resolved diffraction peaks with  $d = 10.3, 6.2$  and  $5.3$  nm, which can be indexed as the (100), (110) and (200) reflections associated with  $p6mm$  hexagonal symmetry [4];  $d(100)$  spacing of 10.3 nm corresponds to a large unit cell parameter  $a = 11.9$  nm ( $a = 2 d_{100}/\sqrt{3}$ ) (see figure 2).



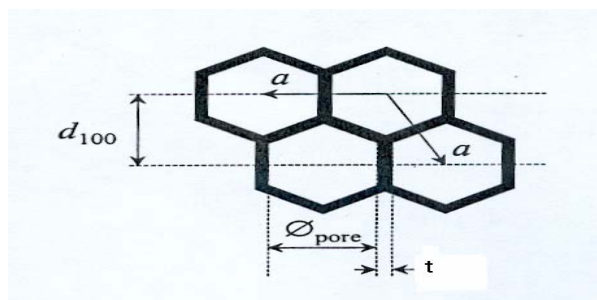


**Fig.2:** Relationship between the cell parameter ( $a$ ), the porous diameter ( $\varnothing_{\text{pore}}$ ) and the wall thickness ( $t$ ) for a hexagonal structure.

**3.2.2.  $\text{N}_2$  adsorption:** Figure 3 shows  $\text{N}_2$  adsorption - desorption isotherm for siliceous SBA-15. A typical irreversible type IV adsorption isotherm with an H1 hysteresis loop, as defined by IUPAC [1] is observed. This clear H1 type hysteresis loop, situated in the range  $0.45 < P/P_0 < 0.85$ , suggests that the material has regular

mesoporous channels with narrow gaussian pore size distribution centred at 7.9nm (Figure 4).

Textural properties of purely siliceous SBA-15 are listed in Table 1. The BET surface area, the pore volume and the mean pore diameter of the siliceous SBA-15 sample are in agreement with those published by other authors [4,5].

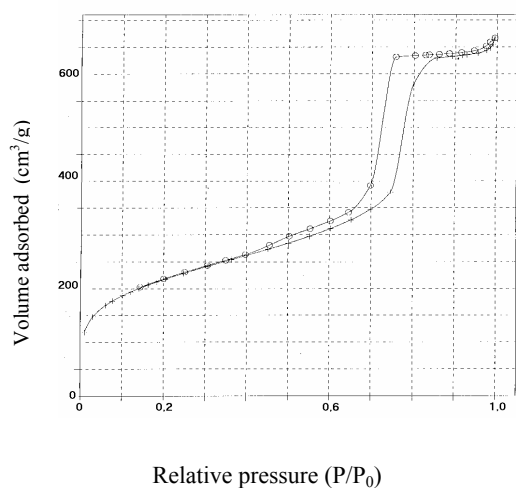


**Fig.3:** Adsorption-desorption isotherm of nitrogen on siliceous SBA-15 at 77 K  
+ : Adsorption    o : Desorption

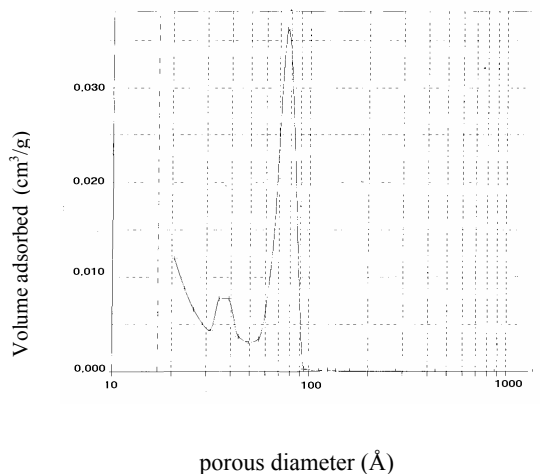


**Fig.4:** the pore size distribution curve of siliceous SBA-15 molecular sieve.

**Table1:** Textural properties of purely siliceous SBA-15.

	SBA-15 calcined
BET area (m <sup>2</sup> /g)	778
Pore volume (cm <sup>3</sup> /g)	1.01
Pore diameter (nm)	5.90
d <sub>100</sub> (nm)	10.34
Unit cell parameter, a (nm) <sup>(a)</sup>	11.94
Pore wall thickness, t (nm) <sup>(b)</sup>	6.04

(a) : Unit cell Parameter  $a = 2 d_{100}/\sqrt{3}$

(b) : Pore wall thickness ,  $t = a - \text{pore diameter}$

**3.2.3. TGA and DTA:** thermal gravimetric and differential thermal analyses show total weight losses of 58 weight % as shown in Fig. 5.

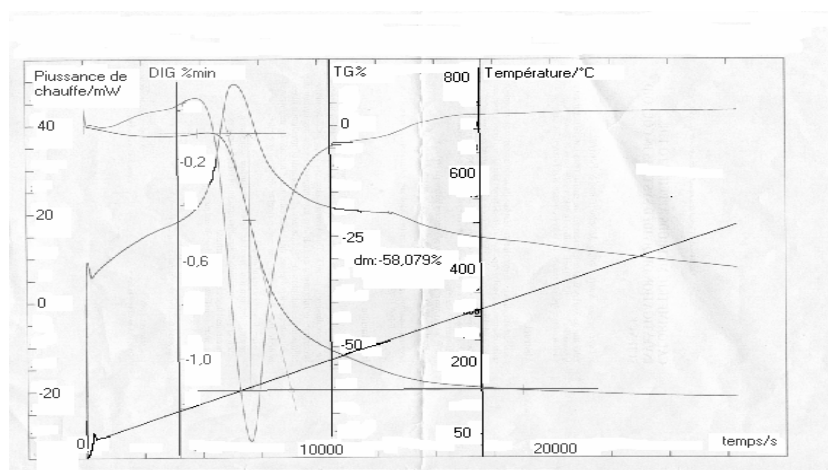


**Fig.5.** TGA and DTA spectra of siliceous material SBA-15 molecular sieve

At 80°C, TGA registers a weight loss accompanied by an endothermic DTA peak because of a desorption of water [13-15]. This is followed by a weight loss at 145°C, which coincides with an exothermic DTA peak associated with decomposition of the organic block copolymer. At about 300°C, a weight loss is assigned to deshydroxylation of silanol.

The temperature of 145°C at which the block copolymer species are decomposed and desorbed from the SBA-15 channels is much lower than the decomposition temperature of pure EO<sub>20</sub>PO<sub>70</sub>EO<sub>20</sub> (~ 250°C). The origin of the low decomposition temperature of the triblock

copolymer in the material SBA-15 comes owing to the fact that SBA-15 material catalyses the decomposition of the triblock [16].

### 3.2. Mesoporous materials Ga-SBA-15

#### 3.2.1. By direct synthesis

The elemental analysis showed that SBA-15 material contains only traces of gallium; for Si/Ga= 60 ratio in the gel mixture, the analysis gives a Si/Ga=178 ratio. This very weak incorporation of gallium by direct synthesis is due probably to the fact that the direct synthesis is synthesized in strong acidic media. A solution is to reduce the time of

the hydrothermal synthesis while operating under microwave like the for the introduction of titanium [8].

### 3.2.2. By post-synthesis

**3.2.2.1.  $N_2$  adsorption:** All samples Ga-SBA-15 (Si/Ga=20 and 60) prepared by post-synthesis and from which the

triblock was eliminated by solvent extraction or calcination present similar isotherms to that of SBA-15 material. The textural characteristics are listed in table 2.

**Table 2.** Textural properties of purely siliceous SBA-15 and Ga-SBA-15 (Si/Ga=20 and 60) prepared by post-synthesis.

Materials	SBA-15	Ga-SBA-15 ext		Ga-SBA-15 calcination
Si/Ga <sup>(a)</sup>	/	20	60	60
$S_{BET}$ ( $m^2/g$ )	778	496	683	952
Pore volume ( $cm^3/g$ )	1.01	0.38	0.58	1.45
Average pore diameter (nm)	5.90	3.89	5.79	7.20
Si/Ga <sup>(b)</sup>	/		94 <sup>(c)</sup> 178 <sup>(d)</sup>	/

(a) : Si/Ga in gel mixture

(b) : Si/Ga followed by elemental analysis

(c) : post-synthesis

(d) : direct synthesis

Table 2 shows the influence of the elimination mode of the triblock copolymer on the textural properties of Ga-SBA-15 materials ; the specific area obtained with the Ga-SBA-15 from which the triblock was eliminated by calcination, is higher than that from which the triblock was eliminated by extraction. This difference is probably due to the fact that the triblock copolymer is not completely eliminated by extraction and blocks porosity. Indeed Kruk et al. [17] showed that the solvent extraction does not involve a complete triblock copolymer elimination. In addition, table 2 shows that for the same Si/Ga=60 ratio in gel mixture, the introduction of gallium by post-synthesis is more effective since the elemental analysis gives a

Si/Ga=94 against Si/Ga=178 for the introduction of gallium by direct synthesis.

In the case of the introduction of gallium by post-synthesis, it would be interesting to characterize the samples by solid NMR of  $^{71}Ga$  to check if gallium is introduced into the framework or extra framework.

**3.2.2.2. FT-IR spectroscopy:** The FT-IR spectra of as-synthesized SBA-15, Ga-SBA-15 (Si/Ga=20 and 60) (figure 6) show the asymmetric Si-O-Si stretch at  $1089\text{ cm}^{-1}$ , the symmetric stretch at  $804\text{ cm}^{-1}$  and the Si-O-Si bending mode at  $463\text{ cm}^{-1}$ . The band at  $953\text{ cm}^{-1}$  is assigned to the Si-OH vibrations generated by the presence of defect sites.



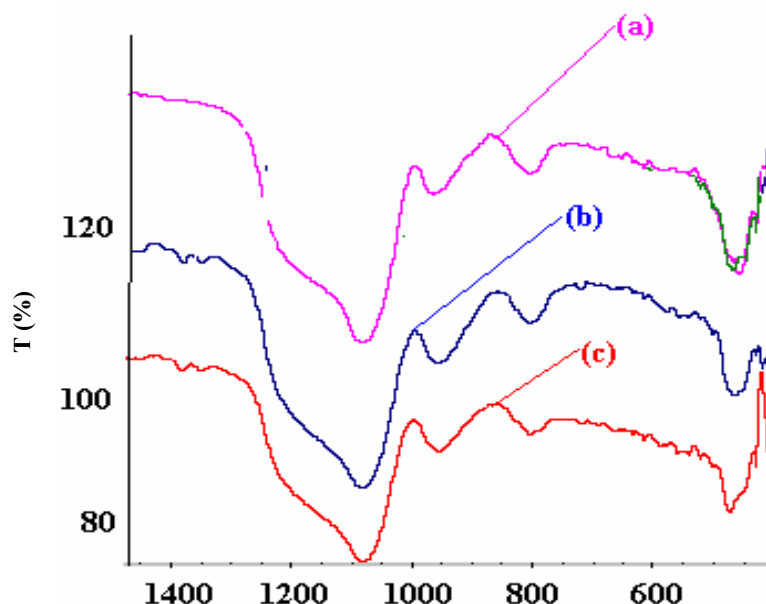


**Fig. 6.** FT-IR spectra of as-synthesized SBA-15(a), Ga-SBA-15 (Si/Ga= 20 (b) , Ga-SBA-15 (Si/Ga=60) (c) .

The wave number of different absorption bands are listed in table 3.

**Table 3.** Absorption bands of purely siliceous SBA-15 and Ga-SBA-15 (Si/Ga=20 and 60)

	$\nu$ (cm <sup>-1</sup> )		
Samples	SBA-15	Ga-SBA-15 ex	Ga-SBA-15 ex
Si/Ga	/	60	20
Asymmetric Si-O-Si stretch	1083.2	1082.7	1083.2
Si-OH Vibration	964.2	956.0	957.9
Symmetric Si-O-Si stretch	806.4	804.0	804.0
Si-O-Si bending mode	456.9	471.6	463.8

We found the same vibration bands in purely siliceous SBA-15 and Ga-SBA-15; about we cannot however

conclude if gallium is intra or extra framework. The Ga-O band is longer than Si-O band, the exchange of Si by Ga

must involve a displacement of Si-O-Si vibration towards the lower wave number, as that were found in the case of La-MCM-41 [18]. In our case, this displacement of Si-O-Si vibration is not checked for all the bands.

#### 4. Conclusion

This study showed that:

- the elimination of triblock copolymer by solvent extraction is not total
- the introduction of gallium by direct synthesis is quasi impossible by traditional hydrothermal synthesis
- gallium could be introduced by post-synthesis but the Si/Ga ratio remains lower than Si/Ga ratio used in gel mixture.

This study doesn't enable us to show if introduced gallium is intra or extra framework; a characterization by solid NMR of  $^{71}\text{Ga}$  and  $^{29}\text{Si}$  will allow to confirm the incorporation of Gallium and to show the coordination state of gallium.

#### References.

- [1] Sing, K. S. W., Everett, D. H. Haul, R. A., Moscou, L. Pierotti, R. A. J. Rouquerol and T. Siemienieuska, *Pure and Appl. Chem.*, 57(4), 603 (1985)
- [2] Kresge, C. T., Leonowickz, M. E., Roth, W. J., Vartuli J. C. and Beck, J. S. *Nature.*, 359, 710. (1992)
- [3] Beck, J. S., Vartuli, J. C., Roth, W. J. M. E. Leonowickz, Kresge, C. T., Schmitt, K. D. C. T. W. Chu, D. H. Olson, E.W. Sheppard, S. B. McCullen, J.B. Higgins and J. Lshlenker, *J. Am. Chem. Soc.*, 114, 10834 (1992)
- [4] Zhao, D. Feng, J. Huo, Q. Melosh, N. G. H. Frederickson, Chmelka B. F. and Stucky, G. D. *Science.*, 279, 548 (1998)
- [5] Yue, Y. -H. Gédéon, A. Bonardet, J. -L. J. B. d'Espinose, Melosh, N. and Fraissard, J. *Studies in Surface Science and Catalysis* 129, A. Sayari and et al. (Editors), Elsevier Science (2000)
- [6] Cheng, M., Wang, Z., Sakurai, K., Kumata, F. T. Saito, T. Komastu, and T. Yashima, *Chem. Letter.*, 131 (1999)
- [7] Zhang, X., Yue, Y. and Gao, Z., *Catal. Letter.*, 83 (1-2), 19 (2002)
- [8] Newalkar, B., L. Olanrewaju, J. and Komarneni, S. *Chem. Mater.*, 13, 552 (2001)
- [9] Coutisito, D., Acevedo, A. O., Dieckmann, G. R. and K. J. Balkus Jr, *Microporous and Mesoporous Mater.*, 54, 249 (2002)
- [10] Aiello, A., Giordano, G. and Testa, F. *Studies in Surface Science and Catalysis.*, 142, 1109 (2002)
- [11] Cheng, C. F., Alba, M. D., Klinowski, J. and J. Chem. Phys. Lett., 250, 328 (1996)
- [12] Cheng, C. F., He, H. Zhou, W. J. Klinowski, J. A. S. Gonçalves, and L. F. Gladden, *J. Phys. Chem.*, 100, 390 (1996)
- [13] Kim, J. M., Kwak, J. H. S. Jun, and R. Ryoo, *J. Phys. Chem.*, 99, 16742 (1995)
- [14] Kim, J. -H. M. Tunabe, and M. Niwa, *Microporous Mater.*, 10, 85 (1997)
- [15] Okumura, K. Nishigaki, K. and Niwa, M. *Chem. Lett.*, 577 (1998).
- [16] Huo, Q. Leon, R. Petroff, P. M. G. D. Stucky, *Science.*, 268, 1324 (1995)
- [17] Kleitz, F. Schmidt, W. and F. Schuth, *Microporous and Mesoporous Materials.*, 65, 1 (2003)
- [18] Kawi, S. Lai, M. W. , *Chem. Commun.*, 1407 (1998)
- [19] Inagaki, S. Sakanoto, Y. . Fukushima, Y, Terasaki, O. *Chem. Mater.*, 8, 2089 (1996)
- [20] Krik, M. and Jaroniec, M. *Chem. Mater.*, 12, 1261 (2000)
- [21] Kuang, Y., He, N., Wang, J. Xiao, P. Yuan, C. and Lu, Z. *Colloids and Surfaces A: Phys. Chem. Eng. Asp.*, 179, 177 (2001).

## Spectrophotometric Determination of Enrofloxacin, Lomefloxacin and Ofloxacin in Pure and in Dosage Forms Through Ion-Pair Complex Formation

Alaa S. Amin<sup>1,\*</sup>, Hassan A. Dessouki<sup>1</sup>, and Ibrahim A. Agwa<sup>2</sup>

<sup>1</sup> Department of Chemistry, Faculty of Science, Benha University, Benha, Egypt

<sup>2</sup> Department of quality control, Spimaco Addwaeih Company, Al-Qassim, King of Saudi Arabia

### Abstract

A spectrophotometric method was described for determination of the antibacterial quinolone derivatives, enrofloxacin (Enro), lomefloxacin (Lome) and ofloxacin (Oflo) through ion-pair complex formation with five different acid dye reagents. Phenol red (I), cresol red (II) and methyl red (III) were utilized for their determination, forming ion-pair complex with maximum absorbance at  $\lambda_{\max}$  408, 406 and 425 nm, respectively. The proposed method was applied for determination of Enroxin injection 10 %, Lomax 400 mg tablet, Oflicin eye drop and Tarivid 200 mg tablet, with mean percentage accuracies between (99.71 and 99.89%), (99.6 and 100.26%), (99.7 and 100.53%), (99.65 – 100.67%), respectively. Also, congo red (IV) and eirochrom black T (V) were utilized in determination of concerned drugs forming ion-pair complexes with maximum absorbance at  $\lambda_{\max}$  496 and 520 nm. The proposed method was applied for determination of Enroxin injection 10 %, Lomax 400 mg tablet, Oflicin eye drop and Tarivid 200 mg tablet, with mean percentage accuracies between (99.58 and 100.01%), (99.97 and 100.23%), (99.73 and 100.41%), (100.39 and 100.57%), respectively. Range of determination, molar absorptivity, Sandell sensitivity, detection and quantification limits were calculated. Statistical analysis of the obtained results showed no significant difference between the proposed, official and reported methods as evident from the t- and F- tests.

**Keywords:** Enrofloxacin, lomefloxacin and ofloxacin determinations; Ion-pair complexes; Spectrophotometry; Dosage forms.

---

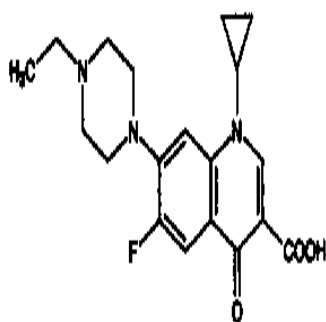
\* Corresponding author: E-mail: [asamin2002@hotmail.com](mailto:asamin2002@hotmail.com)

### 1. Introduction

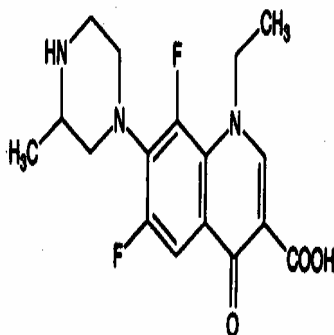
Fluoroquinolones are broad spectrum antibacterial agents, they are effective against most Gram-negative and – positive aerobic bacteria, and also they have some activity against mycobacteria, mycoplasmas, rickettsias and the protozoan *Plasmodium falciparum* [1]. Enrofloxacin, lomefloxacin and ofloxacin are member of this group. Several chromatographic methods have been reported for these compounds [2-8]. Selective determination of fluoroquinolone derivatives from tablets by reverse-phase was investigated [9]. Quantitative determination of lomefloxacin, ofloxacin and enrofloxacin in dosage forms, bulk drugs and process monitoring of enrofloxacin by RP-HPLC was studied [10]. Enrofloxacin was determined in tablets by reversed phase HPLC [11] and also in present of related materials, synthetic intermediates by another HPLC method [12]. A simple, and sensitive HPLC method was developed for the assay of enrofloxacin in raw material and injection [13]. Various spectrophotometric methods were described for determination of ofloxacin and lomefloxacin hydrochloride with some sulphonphthalein dyes [14-16]. Ofloxacin and enrofloxacin were determined in their

pharmaceutical formulations by treating with 3-methyl-2-benzothiazolinone hydrazine hydrochloride and Ce(IV) [17]. Enrofloxacin was determined spectrophotometrically in its dosage forms through formation of complex with Fe(III), charge transfer complex with 2,3-dichloro-5,6-dicyano-p-benzoquinone, ion-pair complex with bromocresol purple [18]. Enrofloxacin and ofloxacin were determined in their dosage forms using fluourometric and chemiluminescence techniques [19-21].

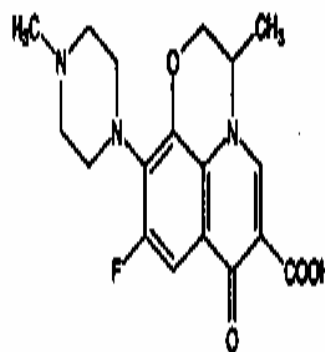
However, no spectrophotometric method for determination of enrofloxacin, lomefloxacin and ofloxacin through ion-pair complexation with phenol red (I), cresol red (II), methyl red (III), congo red (IV) and eirochrom black T (V) has been described. In the present work, attempts were made to determine enrofloxacin, lomefloxacin and ofloxacin through ion-pair complexation with five different acid dye reagents (I-V). The proposed methods are simple and suitable for routine determination of the drugs. Also these methods provide economic procedures, less time consuming and more sensitive compared with other reported spectrophoto-metric methods [14-18].



Enrofloxacin



Lomefloxacin



Ofloxacin

The chemical structure of three drug materials

## 2. Experimental

### 2.1. Instrumentation

A double beam Jasco (UV- Visible) spectrophotometer (Japan), with scanning speed 400 nm/min, and band width 2.0 nm equipped with 10 mm matched quartz cells. The pH values of buffer solutions were measured using Jenway instrument pH meter (combined electrode).

### 2.2. Materials and reagents

All solvents used were of analytical grade. Phenol red (I), cresol red (II), methyl red (III), congo red (IV) and eirochrom black T (V) were supplied from Aldrich (England). Also, chloroform, methylene chloride, carbon tetrachloride, benzene from VWR (England). The drugs under investigations are Enrofloxacin (99.92%), lomefloxacin Hydrochloride (99.95%) and ofloxacin (99.52%) were kindly supplied by Egyptian International Pharmaceutical Industries Company (EIPICO). A stock solutions of ( $2.0 \times 10^{-3}$  M) of phenol red (I), cresol red (II), methyl red (III), congo red (IV) and EBT (V) reagents were prepared by dissolving the appropriate weight of the dye initially in 10 ml methanol followed by dilution in a 100 ml measuring flask by bidistilled water to the mark. A series of buffer solutions of NaOAc – HCl (pH 1.99 – 6.2) and NaOAc – AcOH (pH 3.42 – 5.89) and NaH<sub>2</sub>PO<sub>4</sub> (pH 6.0 – 8.0) were prepared by following standard method. Enroxin injection 10 %, Lomax 400 mg tablet, Oflicin eye drop and Tarivid 200 mg table products were purchased from the marketing.

### 2.3. Stoichiometric ratio

Using the molar ratio method, the concentration of drug is kept constant (0.5 ml of  $2 \times 10^{-3}$  M) while that of the reagent is regularly varied (0.1– 1.8 ml of  $2 \times 10^{-3}$  M). The absorbance of the prepared solutions was measured at the optimum  $\lambda_{\text{max}}$  for each complex. The values were then plotted vs the molar ratio

[reagent]/[drug]. The intersections of the obtained straight lines show the molar ratio of the most stable complexes.

In continuous variation method, a series of solutions were prepared by mixing equimolar solution of drug and reagent in different proportions while keeping the total molar concentration constant (1.0 ml of  $2 \times 10^{-3}$  M). A plot of the absorbance of the solution measured at the recommended wavelength vs the mole fraction of the drug manifests a maximum at molar ratio of the most stable complex.

### 2.4. General procedures

#### 2.4.1. Using reagents I, II and III.

Aliquot portions of enrofloxacin, lomefloxacin and ofloxacin of  $100 \mu\text{g ml}^{-1}$ , (0.1 - 1.7 ml) was transferred into 10 ml calibrated flask and mixed with 2 ml ( $2.0 \times 10^{-3}$  M) reagent I and II or 1.5 ml using reagent III, followed by 3.0 ml buffer solution of pH 3.1 using I, 2.5 ml of pH 3.3 using II and 2.5 ml of pH 2.8 using reagent III and completed to 10 mark with bidistilled water. The solution was transferred into a 25 ml separating funnel and the formed ion-pairs were extracted with 5.0 ml CHCl<sub>3</sub> after shaking for 5.0 min. The absorbance of the extracted solutions was measured at 408, 406 and 425 nm using reagent I, II, and III, respectively, against extracted blank similarly prepared without drug. A calibration graph for each drug was constructed and the concentration of the unknown samples can be deduced using such calibration graph.

#### 2.4.2. Using reagent IV and V.

Aliquot portions of enrofloxacin, lomefloxacin and ofloxacin of  $100 \mu\text{g ml}^{-1}$ , (0.1 - 2.2 ml) was transferred into 10 ml measuring flask and mixed with, 1.5 and 1.0 ml of ( $2.0 \times 10^{-3}$  M) of reagent IV and V, respectively, followed by 2.5 ml of buffer pH 3.2 for IV and 3.0 ml of pH 2.7 for V. The mixed solution was

completed to 10 ml with water and transferred into a 25 ml separating funnel. The formed ion-pair was extracted with 2 x 5 ml  $\text{CH}_2\text{Cl}_2$ , after shaking for 5.0 min. The absorbance of the extracted solutions was measured at 496 and 520 nm, using IV and V, respectively, against extracted blanks similarly prepared without drug. A calibration of each drug was constructed and the concentration of unknown samples can be deduced by using such graph.

#### 2.4.3. Procedure for tablets

Thoroughly powder and mix the contents of 10 tablets of each investigated drug and determine the average weight of each one. An accurately weighed amount of the powder equivalent to 10 mg of the examined drug was dissolved in 10 ml methanol, shaken for 5.0 min and filtered through a filter paper, washed with water. The clear solution was diluted to 100 ml with water in 100 ml measuring flask. The procedures described above were used for the determination of the studied drugs applying the standard addition technique.

#### 2.4.4. Procedure for injection and eye drops

The content of 5.0 bottles of injection or eye drops was mixed and the average volume of one bottle was determined. An accurate volume equivalent to 50 mg of the drug was diluted and completed to the mark with bidistilled water in a 100 ml measuring flask. This solution was further diluted stepwise to the requisite concentration with bidistilled water. The procedures described above were used for the determination of the studied drugs applying the standard addition technique.

### 3. Results and discussion

Preliminary investigations revealed that Enro, Lome and Oflo react with each of reagents (I-V) to yield insoluble ion pair complexes. Investigations were carried out to establish the most favourable conditions for ion-pair complexation reaction of reagents (I-V) with the studied

drugs to achieve maximum colour development in their determination. The influence of the following variables on the reaction has been tested

#### 3.1. Effect of pH

In order to establish the optimum buffer media, different buffers were examined as acetate, borate, thiel, phosphate and universal buffers. It was noticed that the maximum colour intensity and constant absorbance were found using acetate buffer solutions of pH 2.0 – 5.6. Highly and constant absorbances were obtained over the pH range recorded in Table 1,2 and represented in Fig. 1. Moreover the volume of the optimum pH value was examined and found to be 2.5 ml for II, III and IV, whereas, 3.0 ml was sufficiently on using I and V in the total volume of 10 ml.

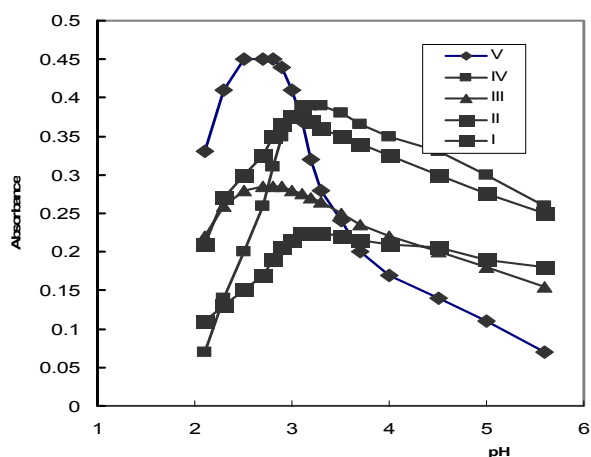
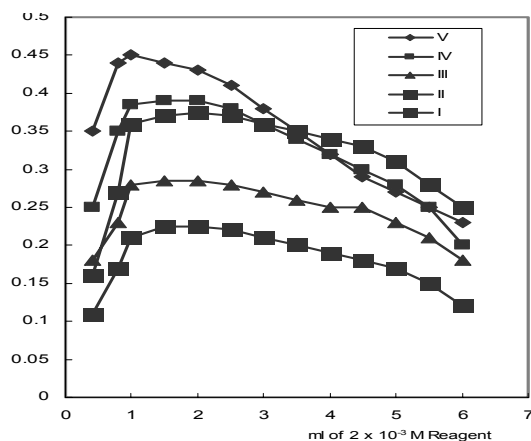


Fig. 1: Effect of pH on the absorbance of  $15 \mu\text{g ml}^{-1}$  of lome complexes with (I-V)

#### 3.2. Effect of reagent concentration

The influence of reagents (I-V) concentration on the absorbance of the ion-pair is investigated. Net absorbance increases with reagent concentration and the optimum values are obtained for the concentrations between  $1.0 \times 10^{-4}$  and  $5.0 \times 10^{-4}$  M. An increase in reagent concentration causes a decrease in absorbance as a result of dissociation of the formed ion-pair. Hence,  $3 \times 10^{-4}$  M in

the final assay solution was selected for reagent III and IV,  $4 \times 10^{-4}$  M using I, and II and  $2 \times 10^{-4}$  M using reagent V in the general procedure, since the results are highly concordant at this level of concentration (Fig. 2).



### 3.3. Effect of time and temperature

Sample solutions containing drug and the blank were treated identically with the reagent, buffer, and extracted solvent within different time and temperature. The results obtained indicated that ion-pairs were formed after shaking for 5.0 min of starting the extraction at room temperature ( $25 \pm 1^\circ\text{C}$ ). The absorption spectra were not altered on varying temperature upto  $45^\circ\text{C}$ , after which the absorbance decay with 10 % for each  $10^\circ\text{C}$  raising. The absorbance remained stable at room temperature for at least 9.0 h, after which it began to fade slowly.

### 3.4. Effect of extracted solvent

The polarity of the solvent affects both extraction efficiency and absorbance intensity. The results using different extracted solvents (benzene, chloroform, carbon tetrachloride, hexane, and methylene chloride), indicated that chloroform was the optimum solvent for all ion-pairs of reagents (I –III), whereas for reagent IV and V ion pair complexes methylene chloride was the best. Those solvents were selected due to their slightly higher sensitivity and the considerably lower extraction of the reagent itself. Complete extraction was attained by

extraction with 5.0 ml of chloroform for one time, whereas twice extraction with 5.0 ml methylene chloride was used.

### 3.5. Molecular ratio of the formed complex

The stoichiometry of the ion-pair complex was established by the molar ratio and continuous variation methods using both variable reagent and drug concentration. The results showed that the stoichiometric ratio of the complex is 1 : 1 and the shape of the resulting curves indicated that, the complex is labile. Consequently, a large excess of reagent must be always used to enhance the complex formation. The stability of the complex was calculated using the data of the molar ratio and Job's continuous variation methods applying Harvey and Manning equation [22]. The results of the stability constants were recorded in Table 1.

### 3.6. Mechanism

Acid dye technique is an ion-pair mechanism in which ion-pair is formed between negative ion producing from ionization of reagent under consideration which convert into  $[\text{R}]^-$  in buffer solution and positive ion of drug  $[\text{D}]^+$ . A representative example for the suggested structure of the formed ion-pair between reagent I and any drug can be shown below.



### 3.7. Method validation

Under the experimental conditions described, standard calibration curves for three studied drugs with different reagents (I-V) were constructed by plotting absorbance versus concentration range of the final dilution cited in Table 1 and 2. The linear regression equation for each method is listed in Table 1 and 2. The correlation coefficients were between 0.9959 and 0.9993 indicating good linearity. Ringbom optimum concentration range was determined by plotting  $\log [\mu\text{g ml}^{-1}]$  against percent

of transmittance and the linearity of S-shape curve gave accurate range of analysis and the results are recorded in Table 1 and 2. The recoveries ranging from 99.0 to 101.0 %, 98.75 to 101.38 % and 99.26 to 100.83 % with reagent I; from 98.54 to 101.56 %, 98.57 to 101.24 % and 99.17 to 101.17 %; with reagent II; from 98.89 to 100.83 %, 99.29 to 101.19 % and 98.75 to 100.63 % with reagent III; from 99.17 to 100.83 %, 98.91 to 100.85 % and 99.24 to 101.14 % with reagent IV; from 98.33 to 101.79 %, 98.33 to 101.44 % and 99.17 to 101.17 % with reagent V for each of Enro, Lome and Oflo, respectively. Furthermore, recoveries were determined on three levels and six replicates per each level.

The reproducibility of the proposed procedure was determined by analyzing ten replicate samples of each drug ( $10.0 \mu\text{g ml}^{-1}$ ). The relative standard deviations and ranges of error obtained are given in Table 1 and 2. The performance of the proposed procedure was assessed by calculation of the t- (for accuracy) and F- (for precision) values compared with the official methods [10-12]. Mean values were obtained in a Student's t- and F- tests and 95% confidence limits for five degrees of freedom [23] and the results showed that the calculated t- and F- values did not exceed the theoretical values (Table 1 and 2).

In order to determine the accuracy and precision of the proposed procedure, solutions containing four different concentrations of the examined drugs were prepared and analysed in quantuplicate. The measured standard deviation, relative standard deviation ( $S_r$ ), the standard analytical error and confidence limit value can be considered satisfactory, at least for the levels of concentrations examined.

### 3.8. Interference studies

The effects of common excipients that often accompany the studied drugs in various pharmaceutical dosage forms were tested for possible interference in the assay. An attractive feature of the procedure is its relative freedom from interference by the usual tablet diluents and

excipients such as talc, sucrose, starch, gelatine, lactose and magnesium stearate. Amounts far in excess of their normal occurrences in dosage forms were added, and no effect due to these excipients was noted in the experimental procedure. Analyzing synthetic mixtures of the drugs (mg) containing the following amounts of excipients (mg) also checked the applicability of the method:

1. Enro (20), talc (60), sucrose (40), starch (50), gelatine (50), lactose (30) and magnesium stearate (60).
2. Lome (20), talc (60), sucrose (30), starch (40), gelatine (50), lactose (30) and magnesium stearate (50).
3. Oflo (20), talc (40), sucrose (35), starch (60), gelatine (50), lactose (35) and magnesium stearate (60).

A Suitable amount of each synthetic mixture was analyzed by following the general procedure described earlier. The percentage recovery was found to be in the range of 98.5 – 101.2 with RSD values  $\geq 1.12$  for six replicates. Moreover, there is no interference from the decarboxylated degradant results from thermal and hydrolytic treatment [24].

### 3.9. Analytical applications

Pharmaceutical formulations containing Enro, Lome, and Oflo was analysed by the proposed methods and the accuracy was assessed by the standard addition method in which variable amounts of pure drug were added to the previously analysed portion of pharmaceutical formulation. Results are shown in Table 3 confirming that the proposed method is not liable to interference by tablet fillers, excipients and additives usually formulated (microcrystalline cellulose, anhydrous dibasic calcium phosphate, magnesium stearate, croscarmellose sodium, titanium dioxide, hydroxypropyl methylcellulose, lactose, and triacetin). The proposed method is highly sensitive, therefore, it could be used easily for the routine analysis of pure form and in its pharmaceutical formulations. Statistical comparison of the



results was performed with regard to accuracy and precision using Student's t-test and F-ratio at 95% confidence level (Table 3). There is no significant difference between the proposed methods with regard to accuracy and precision.

#### 4. Conclusion

The proposed procedure is fairly simple, less time-consuming and more sensitive than the official methods. The principal advantage of the proposed procedure is suitable for the determination of the studied drugs in their dosage forms without interference from excipients and additives such as starch, glucose, magnesium stearate or from common degradation products suggesting application in bulk drug analysis. The proposed procedure is successfully applied to determine Enro, Lome and Oflo in dosage forms. Statistical comparison for the results of the proposed procedure with the official methods indicate that there is no significant difference with regard to accuracy and precision. In comparison with the existing spectrophotometric methods the proposed procedure especially with congo red (IV) are simpler, more sensitive, cheaper and accurate.

#### References

- [1] Martindale, 31st ed., Royal pharmaceutical society, London, 1996, pp. 207-210 and 260-261.
- [2] Souza, M.J.; Bittencourt, C.F.; Morsch, L.M., J. Pharm. & Biomed. Anal. 2002, 28, 1195-1199.
- [3] Zeng, Z.; Dong, G.; Chen, Z.; Huang, X., J. Chromatog. B., 2005, 821, 202-209.
- [4] Sun, H-W.; He, P.; Lu, Y-K.; Liang, S-X., J. Chromatog. B., 2007, 852, 145-151.
- [5] Idowu, O.R.; Peggins, J.O., J. Pharm. & Biomed. Anal., 2004, 35, 143-154.
- [6] Wei, S.; Lin, J.; Li, H.; Lin, J-M., J. Chromatog. A., 2007, 1163, 333-336.
- [7] Wan, G-H.; Cui, H.; Pan, Y-L.; Zheng, P.; Liu, L-J., J. Chromatog. B., 2006, 843, 1-9.
- [8] Zhao, S-J.; Li, C.; Jiang, H-Y.; Li, B-Y.; Shen, J-Z., Chin. J. Anal. Chem., 2007, 35, 786-790.
- [9] Shinde, V. M.; Desai, B. S.; Tendolkar, N. M., Indian Drugs, 1998, 35, 715-717.
- [10] Argekar, A. P.; Kapadia, S. U.; Raj, S. V.; Kunjir, S. S., Indian Drugs, 1996, 33, 261-266.
- [11] Ba, B.B.; Ducint, D.; Fourtillan, M.; Saux, M.C., J. Chromatogr. Biomed. Appl., 1998, 714, 317-324.
- [12] United States Pharmacopeia, XXIV ED., United States convention, Rckville, 2000, p. 420.
- [13] Souza, M. J.; Bittencourt, C. F.; Morsch, L. M.; J. Pharm. & Biomed. Anal., 2002, 28, 1195-1199.
- [14] Issa, Y.M.; Abdel-Gawad, F.M.; Abou Table M.A.; Hussein, H.M., Anal. Lett., 1997, 30, 2071-2084.
- [15] Askal, H.; Refaat, I.; Darwish, I.; Marquouq, M., Chem. Pharm. Bull., 2007, 55, 1551-1556.
- [16] Patel, P.U.; Suhaghia, B.N.; Patel, M.M.; Patel, G.C.; Patel, G.N., Indian Pharm., 2007, 6, 59-61.
- [17] Sastry, C.S.P.; Rao, K.R.; Prasad, D.S., Indian Drugs, 1995, 32, 172-175.
- [18] Shinde, V.M.; Desai, B.S.; Tendolkar, N.M., Indian drugs, 1998, 35, 715-717.
- [19] Ballesteros, O.; Vilchez, J.L.; Taoufiki, J.; Navalon, A., Mikrochim. Acta, 2004, 148, 227-233.
- [20] El-Kommos, M.E.; Saleh, G.A.; El-Gizawi, S.M.; Abou-Elwafa, M. A., Talanta, 2003, 60, 1033-1050.
- [21] Hanwen, S.; Liqing, L.; Xueyan, C., Anal. Sci., 2006, 22, 1145-1149.
- [22] Harvey, A.E.; Manning, D.L., J. Am. Chem. Soc., 1950, 72, 4488.
- [23] Miller, J.C.; Miller, J.N., "Statistics in Analytical Chemistry" Ellis Horwood, Chichester, 3<sup>rd</sup> ed., 1993.
- [24] Florey, K., "Analytical Profile of Drug Substances, Vol. 20, Academic Press, New York, 1991, 557-600.

## Synthesis and Characterization of Two Novel Salent Type Symmetrical Schiff Base Ligands

Iran Shiekhshoaie

*Chemistry Department, Shahid-Bahonar of Kerman, Kerman, Iran*

### Abstract

Two novel Schiff base ligands bis(2-hydroxy-1-naphthaldiamine)-N-2,2-dimethyl-1,3-diaminopropane[L<sub>1</sub>] and bis-(2-hydroxy-1-naphthaldiamine)-N-diethylen triamine[L<sub>2</sub>] have been prepared by condensation of 2,2-dimethyl-1,3-diaminopropane and diethyltriamine with 1-naphthaldehyde. The products have been charactrized by C, H, N, analysis and some spectroscopic methods.

**Keywords:** Schiff base, Napthaldehyde, Diethelentriamine, 2,2-Dimethyl-1,3-diamineopropane.

### 1. Introduction

Schiff base are considered as a very important class of organic compounds. Azomethine compounds have wide application in many biological aspects, viz., proteins visual pigments, enzymic aldolization and decarboxylation reactions[1-4]. Also Schiff bases and the relevant transition metal complexes are still found to be of great interest in inorganic chemistry. Some Schiff bases and their metal complexes exhibit biological activity as antibiotic, antiviral and antitumor agents[5]. In this paper, we report the synthesis and characterization of two tetra and penta dentate Schiff base compounds L<sub>1</sub> and L<sub>2</sub> (Fig. 1).

### 2.Experimental

#### Materials and Methods

1-All chemicals were commercial grade reagents and were used as received from Aldrich, Fluka or Merck companies without any further purification. Fourier transformed infrared (FT-IR) spectra were recorded at room temperature in a KBr disk using a spectrophotometer (Unicam-400). The electronic spectra were recorded on a Beckman DU-7000 UV-vis spectrophotometer in DMF. Elemental analysis (C, H, and N) data were obtained with

an Exeter Analytical CE-440 elemental analyzer. Melting points were taken using an electro thermal IA 9100 apparatus in open capillary tubes.

<sup>1</sup>H-NMR and <sup>13</sup>C-NMR spectra were obtained on Bruker (250 MHz) NMR spectrometer in dimethylsulfoxide DMSO-d<sub>6</sub> solvent. Proton chemical shifts are reported in parts per million (ppm) relative to an internal Me<sub>4</sub>Si standard.

#### Synthesis of L<sub>1</sub> and L<sub>2</sub> Schiff base compounds

Bis-(2-hydroxy-1-naphthaldimine)-N-2,2-dimethyl-1,3-diaminopropane[L<sub>1</sub>] and bis-(2-hydroxy-1-naphthaldimine)-N-diethylene triamine[L<sub>2</sub>] Schiff base compounds were prepared according to a general procedure reported by Schiff[6]. The L<sub>1</sub> and L<sub>2</sub> Schiff bases have been synthesized by adding the ethanolic solution of naphthaldehyde ( 2 mmol) with ethanolic solution of 2,2-dimethyl-1,3-propane diamine ( 1 mmol) or diethylen triamine ( 1 mmol). The reaction mixtures were separately refluxed for 5-6 h, and the condensation products were filtere, throughly washed with the least possible amount of ethanol, recrystallized at room temperature. The purity of

the synthesized compounds was monitored by TLC using silica gel.

**Comp. L<sub>1</sub>.** Yellow crystals, Yields 80%, mp. 125 °C, Molecular weight: 410 g/mol.

Anal. Calcd. For L<sub>1</sub>: C, 79.02; H, 6.34; N, 6.82. Found: C, 78.98; H, 6.20; N, 6.73.

<sup>1</sup>H-NMR (CDCl<sub>3</sub>): δ 2.2 (s, 6H, CH<sub>3</sub>), 3.5 (q, 4H, CH<sub>2</sub>), 6.9 (m, 2H, CH=N), 12.4 (s, 2H, OH), 7.8-8.2 (m, 12H, naphthyl).

**Comp. L<sub>2</sub>.** Yellow crystals. Yield: 57%, mp. 117 °C, molecular weight: 411 g/mol. Anal. Calcd. For L<sub>1</sub>: C, 75.91; H, 6.08; N, 10.21. Found: C, 75.72; H, 6.10; N, 10.11.

<sup>1</sup>H-NMR (CDCl<sub>3</sub>): δ 2.25 (m, 1H, NH), 2.76 (m, 8H, CH<sub>2</sub>), δ (s, 2H, HC=N), 7.11-7.22 (m, 12H, naphthyl).

In the UV-Vis spectra of L<sub>1</sub> and L<sub>2</sub> there is an intense band in high-energy region (about 300 and 259 nm) of their spectra of these ligands which are related to  $\pi \rightarrow \pi^*$  transition of naphthyl rings[7].

### 3. Results and Discussion:

Salen type Schiff base compounds L<sub>1</sub> and L<sub>2</sub> can be rapidly by Schiff method. These compounds are air stable. Infrared spectral data of these ligands displays a sharp band at 1641-1644 cm<sup>-1</sup> that are attributed to  $\nu$  (C=N) stretching frequency. Quantum chemical calculations study shows that the two above mentioned compounds are tetra-denate ligands with N (in C=N groups) and O (in hydroxyl groups) are the active coordination, sites.

### References:

- [1] B. Witkop, L. K. Ramachandran, *Metabolism*, 13, 1016(1964).
- [2] R. A. Morton, G. A. J. Pitt, *Biochem. J.*, 59, 128(1955).

- [3] I. Fridovitch, F. H. Westheimer, *J. Am. Chem. Soc.*, 84., 3208(1962).
- [4] E. Grazi, R. T. Rowley. T. Cheng, O. Tchola. B. L. Horecker, *Biochem. Biophys. Res. Commun.* 9, 38,(1962).
- [5] D. R. Williams, *Chem Rev.*, 72, 203(1972).
- [6] H. Schiff, *Ann. Chim. (Paris)*, 131, 118(1964).
- [7] A. Bottcher, T. Takeuchi, K. I. Hardcastle, T. J. Meade, H. B. Gray, *Inorg. Chem.*, 36, 2498(1997).

المجلة العربية للكيمياء :

Ô Ô - - - -

:

..

éèì ì : . . èèèì è - - -

E-mail: [awarthan@ksu.edu.sa](mailto:awarthan@ksu.edu.sa) , [aalwarthan@yahoo.com](mailto:aalwarthan@yahoo.com)

:

..

. .

E-mail: [abouorabi@yahoo.com](mailto:abouorabi@yahoo.com)

..

- - -

E-mail : [yousrymi@yahoo.com](mailto:yousrymi@yahoo.com)

:

.

éèì ì . - èèèì è - - -

E-mail : [aaltulihe@ksu.edu.sa](mailto:aaltulihe@ksu.edu.sa)